Stretto di Messina

Concessionaria per la progettazione, realizzazione e gestione del collegamento stabile tra la Sicilia e il Continente Organismo di Diritto Pubblico
(Legge n° 1158 del 17 dicembre 1971, modificata dal D.Lgs. n°114 del 24 aprile 2003)

EurolinK

# PONTE SULLO STRETTO DI MESSINA

# PROGETTO DEFINITIVO

## EUROLINK S.C.p.A.

IMPREGILO S.p.A. (MANDATARIA)
SOCIETÀ ITALIANA PER CONDOTTE D'ACQUA S.p.A. (MANDANTE)
COOPERATIVA MURATORI E CEMENTISTI - C.M.C. DI RAVENNA SOC. COOP. A.R.L. (MANDANTE)
SACYR S.A.U. (MANDANTE)
ISHIKAWAJIMA - HARIMA HEAVY INDUSTRIES CO. LTD (MANDANTE)
A.C.I. S.C.P.A. - CONSORZIO STABILE (MANDANTE)

| IL PROGETTISTA | IL CONTRAENTE GENERALE | STRETTO DI MESSINA | STRETTO DI MESSINA |
|---|---|---|---|
| COWI<br>Ing. E.M. Veje<br>Dott. Ing. E. Pagani<br>Ordine Ingegneri Milano<br>n° 15408<br>EurolinK | Project Manager<br>(Ing. P.P. Marcheselli) | Direttore Generale e<br>RUP Validazione<br>(Ing. G. Fiammenghi) | Amministratore Delegato<br>(Dott. P. Ciucci) |

PF0004_F0

| | |
|---|---|
| *Unità Funzionale* | OPERA DI ATTRAVERSAMENTO |
| *Tipo di sistema* | SOTTOSTRUTTURE |
| *Raggruppamento di opere/attività* | FONDAZIONI TORRI |
| *Opera - tratto d'opera - parte d'opera* | Geotechnical Design Reports |
| *Titolo del documento* | Sicily Tower Foundation: evaluation of foundation behaviour via 3D FE analyses and of bearing capacity, Annex |

CODICE: G C 1 0 0 0 | P | C L | D | P | S T | F 3 | T S | 0 0 | 0 0 | 0 0 | 0 1 | F0

| REV | DATA | DESCRIZIONE | REDATTO | VERIFICATO | APPROVATO |
|---|---|---|---|---|---|
| F0 | 20/06/2011 | EMISSIONE FINALE | DL | GR | CV |
| | | | | | |
| | | | | | |
| | | | | | |
| | | | | | |

NOME DEL FILE: PF0004_F0.doc

# INDICE

INDICE ..... 3
EXECUTIVE SUMMARY ..... 4
1 Foreword ..... 6
2 The foundation of the Sicily Tower ..... 7
3 Soil profile and geotechnical characterisation ..... 10
3.1 In situ stress state ..... 11
3.2 Shear strength parameters ..... 12
3.3 Stiffness ..... 12
4 3D FEM model ..... 14
4.1 Soil profile ..... 15
4.2 Finite element mesh ..... 15
4.3 Constitutive soil model and soil parameters ..... 16
4.4 Structural members ..... 20
4.4.1 Footings ..... 20
4.4.2 Diaphragm walls ..... 21
4.5 Calculation sequence ..... 24
4.6 ULS - Loading conditions ..... 26
4.6.1 ULS – STRU (approach 1 combination 1- A1+M1+R1) ..... 27
4.6.2 ULS - GEO (approach 1 combination 2 – A2+M2+R2) ..... 28
4.6.3 ULS - Results of the analyses ..... 30
4.7 SILS - Loading condition ..... 32
4.7.1 SILS - Results of the analysis ..... 33
4.8 SLS2 – Loading condition ..... 34
4.8.1 SLS2 - Results of the analysis ..... 36
5 Bearing capacity via hand calculation ..... 37
5.1 Case A1M1 ..... 39
5.2 Case A2M2 ..... 40
6 Load update from IBDAS new model ..... 41
7 Appendix A – Comparison between loads from IBDAS global model 3.3 b and 3.3 f ..... 98

# EXECUTIVE SUMMARY

**Section §1 - *Foreword*:** the main goals of the numerical analyses report are presented: 1) verify that the ultimate limit state consisting in a failure of the ground beneath the tower foundation is not exceeded; 2) furnish to the structural designer the loading displacement curves essential for evaluating the safety for the ultimate limit state consequent to excessive deformation of the ground. The aforementioned issues are addressed referring to ultimate limit state loading conditions as defined by NTC 2008 (ULS-STRU and ULS-GEO) and structural integrity limit state loading condition as defined by tender documents (SILS). Furthermore, as regards the serviceability limit states, the foundation behaviour is analysed and the displacements are evaluated referring to SLS2 loading condition.

**Section §2 - *The foundation of the Sicily Tower***: the main geometrical features of the tower foundation are described and the considered loading conditions are presented.

**Section §3 - *Soil profile and geotechnical characterisation***: a brief summary of the geotechnical properties of the subsoil is presented. For more details on recent geotechnical investigations and characterisation see the geotechnical report CG1003-P-RG-D-P-SB-G3-00-00-00-00_01_A_Upd_Geot_Char_ANX.

**Section §4 - *3D FEM model***: the numerical model of the tower foundation is described. In particular the following aspects are discussed: the soil profile; the finite element mesh; the constitutive soil model and the adopted soil parameters; the modelisation of the structural members (footings, connecting beam and diaphragm walls); the calculation sequence. The different loading conditions and the corresponding results are presented in specific subsections dealing with: ULS - Loading conditions (ULS – STRU and ULS – GEO); SILS - Loading condition; SLS2 – Loading condition.

Main results obtained by FEM calculations are summarized in the following table:

| Limit state | load/ design load | Vertical displacement (m) | | | | |
|---|---|---|---|---|---|---|
| | | A | B | C | D | E |
| ULS: | | | | | | |
| A1+M1+R1 | 1.00 | -0.060 | -0.091 | -0.123 | | |
| max reached value | 7.29 | -1.40 | -3.12 | -4.87 | | |
| A2+M2+R2 | 1.00 | -0.049 | -0.085 | -0.121 | | |
| max reached value | 7.58 | -0.92 | -3.90 | -6.96 | | |
| SILS | 1.00 | -0.075 | -0.105 | -0.136 | -0.102 | -0.110 |
| SLS2 | 1.00 | -0.072 | -0.085 | -0.098 | -0.082 | -0.089 |

In the table the amplification factor of the design load is reported in the second column while in the columns from 3 to 8 the settlement of five points selected on two orthogonal diameters are recalled. The points refer to only one foundation leg because the adopted 3D model is symmetrical around an axis orthogonal to the seashore, passing in between the two foundation legs. The amplification factors allow to appreciate how large is the distance from any form or collapse detectable via FEM calculations: in other words the FEM model did not show any clear soil collapse until the design loads were multiplied by a number between 7 and 8. The settlements of the five selected points under SLS2 combination range between 72 and 98 mm, showing significant rotation only towards the seashore.

**Section §5 - *Bearing capacity via hand calculation***: hand calculations of the bearing capacity of the foundation referred to ULS loading conditions are presented. Very large overall safety factors are deduced using conventional Brinch-Hansen formulation for bearing capacity of shallow foundations.

**Section §6 – Load update from new IBDAS model:** In this section the main features of the new load combinations on the foundations of the tower provided via IBDAS new model are analysed. The load combinations are divided in ULS, SLS2, SILS and SLS1. Furthermore they are divided in static and seismic combinations, the latter being derived by spectral analysis of the bridge. The ULS static combinations were provided according to the NTC 2008 as ULS-GEO for bearing capacity check. The hand calculations described in section 5 were used to select the worst combinations. The results of the hand calculations together with the load-displacement curves obtained via 3D FEM analyses for the worst selected combinations are reported in this final section of the report.

# 1 Foreword

This report describes the 3D finite element analyses performed for the foundations of the Sicilia tower of the suspended bridge over the Messina Strait. The calculations presented herein are mainly based on the drawings and the geotechnical data provided in the tender design. Any change in the geometry or simplifying assumptions will be clearly outlined.

New geotechnical data from site investigations and laboratory tests are already available and further data will be soon available. Only the data available at the date of the revision of the document are of course taken into account. For more details on this topic see the geotechnical report CG1003-P-RG-D-P-SB-G3-00-00-00-00_01_A_Upd_Geot_Char_ANX.

In the *Progetto Preliminare* a number of assumptions had to be made because some of the necessary information concerning soil properties was not available. These assumptions were based on published data, and were always conservative. The input parameters and the results of the analyses are now updated taking into account the data coming from the geotechnical investigation planned for the *Progetto Definitivo*. In the meanwhile the new Italian technical code *NTC 2008* has been approved and this report is updated also by this point of view.

The numerical analyses presented in this report are primarily concerned with the ultimate limit states in which the strength of soil is significant in providing resistance; the main goals of the analyses are:

1. verify that the ultimate limit state consisting in a failure of the ground beneath the tower foundation is not exceeded;
2. furnish to the structural designer the loading displacement curves essential for evaluating the safety for the ultimate limit state consequent to excessive deformation of the ground.

The aforementioned issues are addressed referring to ultimate limit state loading conditions (ULS-STRU and ULS-GEO) and structural integrity limit state loading condition (SILS).

Furthermore, as regards the serviceability limit states, the foundation behaviour is analysed and the displacements are evaluated referring to SLS2 loading condition.

# 2 The foundation of the Sicily Tower

The Sicily Tower foundation consists of two massive concrete circular footings of diameter D = 55 m with a centre-to-centre distance i = 77.5 m. The two footings are connected by a pre-stressed reinforced concrete beam with a box-shaped cross-section (H = 15.50 m; L = 18.00 m) cast in situ from -11 m a.s.l. to +4.5 m a.s.l.

The ground level in the foundation area is around 5-6 m a.s.l.. The area has a gentle slope towards the sea shore which is located at about 60-70 m aside from the center of the foundation. In front of the tower the seabed has a slope of about 13°.

The excavation required to reach the depth of foundation, at -15 m a.s.l., is supported by circular diaphragm walls, reaching – 45 m a.s.l. The diaphragm consists of reinforced concrete panel 1.00 thick and 3.00 m wide casted in situ from +2.50 m a.s.l. to -45.00 m a.s.l.

The soil below the tower foundation (i.e. below the two footings and the connecting beam) has to be treated using secant jet-grouted columns down to a depth of 41.5 m (from -15 m a.s.l. to -38.5 m a.s.l.). In the tender documents the jet grouting columns were a bit longer: one column out of three were prolonged down to -45 m a.s.l.. The above assumption was agreed as a potential source of savings and a technical simplification not implying any significant worsening of the performance of the foundation.

Furthermore the mechanical properties of the soil around the two footings has to be improved by some kind of grouting mainly with the aim to reduce his liquefaction potential.

The effects on the footings of the bridge of the applied loads were deduced by Table 2.1 at page 7 of the *Relazione specialistica sottostrutture* (PG 2R B0-001 N07 p2). These effects (load to be applied onto the foundation) were confirmed by the structural engineers as the loading combinations to be used also in this stage of the design.

These effects are summarised in Table 1, Table 2, Table 3, as vertical forces, horizontal forces and bending moments. Note that design effects of ULS in Table 1 do not correspond to the sum of the effects of dead and live loads as provided by structural engineers because they do not correspond to the same load combinations. The effects in Table 1, Table 2, Table 3 arise from the analysis of the bridge structures subjected to the design loads as obtained by multiplying characteristics loads by the amplification factors prescribed in the tender documents. The main features of seismic actions, considered via a pseudo-static approach in the structural analyses, leading to the effects reported in the above mentioned tables, are reported in Table 4.

A rather complex issue is that concerning the evaluation of allowable values for displacements and rotations. In such a huge project this evaluation of course cannot be limited to empirical criteria. In this report the calculated values for the displacements are simply reports. With the only aim to remember and to fix some general reference the tender design documentation considered as main requirement to be satisfied in terms of serviceability limit states that the tower rotation should not exceed the allowable value fixed to 1‰.

Finally it is worth to notice that the analysis of the foundation subjected to the design value of forces and moment reported in Table 1, Table 2 and Table 3 do not exhaust the analysis of the foundation performance. In principle the foundation behaviour should be analysed under the actions coming out from each of the loading combinations imposed by the design code; however in the present report until section 5 only the “more severe” effects, as identified by the structural designer, has been considered.

In the section 6 all the new load combinations provided by the global IBDAS model are fully analysed. Hand calculations were carried out on all the provided load combinations in order to select the worst ones. Only these last were used for 3D FEM analyses in order to calculate and illustrate load-displacement performance

*Table 1 Forces on the foundation (elevation +18 m a.s.l.) resulting from loads applied on the bridge structures: ULS*

| | **Vertical force (MN)** | **Horizontal force (MN)** | **Moment (MNm)** |
|---|---|---|---|
| **Dead** | 2422 | 1 | 47 |
| **Live** | 289 | 328 | 20235 |
| **Design** | **2577** | **370** | **21946** |

*Table 2 Forces on the foundation (elevation +18 m a.s.l.) resulting from loads applied on the bridge structures: SILS*

| **Vertical force (MN)** | **Horizontal force (MN)** | **Moment (MNm)** |
|---|---|---|
| **3289** | **376** | **23876** |

*Table 3 Forces on the foundation (elevation +18 m a.s.l.) resulting from loads applied on the bridge structures: SLS2*

| **Vertical force (MN)** | **Horizontal force (MN)** | **Moment (MNm)** |
|---|---|---|
| **3042** | **159** | **11239** |

*Table 4 Main features of seismic actions*

| **limit state** | **peak ground acceleration ($m/s^2$)** | **return period (years)** |
|---|---|---|
| SLS2 | 2.6 | 200 |
| ULS | 5.7 | 2000 |
| SILS | 6.3 | |

# 3 Soil profile and geotechnical characterisation

The geotechnical site investigations carried out between 1988 and 1992 together with the geological and geophysical investigations performed for the preliminary design study allowed to define the general soil profile in the area of the Messina Strait at the time of Progetto Preliminare. The following summary of the soil conditions and geotechnical characterisation is practically the same as in the geotechnical report and is reported here for ease of reference. However being the site investigations still in course and the geotechnical report updated continuously if some minor differences should arise the geotechnical report CG1003-P-RG-D-P-SB-G3-00-00-00-00_01_A_Upd_Geot_Char_ANX must be considered as the reference report. The new site investigations carried out for the Progetto Definitivo made possible to confirm the general validity of the available site characterisation allowing refinements on the definition of some soil parameters.

Figure 1 shows the soil profile on the Sicilian shore of the strait. The present level of the ground at the location of the Sicilian Tower is about 4-5 m a.s.l.; the ground slopes gently towards the sea shore, located at a distance of about 60 to 70 m from the centre of the tower foundation. The inclination of the sea bottom in this area is about 13°. The groundwater level roughly coincides with the sea level, at 0 m a.s.l..

Starting from ground level and moving downwards the following units are encountered:

1 *Depositi Costieri* (Coastal Deposits). Sand and gravel with very little or no fine content; occasionally, silty peaty layers appear in the lower part of the formation. The thickness of this formation is difficult to evaluate as it rests on the very similar formation of the *Ghiaie di Messina*; at this location the thickness of this formation is about 85 m.

2 *Ghiaie di Messina* (Messina Gravel). Gravel and sand, with very occasional silty layers. The thickness of this formation can reach more than 170 m; at this location the estimated value of the thickness of this formation is about 130 m.

3 *Depositi Continentali* (Continental Deposits)/*Calcarenite di Vinco* (Vinco Calcarenite). Clayey-sandy deposit, consisting of layers of silt or silt and sand, with significant gravel content/Bio-calcarenite and fossiliferous calcarenite, with thin silty layers.

4 *Conglomerato di Pezzo* (Pezzo Conglomerate). Soft rock, consisting of clasts of different dimensions in a silty-sandy matrix and sandstone. The thickness of this formation is larger than 200 m.

5 *Cristallino* (Crystalline bedrock). Tectonised granite.

## 3.1 In situ stress state

Values of $K_0$ for the Coastal Deposits can be estimated from the relative density $D_R$ using the relationship proposed by Baldi *et al*. (1987) for normally consolidated silica sands, see Report PP-2R-A24, Fig. 4.3.3. This yields values of $K_0 = 0.43 \div 0.47$ with the lower values associated at shallower depths (z < 30÷35 m b.g.l.)

The Messina Gravel is geologically over-consolidated by erosion of an estimated thickness of at least 100 m, and, in the area of the Sicilian Tower foundation, presently overlain by about 80 m of *Depositi Costieri*. The effects of mechanical over-consolidation on $K_0$ may be estimated as:

$$\frac{K_0}{K_0(NC)} = \left(\frac{\sigma'_{v\,max}}{\sigma'_{v0}}\right)^{0.45}$$

in which $\sigma'_{v0}$ is the in situ effective stress and $\sigma'_{v\,max} = \sigma'_{v0} + \Delta\sigma'_v$, in which $\Delta\sigma'_v$ is the vertical stress once transmitted by the eroded thickness less the load presently transmitted by the Coastal Deposits, estimated at about 10×(100-80) = 200 kPa. At a depth of 100 m, geological over-consolidation can account for an increase of the values of $K_0$ of about 9%; the effect of geological over-consolidation decreases with depth.

The order of magnitude of ageing effects can be estimated using the following relationship (Mesri, 1993):

$$\frac{K_0}{K_0(NC)} = \left(\frac{t}{t_p}\right)^{C_{\alpha e}/C_c}$$

In which t is the time elapsed from the deposition of the Messina Gravel, between $4\times10^5$ and $6\times10^5$ years, $t_p$ is the end of primary consolidation time, about 1 year, $C_{\alpha e}$ is the secondary compression coefficient, and $C_c$ is the compression index. For granular soils typical values of the ratio $C_{\alpha e}/C_c$ are about 0.02 (Mesri, 1989) and therefore the maximum estimated increase of $K_0$ due to ageing effects is of the order of 30%.

It follows:

$K_0 = 1.09 \times 1.3 \times K_0(NC) = 1.42 \times (1\text{-}\sin\varphi'_p) = 0.47$

in which $\varphi'_p = 42°$ (see following section).

## 3.2 Shear strength parameters

The friction angle has been estimated from the relative density obtained from the SPT results using the relationships by Schmertmann (1978).

for $z < 30 \div 35$ m  $D_R = 0.80$  $\varphi'_p = 44°$
for $z > 30 \div 35$ m  $D_R = 0.55$  $\varphi'_p = 42°$

This values of friction angle can be considered representative of the peak shear strength corresponding to an effective stress on the plane of failure of 272 kPa.

As far as the constant volume friction angle is concerned, following Bolton (1986):

$\varphi'_{cv} = \varphi'_p - 3\, D_R(10 - \mathit{ln}p') + 3°$

with $\sigma'_v = 272$ kPa, or $p' = 180$ kPa, it follows that:

for $z < 30 \div 35$ m  $D_R = 0.80$  $\varphi'_{cv} = 35°$
for $z > 30 \div 35$ m  $D_R = 0.55$  $\varphi'_{cv} = 37°$

These values are only slightly larger than those indicated by Negussey *et al*. (1986) for silica (quartz and feldspars) materials independently of grain size and shape, relative density, and effective stress state, $\varphi'_{cv} = 33° \div 35°$.

## 3.3 Stiffness

The stiffness characteristics of the deposits were obtained from one cross-hole test carried out in the vicinity of the Sicilian Tower foundation (FS-BH1), using three boreholes reaching a maximum depth of 100 m b.g.l., at a distance of 5 m from one another. The results of the cross-hole test in terms of shear wave velocity, $V_s$, versus depth are given in Figure 4.3.59 of Report PP-2R-A24. In Figure 2 the same results are shown as profiles of small strain shear modulus, $G_0$. This has been obtained from the shear wave velocity as:

$$G_0 = \rho V_S^2$$

The three data sets refer to the values obtained in each of the three boreholes, while the continuous line is the average of the three data at each depth.

The data show that in the Coastal Deposits $G_0$ varies from about 50 MPa at surface to about 200 MPa at a depth of 68 m b.g.l.; from this depth to 84 m b.g.l. there is a transition layer where $G_0$ takes values of about 350 MPa. Despite the fact that the Coastal Deposits and the Messina Gravel have otherwise very similar characteristics, the contact between the two formations is readily identified at a depth of 84 m b.g.l. by a sharp increase of the values of shear modulus to a values of about 2.5 GPa.

The comparison of the values of small strain shear modulus measured in the cross-hole test and those obtained by correlation with the results of three CPT tests carried out in this area (Baldi et al., 1986) is rather good indicating that, at least in the first 50 m b.g.l. where there are CPT data, there is little horizontal variability of the stiffness of these deposits (see Geotechnical Report PP-2R-A24, Fig. 4.3.69).

Table 5 summarises the main mechanical parameters obtained from the geotechnical characterization above.

*Table 5 Summary of main mechanical parameters from geotechnical characterization*

| | **depth (m bgl)** | **Dr * (%)** | **$K_0$*** | **$\varphi'_p$ (°)** | **$\varphi'_{cv}$ (°)** | **$K_h$ (m/s)** | **$G_0$ (MPa)** |
|---|---|---|---|---|---|---|---|
| **Coastal Deposits** | 0÷68 | 80÷55 | 0.43÷0.47 | 44 | (33÷35)÷(35÷37) | $5\times10^{-3}$ | 50÷200 |
| **transition layer** | 68÷84 | 55 | 0.47 | 42 | 35÷37 | $5\times10^{-3}$ | 350 |
| **Messina Gravel** | 84÷210 | 55 | 0.47 | 42 | 35÷37 | $5\times10^{-3}$ | 2500 |

* the first value of the range refers to shallower depths, z≤30÷35 m b.g.l.

# 4 3D FEM model

The analyses were carried out using the commercial code Plaxis$^{3D}$ Foundation ver. 2.2. The adopted version is the last release of the same code applied in the *Progetto Preliminare*.

According to the current Italian Code (*Norme Tecniche per le Costruzioni - Testo Unico - DM 14.01.2008*) a shallow footing comply with the ultimate limit state concerned with soil strength if the design action do not exceed design resistance. If the design action is lower or equal to the design resistance, the footing performance is satisfactory in terms of this ultimate limit state. Hence the main problem to be solved is to evaluate the design resistance (i.e. the bearing capacity of the foundation). The FEM analysis described in the following primarily consists into solving the statical problem of the tower foundations loaded by the design action. When the numerical algorithm is capable to find a solution it obviously follows that the design resistance is higher than the design action; as a matter of fact in this case the adopted design actions represent a lower bound for the maximum allowed design actions which, according to the code, could be equal to the design resistance.

In order to get a deeper insight into the new version of the code some further comments are needed.

The new version of the code (*Norme Tecniche per le Costruzioni - Testo Unico - DM 14.01.2008*) introduces two approaches while the elder version of 2005 allowed just one approach. According to the approach 1 of the latest and current version of the code two types of calculations must be carried out. In the first case, called approach 1 comb. 1 (A1+M1+R1) all applied loads are amplified while the strength parameters of the foundation soil are set to their characteristic values; in the second case (A2+M2+R2) only live loads are amplified while the characteristic values of the strength parameters of the foundation soils are reduced. In the first case the dead loads are multiplied by 1.3 while the live loads are multiplied by 1.5. In the second case the live loads only are multiplied by 1.3 and in terms of effective stress both the cohesion c' and tan$\varphi$' are divided by 1.25. The second case should be the most appropriate for ULS referred to geotechnical bearing capacity but, however, in this report both combinations of the approach 1 are verified. The new version of the code (2008) compared to the old version (2005) has also introduced the coefficients $\gamma$R which in the short representation of the combination reported above are included in the term R1 or R2. According to the present version of the code in the approach 1 comb. 1 the coefficient $\gamma$R is equal to 1 while in the approach 1 comb. 2 the coefficient $\gamma$R is equal to 1.8 for the ULS known as bearing capacity, and 1.1 for ULS known as pure sliding. The coefficients $\gamma$R, as a matter of fact, represent further reduction of the calculated design resistance or, which is the same, further amplifications of the design actions.

However an ultimate limit state in the structure could also result from an excessive deformation of the ground. Therefore an incremental loading procedure has to be adopted to evaluate the loading displacement curves. The load-displacement curves provided in this report should be used by the structural engineers in order to check the occurrence of such ultimate limit state.

## 4.1 Soil profile

Figure 1 which was already mentioned before shows the extent of the mesh that was adopted for the 3D finite element analyses of the Sicilian Tower foundation. The bottom of the mesh -see following section- is at about 210 m b.g.l. i.e. shallower than the contact between the Messina Gravel and the Continental Deposits. It follows that, in this context, the geological units of relevance are only those of the Coastal Deposits and of the Messina Gravel.

## 4.2 Finite element mesh

Figure 7 and Figure 8 show the 3D finite element mesh used in the analyses, extending 550 m parallel to the sea, 300 m orthogonal to the sea and 210 m below ground level. The horizontal part of the ground is at a level of +2,5 m a.s.l.; the ground slopes down towards the sea with an average angle of 13°. The contact between the Messina Gravel and the Coastal Deposits is substantially horizontal. The initial distribution of pore water pressure is hydrostatic, with a total head of 0.0 m a.s.l.
The adopted mesh is made of 46596 wedge 15-nodes elements (122254 nodes and 279576 stress points in total). The boundary conditions consist of totally restrained displacements on the bottom boundary; restrained displacements in the normal direction on sides, front and rear boundaries. A free displacement condition is assumed on the top boundary; however linearly varying distributed loads are applied on the portion of the ground slope situated below the sea level to simulate the sea-water pressure, and on the rear part of the surface to model the ground slope.

## 4.3 Constitutive soil model and soil parameters

The behaviour of the tower foundation was analysed through finite element analyses performed using the code *Plaxis 3D Foundation*. The mechanical behaviour of the soil was described using the constitutive model *Hardening Soil* available in the model library of the code. The model is capable of reproducing soil non-linearity due to the occurrence of plastic strains from the beginning of the loading process; this implies that for undrained conditions an increase of the stress deviator *q* produces excess pore water pressure. The computed non linear stress-strain relationship has tangent initial modulus equal to $E'_i$; upon unloading, the model assumes elastic behaviour with Young's modulus $E'_{ur} \geq E'_i$, thus it is capable of reproducing a significant change in stiffness. In the model, soil stiffness depends on the effective stress state.

The same constitutive model has been used in the coupled, effective stress dynamic analyses carried out under plane strain condition to study the soil structure interaction of the simplified 2D bridge model. Under earthquake loading conditions the model predicts plastic strains and excess pore water pressures until peak acceleration is attained at the element location, since increasing values of accelerations produce a progressive enlargement of the yield surfaces. Elastic behaviour is assumed within the elastic domain so that the model is not capable to reproduce strain accumulation and pore pressure build up for loading cycles contained within the yield domain.

The calibration of the constitutive model was performed using the results from the cross hole test carried out at the site and from published results of compression triaxial tests carried out on undisturbed frozen samples of gravely soils (Tanaka et al., 1987). The cross hole test was used to evaluate the shear modulus at small strains $G_0$ and to describe its variation with effective stress. The remaining soil parameters were selected to obtain a satisfactory description of the soil non-linearity observed in the triaxial tests.

Hardening soil model is an elastic-plastic rate independent model with isotropic hardening. The elastic behaviour is defined by isotropic elasticity through a stress-dependent Young's modulus:

$$E'_{ur} = E_{ur}^{\mathrm{ref}} \left( \frac{c' \cdot \cot\phi' + \sigma_3'}{c' \cdot \cot\phi' + p^{\mathrm{ref}}} \right)^{\mathrm{m}} \qquad (1)$$

where $\sigma'_3$ is the minimum principal effective stress, $c'$ is the cohesion, $\varphi'$ is the angle of shearing resistance, $p^{\mathrm{ref}}$ = 100 kPa is a reference pressure; $E_{ur}^{ref}$ and *m* are model parameters.

The model has two yield surfaces $f_s$ and $f_v$ with independent isotropic hardening depending on distortional plastic strain $\gamma^p = (2 \cdot \varepsilon^p{}_1 - \varepsilon^p{}_v)$ and on volumetric plastic strains $\varepsilon^p{}_v$, respectively; the two surfaces have the following equations:

$$f_s = \frac{1}{E'_{50}} \frac{q}{(1 - 0.9 \cdot q/q_f)} - \frac{2q}{E'_{ur}} - \gamma^p = 0 \tag{2}$$

$$f_v = \frac{\tilde{q}^2}{\alpha^2} + p'^2 - p'^2_c = 0 \tag{3}$$

In eqn. 2, $E'_{50}$ is given by an expression similar to eqn. 1, but, in contrast to $E'_{ur}$, it is not used within a concept of elasticity. Hardening of the $f_s$ surface is isotropic and depends on the plastic distortional strain $\gamma^p = (2 \cdot \varepsilon^p{}_1 - \varepsilon^p{}_v)$.

In eqn. 3, $p'$ is the mean effective stress; $\tilde{q}$ is a generalised deviator stress, that accounts for the dependence of strength on the intermediate principal effective stress $\sigma'_2$; $\alpha$ controls the shape of the $f_v$ surface in the $\tilde{q}$ -$p'$ plane and can be related to the coefficient of earth pressure at rest $K_0$ for normally consolidated states. The hardening parameter $p'_c$ is the size of the current $f_v$ surface and is related to the plastic volumetric strains $\varepsilon_v{}^p$ through the hardening law, written in the incremental form as:

$$\mathrm{d}\varepsilon^p_v = \frac{\beta}{p^{ref}} \left( \frac{p'_c}{p^{ref}} \right)^m \cdot \mathrm{d}p'_c \tag{4}$$

where $\beta$ is a parameter that controls the variation of $p'_c$ with the plastic volumetric strains. In the model formulation implemented in *Plaxis*, the parameter $E'_{oed}$, which is related to $\beta$, has to be specified. This is the constrained modulus for one-dimensional plastic loading, and depends on the maximum principal effective stress $\sigma'_1$ through the relationship:

$$E'_{oed} = E'^{ref}_{oed} \cdot \left( \frac{c' \cdot \cot\phi' + \sigma_1'}{c' \cdot \cot\phi' + p^{ref}} \right)^m \tag{5}$$

where $\sigma'_1$ is the maximum principal effective stress.

The initial value of the hardening parameter $p'_c$ is related to the one-dimensional vertical yield stress, and can therefore be specified by assigning a value for the overconsolidation ratio OCR. It is worth mentioning that OCR has to be regarded as a yield stress ratio defined in the framework of strain hardening plasticity, so that values of OCR > 1 can be specified also for geologically normally consolidated soil deposits exhibiting a yield stress larger than the in situ stress.

The flow rule is associated for states lying on the surface $f_v$, while a non associated flow rule is used for states on the surface $f_s$. The latter is derived from the theory of stress dilatancy by Rowe (1962): the mobilised dilatancy angle $\psi_m$ depends on the current stress state through the angle of mobilised friction $\varphi'_m$ and the angle of friction at constant volume $\varphi'_{cv}$:

$$\sin\psi_m = \frac{\sin\phi'_m - \sin\phi'_{cv}}{1-\sin\phi'_m \sin\phi'_{cv}} \tag{6}$$

In turn, $\varphi'_{cv}$ can be obtained from the angle of shearing resistance $\varphi'$ and the angle of dilatancy $\psi$ at failure:

$$\sin\phi'_{cv} = \frac{\sin\phi' - \sin\psi}{1-\sin\phi' \sin\psi} \tag{7}$$

Figure 3 shows the shape of the yield surfaces fv and fs and schematically indicates their evolution.

For plastic loading from isotropic stress states, the model predicts a non linear stress-strain relationship with tangent initial modulus equal to

$$E_i^{'} = \frac{2E_{50}^{'}}{2-0.9} \approx 1.82 E_{50}^{'}$$

However for unloading and reloading (i.e. initially elastic loading), the value of $E_i'$ coincides with $E'_{ur}$ and is related to the shear modulus at small-strain $G_0$ obtained from the cross-hole test carried out in the site.

Figure 4 shows the profile of $G_0$ against the elevation a.s.l.. The continuous line in the figure represents the prediction of $G_0$ obtained using eqn. (1) with the values of $c'$, $\varphi'$, $E'^{ref}_{ur}$ and $m$ reported in Table 6. Specifically, the values of $\sigma'_3$ was obtained using the values of $K_0$ given in Table 5. Values of $E'^{ref}_{ur}$ and $m$ were obtained by best fitting the cross-hole test results and assuming $\nu' = 0.2$.

The remaining model parameters $E'^{ref}_{50}$ and $E'^{ref}_{oed}$ were calibrated on the results of triaxial compression tests carried out on large-diameter reconstituted samples of gravely soils (Tanaka et al., 1987).

Figure 5 shows the comparison between the model simulations and the test results. It was found that a good agreement for the stiffness decay with the shear strain was obtained using ratios of $E'_{ur}{}^{ref}$ / $E'_{50}{}^{ref}$ = 7 and of $E'_{50}{}^{ref}$ / $E'_{oed}{}^{ref}$ = 1.0 and a value for the angle of dilatancy at failure $\psi$ = 0. A constant shear stiffness was assumed for the layer of Messina gravel with a stiffness decay ($E'_{ur}{}^{ref}$ / $E'_{50}{}^{ref}$ = 3 and of $E'_{50}{}^{ref}$ / $E'_{oed}{}^{ref}$ = 1.0) lower than that assumed for the overlying layers.

*Table 6 Hardening soil parameters for the foundation soil*

| **Soil** | **$\gamma$ (kN/m$^3$)** | **$c'$ (kPa)** | **$\varphi'$ (°)** | **$K_0$** | **OCR** | **$E'_{ur}{}^{ref}$ (kPa)** | **m** | **$E'_{50}{}^{ref}$ (kPa)** | **$E'_{oed}{}^{ref}$ (kPa)** |
|---|---|---|---|---|---|---|---|---|---|
| **coastal deposit** | 20.0 | 4.2 | 40 | 0.47 | 2.0 | $2.28 \cdot 10^5$ | 0.2 | $3.26 \cdot 10^4$ | $3.26 \cdot 10^4$ |
| **transition soil** | 20.0 | 13.5 | 42 | 0.47 | 2.0 | $6.24 \cdot 10^5$ | 0.2 | $8.91 \cdot 10^4$ | $8.91 \cdot 10^4$ |
| **Messina gravel** | 20.0 | 20.0 | 42 | 0.47 | 2.0 | $6.00 \cdot 10^6$ | 0.0 | $2.00 \cdot 10^6$ | $2.00 \cdot 10^6$ |

Soil permeability was evaluated from the in situ measurements; a constant value of k = $10^{-3}$ m/s was adopted in the analyses.

The soil below the tower foundation is to be treated using secant jet-grouted columns down to a depth of 41.5 m (from -15 m a.s.l. to -38.5 m a.s.l.); the jet-grouted columns will be confined by the diaphragm walls. Mechanical properties of the jet-grouted columns were selected using published results (Croce et al., 2004). Table 7 summarises the adopted quantities; specifically, an unconfined strength $\sigma_c$ = 6 MPa was assumed for the columns, with a ratio $E'/\sigma_c$ = 500 and a low stiffness decay, $E'^{ref}/E'_{50}{}^{ref}$ = 2 and $E'_{50}{}^{ref}/E'_{oed}{}^{ref}$ = 1.

*Table 7. Hardening soil parameters for the jet-grouted soil*

| **Soil** | **$\gamma$ (kN/m$^3$)** | **$c'$ (kPa)** | **$\varphi'_{cv}$ (°)** | **$E'^{ref}$ (kPa)** | **m** | **$E'_{50}{}^{ref}$ (kPa)** | **$E'_{oed}{}^{ref}$ (kPa)** |
|---|---|---|---|---|---|---|---|
| **jet-grouting** | 22.0 | 1560 | 35 | $3 \cdot 10^6$ | 0.2 | $1.5 \cdot 10^6$ | $1.5 \cdot 10^6$ |

A constant value for the permeability coefficient k = $10^{-7}$ m/s was assumed in the analyses. Conservatively the soil improvement of the zone external to the foundation is not considered in the calculations presented in this report.

## 4.4 Structural members

### 4.4.1 Footings

The upper part of the Sicily Tower foundation, above -2.0 m a.s.l., has a conical shape reaching elevation +18.0 a.s.l. In the numerical model the upper part of the foundation has been simulated as cylindrical with the same diameter of the bottom part (D=56 m) and height of 7.0 m (between -2.0 m a.s.l. and + 5.0 m a.s.l.). Therefore, an equivalent unit weight was computed for the upper portion of the foundation by equating the self-weight of the real foundation to the self-weight of the equivalent foundation:

$$\gamma_{eq} = \gamma \cdot \frac{D_{real}{}^2 \cdot h_{real}}{D_{model}{}^2 \cdot h_{model}} = 18{,}4\ \frac{kN}{m^3}$$

The total weight of each of the two footings on the Sicilian side is:

$$Q_{footing} = Q_{upper\ footing} + Q_{lower\ footing} = \gamma_{upp} \cdot V_{upp} + \gamma_{low} \cdot V_{low} = \gamma_{upp} \cdot \frac{\pi \cdot D^2 \cdot h_{upp}}{4} + \gamma_{low} \cdot \frac{\pi \cdot D^2 \cdot h_{low}}{4} =$$

$$= \left( 18{,}4 \cdot \frac{\pi \cdot 56^2 \cdot 7}{4} + 24{,}0 \cdot \frac{\pi \cdot 56^2 \cdot 13}{4} \right) kN = 1086\,MN$$

The concrete has been modelled as an elastic material. The unit volume weight $\gamma$ has been taken equal to 24 kN/m$^3$. The Young's modulus E has been assumed equal to 30 GPa; the Poisson's ratio $\nu$ = 0,15.

The beam connecting the two separate footings was briefly described in the section 2. This beam should of course influence the foundation behaviour limiting the relative displacement and rotations. However in the numerical analyses carried out in this report the considered loading conditions and the subsoil are symmetric in respect of the vertical plane normal to the connecting beam. It follows that the connecting beam should work only as consequence of the rotations of each footing in a plane parallel to the seashore. Even if such rotations are expected as a consequence of the interaction between the two footings (i.e. the settlements induced below one footing by the load applied on the other footing) in the calculations presented in this report the connecting beam is not considered. As a consequence the aforementioned rotations may be overestimated.

### 4.4.2 Diaphragm walls

The circular diaphragm walls have an external diameter $D_e$ = 57 m and a thickness t = 1 m. They have a total length L = 47.5 m extending from 2.5 m a.s.l. to – 45 m a.s.l. Three annular beams at depths of -6.5 m a.s.l., -11.0 m a.s.l., and -15 m a.s.l., are used to cooperate with the diaphragm wall in order to support the excavation. The cross section of the beams is 1.0 m x 1.5 m. The beams will be connected to the diaphragm wall with shear bars and will be removed prior to the construction of the foundation, in order to prevent vertical load transfer from the footing to the diaphragm walls. However, due to computational problems, no interfaces were activated between the diaphragm wall and the foundation nor between the diaphragm wall and the in situ soils.

The diaphragm walls were modelled as Plaxis WALL elements. These are shell elements (seeFigure 6), with thickness d = t = 1 m and weight w. The code requires 6 stiffness values, namely $E_1$, $E_2$, $E_3$, $G_{12}$, $G_{13}$, $G_{23}$, to completely define their behaviour. The required values of stiffness moduli were obtained using the procedure outlined below.

The stiffness along direction 1 was obtained as:

$$E_1 = \frac{12 \cdot E_c \cdot I_1}{d^3} = E_{cls} = 30 \text{ GPa} = 3 \cdot 10^7 \text{ kPa}$$

in which:

$$I_1 = \frac{1 \times s^3}{12} \quad \frac{m^4}{m} \text{ (inertia per unit length)}$$

The stiffness along direction 2 was obtained as:

$$E_2 = \frac{12 \cdot E_c \cdot I_2}{d^3}$$

in which $I_2$ is the moment of inertia along direction 2, mainly determined by the presence of the 3 annular beams, whose section is rectangular with a size of 1.0 m x 1.5 m. The moment of inertia of the single beam is:

$$I_{beam} = \frac{a \cdot b^3}{12} = 0{,}28\,m^4 \Rightarrow 3 \cdot I_{beam} = 0{,}84\,m^4 \;.$$

The bending stiffness of the 3 beams was distributed over the entire excavated depth of the diaphragm wall (17,5 m):

$$I_2 = I_{eq} = \frac{3 \cdot I_{beam}}{h_{excavation}} = \frac{3 \cdot 0{,}84}{17{,}5} = 0{,}048\,\frac{m^4}{m}$$

and therefore:

$$E_2 = \frac{12 \cdot E_c \cdot I_2}{d^3} = \frac{12 \cdot 30 \cdot 0{,}048}{1^3} = 17{,}4\,GPa = 1{,}74 \cdot 10^7\,kPa$$

Following the same criteria the shear stiffness $G_{12}$ and $G_{13}$ were calculated based on the dimensions of the diaphragm walls while the shear stiffness $G_{23}$ was calculated based on the dimensions of the annular beams:

$$G_{12} = G_{13} = \frac{E_{cls}}{2 \cdot (1+\nu)} = 1{,}30 \cdot 10^7\,kPa.$$

$$G_{23} = \frac{E_{cls} \cdot A_{23}}{2 \cdot (1+\nu) \cdot d}$$

The area $A_{23}$ of the beams is equal to:

$$A_{23beam} = a \cdot b = 1{,}5\,m^2 \Rightarrow 3 \cdot A_{23beam} = 4{,}5\,m^2.$$

Distributing the area of the 3 beams over the excavated length of the diaphragm wall:

$$A_{23} = \frac{3 \cdot A_{23beam}}{h} = \frac{4{,}5}{17{,}5} = 0{,}26\,\frac{m^2}{m}$$

The following value is obtained for $G_{23}$:

$$G_{23} = \frac{E_c \cdot A_{23}}{2 \cdot (1+\nu) \cdot d} = 3{,}35 \cdot 10^6 \text{ KPa}$$

As a matter of fact the values of the shear stiffness $G_{ij}$ do not have a significant influence on the calculations.

The length of the diaphragm wall below the excavation depth was characterized using the same values of $E_1$, $G_{12}$ and $G_{13}$ and lower values of $E_2$ and $G_{23}$, to take into account that there are no annular beams.

Early calculations showed a significant vertical load transfer from the footing to the diaphragm wall due to the impossibility to activate low strength interface. To prevent such load transfer the value of $E_1$ was reduced everywhere in the diaphragm wall, resulting in a substantial reduction of its axial stiffness. Final calculations were carried out according to this assumption after the excavation step.

Table 8 summarises the geometrical and mechanical properties of the diaphragm walls.

*Table 8 Properties of the diaphragm walls*

| Diaphragm walls | **$\gamma$ (kN/m$^3$)** | **d (m)** | **$E_1$ (kPa)** | **$E_2$ (kPa)** | **$G_{12}$ (kPa)** | **$G_{23}$ (kPa)** | **$G_{23}$ (kPa)** | **$\nu$** | **$E_{cls}$ (kPa)** |
|---|---|---|---|---|---|---|---|---|---|
| Upper portion with beams | 24.0 | 1.0 | $3.00\times10^7$ | $1.74\times10^7$ | $1.30\times10^7$ | $1.30\times10^7$ | $3.35\times10^6$ | 0.15 | **$3.00\times10^7$** |
| bottom part | 24.0 | 1.0 | $3.00\times10^7$ | $3.00\times10^5$ | $1.30\times10^7$ | $1.30\times10^7$ | $1.30\times10^5$ | 0.15 | **$3.00\times10^7$** |
| stiffness. reduction | 24.0 | 1.0 | $3.00\times10^3$ | $3.00\times10^3$ | $1.30\times10^3$ | $1.30\times10^3$ | $1.30\times10^3$ | 0.15 | $3.00\times10^7$ |

## 4.5 Calculation sequence

The main aim of the calculations reported in this document have been already clarified in the previous chapters. The interest of the report is focused on the load-displacement relationship of the footings of the bridge. However the full construction sequence of the footings including the excavation stage was judged as significant for the aim of the report. For this reason even the main steps of the construction sequence were selected and analysed. Only minor details of the preliminary stages of the construction were neglected.

In order to clarify such point in the following the full construction sequence modelled in the 3D finite element analyses of the foundation of the Sicilian Tower is summarized:

- construction of the diaphragm walls as wish in place;
- realisation of the jet grouting columns below the foundation base by changing soil properties in the cluster interested by soil treatment;
- excavation of the soil to reach the foundation base made by removing soil clusters;
- casting in place of the concrete footings;
- applications of the vertical, horizontal and moment loadings.

It is worthy mentioning that all the preliminary steps (i.e. steps before the applications of the structural load coming from the towers) have been included in the analyses for their influence on the stress state in the soil below the foundation; however, the displacement that will be presented in the report refer only to the steps were external load are applied.

The calculation phases as introduced in the code Plaxis are reported in Table 9.

*Table 9 Calculation phases*

| ***step*** | ***Description*** |
|---|---|
| **0** | **gravity loading with double unit weight of all soils and increased stiffness (×10)** |
| **1** | **unit weight back to true values; maintain increased stiffness** |
| **2** | **decrease stiffness to true values** |
| **3** | **displacement reset and activation of diaphragm walls and jet-grouting** |
| **4** | **excavation to -15 m a.s.l.** |
| **5** | **displacement reset, activation of tower foundation,** |
| **6** | **displacement reset and application of vertical loads** |
| **7** | **application of horizontal loads and moments** |

The initial three steps (steps 0-2) are needed to generate the correct initial stress state in the soil mass. In calculation step 0 the of bulk weight, $\gamma$, of all soil layers were doubled to simulate an overconsolidated state; at the same time, the values of $E_{ur}$, $E_{50}$ and $E_{oed}$ were multiplied by ten. In calculation step 1 the true values were assigned to $\gamma$ while the increased values of the stiffness parameters of the hardening soil model were maintained. Finally, in calculation step 2, the true values of $E_{ur}$, $E_{50}$ and $E_{oed}$ were assigned to the soil layers. In this manner it was possible to obtain an overconsolidation ratio OCR = 2 while avoiding hardening of the yield surface in shear, such that, in the following loading processes, the soil would develop plastic strains for even very small increments of shear stresses.

After generating the initial stress state, the diaphragm walls and the jet grouting are activated using a wished in place technique, i.e. changing the properties of the corresponding soil element clusters.

Figure 11 (a) and (b) are two orthogonal sections of the 3D FE mesh showing the location of the footing and the extent of the jet grouted soil below the tower foundations.

In all the analyses, the vertical loads are applied first while the horizontal loads and moments are applied simultaneously in a subsequent step. The vertical loads are simulated with 4 forces on each footing. The applied loads and moments were calculated starting from the values provided by the structural analyses of the bridge and taking into account the difference between the height of the FEM model of the footing and the true height. Both the horizontal loads and the moments were applied in the direction of the seashore (submarine slope).

As already anticipated in the section 1, the analyses were carried out for ULS, SILS and SLS2 loading conditions.

## 4.6 ULS - Loading conditions

The loads to be applied to the footings of the bridge were deduced by Table 2.1 at page 7 of the *Relazione specialistica sottostrutture* (PG 2R B0-001 N07 p2). Table 10 details the different components of the loads applied to the foundation. Note that design loads do not correspond to the sum of dead and live loads as they come from different load combinations as stated by structural designers.

*Table 10 Forces on the foundation (elevation +18 m a.s.l.) resulting from loads applied on the bridge structures: ULS*

| | **Vertical force (MN)** | **Horizontal force (MN)** | **Moment (MNm)** |
|---|---|---|---|
| **Dead** | 2422 | 1 | **47** |
| **Live** | 289 | 328 | **20235** |
| **Design** | **2577** | **370** | **21946** |

### 4.6.1 ULS – STRU (approach 1 combination 1- A1+M1+R1)

In this analysis, which in the report for the Progetto preliminare was called as Standard analysis, the loads applied at +18 m a.s.l. are the design loads reported in Table 10. In the FE model the footings are cut to the elevation of +5,0 m, so the applied moment has to be incremented:

$$M_{tot} = M + \Delta M = M + H \times \Delta h_{footing} = (21946 + 370 \times 13)\,\mathrm{MN\,m} = 26756\,\mathrm{MN\,m}.$$

The loads adopted in the standard analysis are summarised in Table 11.

*Table 11 Loads applied at +5.0 m. ULS- STRU (APPROACH 1 COMBINATION 1- A1+M1+R1)*

| Q (MN) | H (MN) | M (MNm) |
|---|---|---|
| **2577** | **370** | **26756** |

The loads have been applied to each footing by means of four point load (i.e. concentrated forces). The four nodes were selected on the edge of the top part of the footing. In each node vertical forces were calculated in order to simulate also the presence of the bending moments.

In the first phase, to each point-force on the footings a vertical load $Q_{node}$ is applied:

$$Q_{node} = \frac{Q}{8} = 322\,\mathrm{MN}.$$

In the following loading phase horizontal loads and moments are added, both ap plied in the direction of the seashore.

Moments are produced applying vertical forces in the nodes, with the same magnitude and of opposite sign, generating in the center of the footings a resulting moment equal to the design value. The distance between the load-points in the z direction (orthogonal to the seashore) is 28 m. To obtain a resulting bending moment of 26756 MNm a vertical force of 239 MN has been applied, directed downward for the nodes nearest to the seashore, upward for the others (y-axes positive verse is directed upward). It results:

$$M_{tot} = 8 \times \left( F \times \frac{\Delta z}{2} \right) = 8 \times (239 \times 14)\,\text{MN m} = 26756\,\text{MN m}$$

Finally, the vertical loads applied downward on the 8 nodes are:

$$Q^{+}_{node} = Q_{node} + F = (322 + 239)\text{MN} = 561\text{MN} \qquad \text{(nodes near to the seashore)}$$
$$Q^{-}_{node} = Q_{node} + F = (322 - 239)\text{MN} = 83\text{MN} \qquad \text{(nodes far from the seashore)}$$

Furthermore, in each of the 8 nodes a horizontal load, $H_{node}$, is applied:

$$H_{node} = \frac{H}{8} = 46\,\text{MN}.$$

### 4.6.2 ULS - GEO (approach 1 combination 2 – A2+M2+R2)

In this analysis which in the progetto preliminare was called DeltaPHI, the mechanical properties of the foundation soils were reduced according to the current Italian Codes (*Norme Tecniche per le Costruzioni - Testo Unico - DM 14.01.2008)*. In this case only the live loads should be amplified. On the side of the resistance the Italian Code require that both the effective cohesion and the tangent of the friction angle of the soil should be reduced by 20%:

$$c' = \frac{c}{1{,}25}$$
$$(\tan\phi)' = \frac{\tan\phi}{1{,}25}$$

The resulting values of the reduced strength parameters for the two soil layers are reported below:

a) Coastal Plain Deposits

$$c' = \frac{c}{1{,}25} = \frac{4{,}2}{1{,}25}\,kPa = 3{,}4\,kPa$$
$$(\tan\phi)' = \frac{\tan\phi}{1{,}25} = \frac{\tan 40°}{1{,}25} = 0{,}67 \Rightarrow \phi' = 34°$$

b) Transition Layer

$$c' = \frac{c}{1{,}25} = \frac{13{,}5}{1{,}25}\,kPa = 10{,}8\,kPa$$

$$(\tan\phi)' = \frac{\tan\phi}{1{,}25} = \frac{\tan 42°}{1{,}25} = 0{,}72 \Rightarrow \phi' = 36°$$

c) Messina Gravel

$$c' = \frac{c}{1{,}25} = \frac{20{,}0}{1{,}25}\,kPa = 16{,}0\,kPa$$

$$(\tan\phi)' = \frac{\tan\phi}{1{,}25} = \frac{\tan 42°}{1{,}25} = 0{,}72 \Rightarrow \phi' = 36°$$

4) Jet grouting

$$c' = \frac{c}{1{,}25} = \frac{1560}{1{,}25}\,kPa = 1248\,kPa$$

$$(\tan\phi)' = \frac{\tan\phi}{1{,}25} = \frac{\tan 35°}{1{,}25} = 0{,}51 \Rightarrow \phi' = 29°$$

The live loads should be amplified using a factor equal to 1,3 while the dead loads should have their characteristic value.

As already mentioned, in such case the writers have not received the load combination A2 which should include the above load factors: only the load combination A1 reported in Table 10 has been provided. Conservatively the writers have decided to proceed with the analyses using the combination A1 in place of A2.

The load applied to the footings are thus the same applied in the combination called approach 1 comb. 1 (A1+M1+R1). The only difference is in the weight of the foundation which is a dead load and as such in this analysis has not been amplified.

### 4.6.3 ULS - Results of the analyses

The ULS analyses aimed to investigate the bearing capacity ULS and the ULS which could derive by excessive displacements, or better, by their consequence on the superstructure of the suspended bridge. According to this aims the analyses carried out are two. The former refers to the loading combination called A1+ M1 in the T.U. D.M. 14.01.2008 while the latter refers to the loading condition called A2+M2 in the same code. In both cases after the application of the loading condition above mentioned the analyses have been pushed further increasing the applied load while keeping constant the ratios among the various components of the load vector (i.e vertical load, horizontal load, bending moment). This means that after the steps reported in the *Table 9* further incremental steps have been added to explore the behaviour of the foundation under increasing load. The analyses have been carried out until the code Plaxis has stopped calculations having reached a *"soil body collapse".*

A first short view on the obtained results is available in Figure 13. In this figure the vertical displacement of the selected three points A, B, C (reported in Figure 12) are plotted against the applied load. The applied load is represented with the ratio between the applied load and design action according to the only available combination A1. When this ratio is equal to 1 all the design action are applied (vertical and horizontal loading, bending moments) up to the values corresponding to the combination A1. In the top part of the figure the full load-settlement relationships are represented. The maximum reached value of the load ratio ranges between 7 and 8. The reached values of the settlement are clearly very large and ranges between -1.38 and -4.76 m for the case A1+M1 and between -0.92 and -6.96 m for the case A2 +M2. The shape of the load-settlement response is not yet showing any distinct point of collapse. In the lower plot a zoom view is available for the settlement calculated up to a load ratio equal to 2.

In this zoom view the values of the settlement of the three selected points at a load ratio equal to about 1.8 are explicitly reported. This choice was made because in the Italian code the application of the loading combination A2+M2 (approach 1 combination 2) requires a further safety factor $\gamma R$ to be guaranteed which is equal to 1.8 for bearing capacity failures.

At this value of the load ratio the settlement of the three selected points ranges approximately between -0.13 m and -0.50 m. The values of the settlement are indeed rather large but a true collapse mechanism in the foundation is clearly not yet activated.

It is worthy clarifying that the apparent yielding at a load ratio equal to 1 is only due to the fact that a straight line is drawn between the origin and the point representative of the settlement under a load ratio equal to 1. As a matter of fact this settlement was obtained applying first the vertical action and later the horizontal loading and the bending moment. This load-settlement path cannot obviously be represented in such a plot.

In Figure 14 the horizontal displacement of the selected three points are plotted against the applied load. The horizontal displacement are practically coincident for all the points so a unique curve is found in the plot. The applied load is represented using the same load ratio explained before. In the top part of the figure the full load-settlement relationships are represented. The maximum reached value of the load ratio ranges between 7 and 8. The reached values of the horizontal displacement are clearly very large and ranges between 1.25 and 2.2 m for the two cases A1+M1 and A2 +M2.

The shape of the load-settlement response is not yet showing any distinct point of collapse. In the lower plot a zoom view is available for the horizontal displacement calculated up to a load ratio equal to 2.

In this zoom view the values of the horizontal displacement of the three selected points at a load ratio equal to about 1.8 are explicitly reported. This choice was made because in the Italian code the application of the loading combination A2+M2 (approach 1 combination 2) requires a further safety factor $\gamma R$ to be guaranteed which is equal to 1.8 for bearing capacity failures.

At this value of the load ratio the horizontal displacement of the three selected points is equal to 0.135 m for the combination A2+M2. The value of the displacement is rather large but a true collapse mechanism for sliding of the foundation is clearly not yet activated.

In Figure 15 the rotations towards the seashore of the rigid foundation is plotted against the applied load.

The applied load is represented using the same load ratio explained before. In the top part of the figure the full load-rotation relationship is represented. The maximum reached value of the load ratio ranges between 7 and 8. The reached values of the rotation are obviously very large ranging between 6% and 10% for the two cases A1+M1 and A2 +M2.

The shape of the load-rotation response is not yet showing any distinct point of collapse. In the lower plot a zoom view is available for the rotation calculated up to a load ratio equal to 1.8 .

At this value of the load ratio (1.8) the rotation of the footing ranges between 5‰ and 6‰ for the two load combinations while for a load ratio equal to 1 the calculated rotation of the footing is about

1.1‰. The above values of the rotations are indeed very large but a true collapse mechanism for the rotation of the foundation is clearly not yet activated even at the highest explored load levels.
In the Figure 16 and Figure 17 the vertical and horizontal displacement of the ground level (+2.5 m asl) at a load ratio equal to 1 (i.e. load combination A1+M1) are plotted by using shading coloured maps.
In the Figure 18 and Figure 19 the same displacement are plotted with reference to the plan located at -15 m asl which correspond to the bottom of the towers footing.
In the Figure 20 and Figure 21 the same displacement are plotted with reference to a vertical section passing trough the center of a footing.
In the Figure 22,Figure 23,Figure 24,Figure 25,Figure 26 and Figure 27 the same displacement mentioned above are plotted with reference to the ultimate step of the incremental loading stage.
All these figures have the only aim to show that even at very large displacement (the figures show just such displacements at different levels or in different sections) the code is capable of finding a solution to the problem of the foundation of the tower loaded by 7 to 8 times the design actions as fixed by the Italian code (NTC 2008). Furthermore an ULS in the structure caused by high displacement at the foundation level could be evaluated starting from the load-settlement relationship reported.

## 4.7 SILS - Loading condition

In this analysis the loads applied at +18 m a.s.l. are the design loads reported in Table 2. The applied moment at +5.0 m a.s.l. is:

$$M_{tot} = M + \Delta M = M + H \times \Delta h_{footing} = (23876 + 376 \times 13)\,\mathrm{MN\,m} = 28764\,\mathrm{MN\,m}.$$

The loads adopted are summarised in Table 12.

*Table 12 Loads applied at +5.0 m. SILS*

| Q (MN) | H (MN) | M (MNm) |
|---|---|---|
| 3289 | 376 | 28764 |

After all the steps uses to simulate the construction sequence in the first phase of loading, to each point-force on the footings a vertical load $Q_{node}$ is applied:

$$Q_{node} = \frac{Q}{8} = 411\,\text{MN}\,.$$

In the following loading phase horizontal loads and moments are added, both applied in the direction of the seashore.

Moments are produced applying vertical forces in the nodes, with the same magnitude and of opposite sign, generating in the center of the footings a resulting moment equal to the design value. The distance between the load-points in the z direction (orthogonal to the seashore) is 28 m. To obtain a resulting bending moment of 28764 MNm a vertical force of 257 MN has been applied, directed downward for the nodes nearest to the seashore, upward for the others (y-axes positive verse is directed upward). It results:

$$M_{tot} = 8\times\left(F\times\frac{\Delta z}{2}\right) = 8\times(257\times14)\,\text{MN m} = 28764\,\text{MN m}$$

Finally, the vertical loads applied downward on the 8 nodes are:

$$Q^{+}_{node} = Q_{node} + F = (411+257)\,\text{MN} = 668\,\text{MN} \qquad \text{(nodes near to the seashore)}$$
$$Q^{-}_{node} = Q_{node} + F = (411-257)\,\text{MN} = 154\,\text{MN} \qquad \text{(nodes far from the seashore)}$$

Furthermore, in each of the 8 nodes a horizontal load, $H_{node}$, is applied:

$$H_{node} = \frac{H}{8} = 47\,\text{MN}\,.$$

### 4.7.1 SILS - Results of the analysis

The SILS analysis aimed to evaluate the foundation displacement under a loading condition which could completely affect the functional effectiveness of the bridge as stated in the definition of such a limit state; however as stated in the tender documents under such design condition the survival of several main structural members have to be assured. The check of such a limit state is thus a structural issue which can take advantage of the calculated load-displacement response provided in this report.

A first short view on the obtained results is available in Figure 28. In this figure the vertical displacement of the selected five points A, B, C, D and E (reported in Figure 12) are plotted against the applied load. The applied load is represented with the ratio between the applied load and design action. When this ratio spans between 0 and 1 the vertical loadings are linearly applied; then, when it varies from 1 to 2, the horizontal loading and bending moments are progressively added to the vertical ones up to reach the design values. It is worthy clarifying that the apparent yielding at a load ratio equal to 1 is only due to the fact that this settlement curve was obtained applying first the vertical action and later the horizontal loading and the bending moment. The reached values of the settlement ranges between -0.136 m and -0.075 m, indicating that the tower rotate towards the seashore.

In Figure 29 the horizontal displacement of the selected five points are plotted against the applied load. The horizontal displacement are practically coincident for all the points (maximum 0.0231 m, minimum 0.0213 m). The applied load is represented using the same load ratio explained before.

In Figure 30 the rotations towards the seashore of the rather rigid foundation is plotted against the applied load. The applied load is represented using the same load ratio explained before. The reached value of the rotation is 1.1‰.

In the Figure 31 and Figure 32 the vertical and horizontal displacements of the ground level (+2.5 m asl) are plotted by using shading coloured maps.

In the Figure 33 and Figure 34 the same displacements are plotted with reference to the plan located at -15 m asl which correspond to the bottom of the towers footing.

In the Figure 35 and Figure 36 the same displacements are plotted with reference to a vertical section passing trough the center of a footing.

## 4.8 SLS2 – Loading condition

In this analysis the loads applied at +18 m a.s.l. are the design loads reported in Table 2. The applied moment at +5.0 m a.s.l. is: (correggere 11239)

$$M_{tot} = M + \Delta M = M + H \times \Delta h_{footing} = (1123 + 159 \times 13)\,\mathrm{MN\,m} = 13306\,\mathrm{MN\,m}\ .$$

The loads adopted are summarised in Table 13.

*Table 13 Loads applied at +5.0 m. SILS*

| Q (MN) | H (MN) | M (MNm) |
|---|---|---|
| **3042** | **159** | **13306** |

In the first phase, to each point-force on the footings  a vertical load $Q_{node}$ is applied:

$$Q_{node} = \frac{Q}{8} = 380\,\mathrm{MN}\,.$$

In the following loading phase horizontal loads and moments are added, both applied in the direction of the seashore. Moments are produced applying vertical forces in the nodes, with the same magnitude and of opposite sign, generating in the center of the footings a resulting moment equal to the design value. The distance between the load-points in the z direction (orthogonal to the seashore) is 28 m. To obtain a resulting bending moment of 13306 MNm a vertical force of 119 MN has been applied, directed downward for the nodes nearest to the seashore, upward for the others (y-axes positive verse is directed upward). It results:

$$M_{tot} = 8 \cdot \left( F \cdot \frac{\Delta z}{2} \right) = 8 \cdot (119 \cdot 14)\,\mathrm{MN\ m} = 13306\,\mathrm{MN\ m}$$

Finally, the vertical loads applied downward on the 8 nodes are:

$$Q^{+}{}_{node} = Q_{node} + F = (380 + 119)\,\mathrm{MN} \ = 499\,\mathrm{MN} \qquad \text{(nodes near to the seashore)}$$
$$Q^{-}{}_{node} = Q_{node} + F = (380 - 119)\,\mathrm{MN} = 261\,\mathrm{MN} \qquad \text{(nodes  far from the seashore)}$$

Furthermore, in each of the 8 nodes a horizontal load, $H_{node}$, is applied:

$$H_{node} = \frac{H}{8} = 20\,\mathrm{MN}\,.$$

### 4.8.1 SLS2 - Results of the analysis

The SLS2 analysis aimed to evaluate the foundation displacements under a loading condition which could preclude the bridge transit to street vehicles but without affecting railway functionality.

A first short view on the obtained results is available in Figure 37. In this figure the vertical displacement of the selected five points A, B, C, D and E (reported in Figure 12) are plotted against the applied load. The applied load is represented with the ratio between the applied load and design action. When this ratio spans between 0 and 1 the vertical loadings are linearly applied; then, when it varies from 1 to 2, the horizontal loading and bending moments are progressively added to the vertical ones up to reach the design values. It is worthy clarifying that the apparent yielding at a load ratio equal to 1 is only due to the fact that this settlement curve was obtained applying first the vertical action and later the horizontal loading and the bending moment. The reached values of the settlement ranges between -0.098 m and -0.072 m, indicating that the tower rotate towards the seashore.
In Figure 38 the horizontal displacement of the selected five points are plotted against the applied load. The horizontal displacement are practically coincident for all the points (maximum 0.010 m, minimum 0.009 m). The applied load is represented using the same load ratio explained before.
In Figure 39 the rotations towards the seashore of the rather rigid foundation is plotted the applied load. The applied load is represented using the same load ratio explained before. The reached value of the rotation is ~0.5‰ quite smaller than the allowable value fixed in the tender design documentation. The rotations produced by the interaction between the two footings is even smaller and is approximately ~0.1‰. This result, at least within the limits of the analysed loading combinations, support the choice of neglecting the presence of the beam connecting the two footings.
In the Figure 40 and Figure 41 the vertical and horizontal displacements of the ground level (+2.5 m asl) are plotted by using shading coloured maps.
In the Figure 34 and Figure 43 the same displacements are plotted with reference to the plan located at -15 m asl which correspond to the bottom of the towers footing.
In the Figure 44 and Figure 45 the same displacements are plotted with reference to a vertical section passing trough the center of a footing.

# 5 Bearing capacity via hand calculation

In general, bearing capacity does not control the design of large footings on granular soils. Simple hand calculations are carried out in the following to support this statement in the case of the foundations of the tower.

According to the current Italian Code (Norme Tecniche per le Costruzioni - Testo Unico - DM 14.01.2008), which introduces partial safety factors for limit state design, the designer of a shallow footing should evaluate and compare Design Actions and Design Resistances. If the design actions are lower or equal to the design resistances, footing performance is satisfactory in terms of ULS.

The new version of the code introduces two approaches while the elder version of 2005 allowed just one approach. According to the approach 1 of the latest and current version of the code two types of calculations must be carried out. In the first case, called approach 1 comb. 1 (A1+M1+R1) all applied loads are amplified while the strength parameters of the foundation soil are set to their characteristic values; in the second case (A2+M2+R2) only live loads are amplified while the characteristic values of the strength parameters of the foundation soils are reduced. In the first case the dead loads are multiplied by 1,3 while the live loads are multiplied by 1,5. In the second case the live loads only are multiplied by 1,3 and in terms of effective stress both the cohesion c' and tanφ' are divided by 1,25. The second case should be the most appropriate for ULS referred to geotechnical bearing capacity but, however, in this report both combinations of the approach 1 are verified. The new version of the code (2008) compared to the old version (2005) has also introduced the coefficients $\gamma R$ which in the short representation of the combination reported above are included in the term R1 or R2. According to the present version of the code in the approach 1 comb. 1 the coefficient $\gamma R$ is equal to 1 while in the approach 1 comb. 2 the coefficient $\gamma R$ is equal to 1,8 for the ULS known as bearing capacity, and 1,1 for ULS known as pure sliding. The coefficients $\gamma R$, as a matter of fact, represent further reduction of the calculated design resistance or, which is the same, further amplifications of the design actions.

The foundations of the towers of the bridge have a circular shape in plan and are subjected to a combination of vertical load, horizontal load and bending moment. Furthermore the ground level is inclined toward the seashore and under the sea level. All these factors have to be taken into proper account in hand calculations to check the safety against ULS.

The loads to be considered for ULS are those already given in Table 7. As reported in the report on the design of the bridge structures this loads already includes load factors. They thus correspond to the combination A1 of the Italian code while the combination A2 was not available. Conservatively both the combinations will be checked assuming A2 = A1.

The subsoil below the footing base (elevation -15 m asl) will be conservatively characterized by a friction angle $\varphi' = 36°$ and a cohesion $c' = 0$. The unit weight of the soil below the water table (which is assumed at sea level), is $\gamma_{sat} = 20$ kN/m$^3$; the submerged unit weight is $\gamma' = 10$ kN/m$^3$. The ground surface is at an elevation of +4.0 m a.s.l. and the unit weight above the water table is $\gamma = 18$ kN/m$^3$. The improvement of the soil by jet grouting below the foundation has been conservatively neglected.

The bearing capacity calculations will be carried out considering the load acting at the base of the footing (elevation -15 m asl) and characterizing the jet grouting below the foundation and all the soil layers as an homogeneous material with no cohesion and with a rather low characteristic value of the friction angle $\varphi$ compared to the values deduced by the site investigations. Furthermore the positive contribution of the diaphragm walls on the perimeter of the footing is also neglected. In the opinion of the writers such a simplified scheme is obviously conservative and make possible the adoption of the Terzaghi's theory of the bearing capacity.

To obtain the loads acting on one footing, the weight of one footing (1086 MN) must be added to the loads obtained dividing by two the loads reported in Table 7, that represent the total loads acting on the foundation of the tower.

The loads acting at the level of the foundation base for case A1M1 are summarized in Table 14. The moment was obtained transporting the horizontal load at the level of foundation base.

*Table 14 Conventional loads at the base of each footing (-15 m a.s.l.)*

| Case | Vertical Q (MN) | Horizontal H (MN) | Bending Moment M (MN m) | Eccentricity e (m) |
|---|---|---|---|---|
| A1M1 | 2713 | 185 | 17078 | 6,29 |
| A2M2 | 2441,5 | 185 | 17078 | 6,99 |

The bearing capacity of the foundation is computed using Terzaghi's expression in effective stress with appropriate correction factors to take into account the inclination of the applied load, the shape of the foundation, and the sloping ground surface. To account for the eccentricity of the load, the bearing capacity is computed for an equivalent rectangular foundation, whose width B' and length L' are such that the load is centred, as detailed in Figure 46.

$$q_{ult} = N_q \cdot [\gamma z_w + \gamma'(z - z_w)] \cdot \zeta_q \cdot \xi_q \cdot \beta_q + N_\gamma \cdot \gamma' \cdot \frac{B'}{2} \cdot \zeta_\gamma \cdot \xi_\gamma \cdot \beta_\gamma + \gamma_w (z - z_w)$$

where $z_w$ = 4 m and z = 19 m are the depths of the groundwater table and of the foundation base below ground level.

## 5.1 Case A1M1

Simple calculations yield B' = 36.58 m and L' = 46.18 m.

For $\varphi'$ = 36° the bearing capacity coefficients have the following values:

$N_q$ = 37.75
$N_\gamma$ = 43.76

the correction factors for load inclination are:

$\zeta_q = (1 - H/Q)^m = 0.896$ m = (2 + B'/L')/(1 + B'/L')
$\zeta_\gamma = (1 - H/Q)^{m+1} = 0.835$

the correction factors for foundation shape are:

$\xi_q$ = 1 + (B'/L')×tanφ' = 1.570
$\xi_\gamma$ = 1 - 0.4×(B'/L') = 0.683

the correction factors for sloping ground surface (average slope ω = 12°) are:

$\beta_q = (1 - \tan\omega)^2 = 0.62\beta_\gamma = \beta_q = 0.620$

Substituting into Terzaghi's formula:

$q_{ult}$ = 7334 + 2831 +150 = 10315 kPa

According to the current Italian Code, the design bearing capacity, $q_{ult}$ must not be smaller than the applied design actions $q_{app}$ obtained dividing the vertical load by the area of the equivalent foundation, A = B'×L' = 1689.48m$^2$

$q_{app}$ = Q/A = 1606 kPa.

It is obvious that the requirements of design approach A1M1 are amply met.

## 5.2 Case A2M2

Simple calculations yield B' = 35.28 m and L' = 45.76 m

For $\varphi'_{des} = \tan^{-1}[(\tan\varphi')/1.25]$ = 30.2°, the bearing capacity coefficients have the following values:

$N_q$ = 19.00
$N_\gamma$ = 16.57

the correction factors for load inclination are:

$\zeta_q = (1 - H/Q)^m = 0.884$ m = (2 + B'/L')/(1 + B'/L')
$\zeta_\gamma = (1 - H/Q)^{m+1} = 0.817$

the correction factors for foundation shape are:

$\xi_q$ = 1 + (B'/L')×tanφ' = 1.448
$\xi_\gamma$ = 1 - 0.4×(B'/L') = 0.692the correction factors for sloping ground surface (average slope ω = 12°) are:

$\beta_q = (1 - \tan\omega)^2 = 0.62\beta_\gamma = \beta_q /\cos\omega = 0.620$

Substituting into Terzaghi's formula:

$q_{ult}$ = 3350+ 1024 + 150 = 4524 kPa

According to the current Italian Code, the design bearing capacity, $q_{ult}$ must not be smaller than the 1.8 times the applied design actions $q_{app}$ obtained dividing the vertical load by the area of the equivalent foundation, A = B'×L' = 1614.78 $m^2$

$q_{app}$ = Q/A = 1511.98 kPa.

The ratio between the design bearing capacity and the applied design action is 2.99 which is higher than 1.8.

It is obvious that also the requirements of design approach A2M2 are amply met.

# 6 Load update from IBDAS new model

Recently new load combinations on the tower foundations corresponding to the A2 set (for ULS) as defined by NTC 2008 have been provided. Furthermore also new load combinations referring to SILS, SLS2 and SLS1 have been provided all coming from new IBDAS model.

The load combinations have been extracted by datasheets where load vectors made by six components (3 forces and 3 moments) were provided at the elevation of -15 m asl (corresponding to the footings basement) and separately for the two legs of the tower (y=+39.225 m and y=-39.225m). It is also worthy mentioning that separate load combinations for static and seismic conditions were provided by the global IBDAS model, the seismic ones being the result of a spectral analysis.

It is worthy to keep in mind that every previous stage of the design of the foundations of the bridge over Messina strait until now has been always characterized by a unique load combination obtained by the simple summation of the load combinations on the two separate legs of the towers. The resultant forces at +18 m asl reported in the table from 1 to 3 show such combinations which were always shared exactly between the two legs of the tower in each analyses previously shown.

The writers have faced the new complex problem following these steps:

i) all the combinations provided for each individual leg of the towers have been applied on the foundation and via hand calculations the value of the coefficient $\gamma R$ (defined as the ratio between the design action and the design resistance) has been calculated;

ii) such step for ULS combinations has been used to estimate the safety margins against bearing capacity failure (being now A2 available only the geotechnical combination A2+M2+R2 of the approach 1 of the NTC 2008 has been considered);

iii) this hand calculations have been used to select among all the provided SLS and SILS load combinations only the worst ones; such combinations have been used in FEM 3D model in order to calculate load-displacement response of each leg of the footings.

More precisely for every limit state both the combinations coming out either with the lowest $\gamma R$ or with the maximum value of the vertical force have been considered. In the subgroup made only by static combinations the two criteria select the same load combinations while for the seismic subgroup the two criteria provide two different load combinations. Attention has been paid in such a case to both criteria and the calculations via FEM 3D model have been carried out on all these selected combinations.
About the step ii) all calculations have been carried out according to the procedure described in the section 5 using $\varphi' = 40°$ and $c' = 0$.

The hand calculations on the worst static ULS gave a minimum value of $\gamma R$ on the single footing equal to 6.2. This value is largely compatible with the value of 1.8 required the NTC 2008. The same calculations applied to the worst seismic ULS combinations gave a minimum value of $\gamma R$ on the single footing about 1.4. This value is lower than the value of 1.8 required by the NTC 2008. On this number two main comments are opportune. First of all if we take into account that according to the new Italian code the tan $\varphi$ has been divided by 1.25 it must be underlined that in this case the overall safety factor is about 3.3, larger than 3, which was the minimum overall safety factor required by the old Italian geotechnical code. Furthermore the hand made calculations of bearing capacity are affected by a number of conservative assumptions:

a) for instance the calculations have been carried out in the hypothesis that the plane with the maximum slope of the ground surface is the same of the plane which contains the maximum shear and the maximum bending moments; this is not true and it is also largely conservative but hand calculations cannot be done under different hypotheses;

b) no depth factor has been taken into account;

c) one of the most conservative proposal for the value of the coefficient $N\gamma$ has been taken among many authoritative suggestions presented in literature.

For all these reasons and without wanting to push the use of the simple bearing capacity formula beyond its limits the worst ULS combinations were also analysed via 3D FEM model reaching a maximum value of the applied loadings of at least 2 times the design action without showing any distinct collapse. In other words the FEM calculations allowed to estimate a value of $\gamma R$ not less than 2, thus compatible with the minimum values required by the NTC 2008. Some details of these calculations are briefly shown in the following.

In Figure 47 the load-settlement response for both ULS worst static and seismic combinations as deduced via FEM 3D model are plotted. In Figure 48 the load-displacement response in the horizontal direction (towards the seashore) for both ULS worst static and seismic combinations as deduced via FEM 3D model are plotted. The maximum value of the vertical settlement and of the horizontal displacement under actions which represent two times the design actions are summarized in Table 15 for ten points of the two foundations (see Figure 12). In Table 16 the ULS worst load combinations as selected by the output of the global IBDAS model are reported for completeness. It must be noted that the label of the reference axes in the IBDAS model are different from the labels adopted in the FEM 3D model of the foundation.
Both the settlement and horizontal displacement towards the seashore reported in table 15, calculated under loading conditions that according to the NTC 2008 should be considered as failure loads, show that, even in this extreme scenario, the behaviour of the foundation is rather satisfactory and rather small differential settlement arises between the two legs of the Sicilia tower.

*Table 15 Values of the settlement and of the horizontal displacement under two times the design actions (ULS, STATIC AND SEISMIC)*

| | A | B | C | D | E | F | G | H | I | J |
|---|---|---|---|---|---|---|---|---|---|---|
| | uy [m] | uy [m] | uy [m] | uy [m] | uy [m] | uy [m] | uy [m] | uy [m] | uy [m] | uy [m] |
| ULS_STATIC | -0.432 | -0.453 | -0.469 | -0.489 | -0.427 | -0.639 | -0.658 | -0.667 | -0.743 | -0.581 |
| ULS_SEISMIC | -1.058 | -1.079 | -1.090 | -1.118 | -1.057 | -1.237 | -1.256 | -1.261 | -1.335 | -1.192 |
| | uz [m] | uz [m] | uz [m] | uz [m] | uz [m] | uz [m] | uz [m] | uz [m] | uz [m] | uz [m] |
| ULS_STATIC | 0.008 | 0.009 | 0.011 | 0.009 | 0.009 | 0.006 | 0.008 | 0.010 | 0.008 | 0.007 |
| ULS_SEISMIC | 0.002 | 0.004 | 0.007 | 0.003 | 0.005 | -0.002 | 0.001 | 0.005 | 0.001 | 0.001 |

*Table 16 Worst ULS selected combinations under static and seismic conditions.*

Sicilia FOUNDATION – IBDAS GLOBAL MODEL RESULTS –

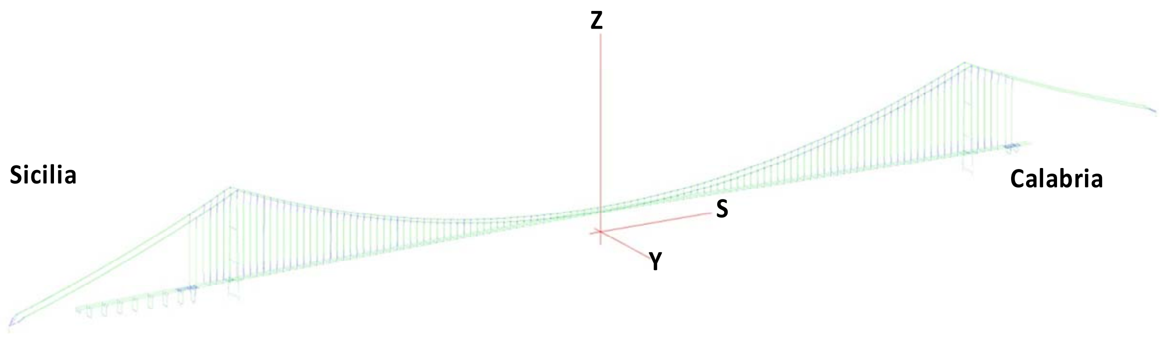


| | s[m] | y[m] | z[m] | Ps[MN] | Py[MN] | Pz[MN] | Ms[MNm] | My[MNm] | Mz[MNm] |
|---|---|---|---|---|---|---|---|---|---|
| ULS_STATIC | -1650 | -39.225 | -15 | -11 | -4 | -3276 | 5730 | -1138 | 167 |
| ULS_STATIC | -1650 | 39.225 | -15 | -12 | -81 | -2733 | 2864 | -1323 | -87 |
| ULS_SEISMIC | -1650 | -39.225 | -15 | -44 | -112 | -4680 | 5003 | -1095 | 97 |
| ULS_SEISMIC | -1650 | 39.225 | -15 | -42 | -195 | -4248 | 1717 | -1039 | -135 |

The step iii) is related to the displacement of the foundation under different limit state. SLS 2 and SILS static conditions are here considered. As stated before the worst combinations have been selected on the basis of the minimum safety factor. For static conditions this criterium lead to the selection of the load combination with the maximum applied vertical load.

In Table 17 the selected load combination as obtained by the output of the global IBDAS model are reported.

*Table 17* SLS2 and SILS worst load combination extracted by IBDAS GLOBAL MODEL OUTPUT

SICILIA FOUNDATION – IBDAS GLOBAL MODEL RESULTS –

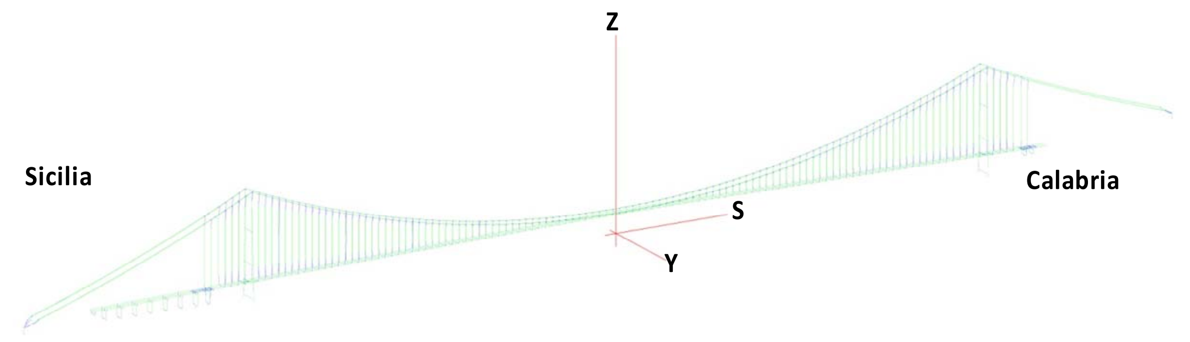


| | s[m] | y[m] | z[m] | Ps[MN] | Py[MN] | Pz[MN] | Ms[MNm] | My[MNm] | Mz[MNm] |
|---|---|---|---|---|---|---|---|---|---|
| SLS2_STATIC | -1650 | -39.225 | -15 | -9 | 3 | -3141 | 4699 | -1402 | 166 |
| SLS2_STATIC | -1650 | 39.225 | -15 | -9 | -71 | -2713 | 2058 | -1563 | -96 |
| SILS_STATIC | -1650 | -39.225 | -15 | -15 | -1 | -4564 | 12930 | -1886 | 151 |
| SILS_STATIC | -1650 | 39.225 | -15 | -15 | -95 | -2908 | 9086 | -2001 | -100 |

Both the combinations where used in the 3D FEM model in order to calculate load displacement behaviour of both the legs of the Sicilia tower.

In Figure 49 the load – settlement curves and the curves for load-horizontal displacements towards the seashore are plotted for the 5 selected points for each leg of the Sicily tower.

In Figure 50 the curves for load-horizontal displacements parallel to the seashore for the same overall 10 points and the rotations towards the seashore for the two legs are plotted.

The performance of the foundations under this loading condition is rather satisfactory: the maximum values of all the plotted movements are summarized in the Table 18. In the same table also the maximum calculated values for the same components of the movements of the foundations under the SILS worst static loading condition are reported. For this latter condition the movements are generally larger than those obtained under SLS2 loading condition but they can be still considered as rather small and acceptable.

*Table 18* Displacements of ten selected points on both legs of the foundation of Sicilia Tower under SLS2 and SILS static worst conditions.

| | **A** | **B** | **C** | **D** | **E** | **F** | **G** | **H** | **I** | **J** |
|---|---|---|---|---|---|---|---|---|---|---|
| **SLS2_Static** | **uy [m]** | **uy [m]** | **uy [m]** | **uy [m]** | **uy [m]** | **uy [m]** | **uy [m]** | **uy [m]** | **uy [m]** | **uy [m]** |
| | -0.069 | -0.071 | -0.073 | -0.068 | -0.075 | -0.099 | -0.101 | -0.102 | -0.108 | -0.094 |
| | **ux [m]** | **ux [m]** | **ux [m]** | **ux [m]** | **ux [m]** | **ux [m]** | **ux [m]** | **ux [m]** | **ux [m]** | **ux [m]** |
| | 0.002 | 0.002 | 0.002 | 0.002 | 0.002 | -0.002 | -0.002 | -0.002 | -0.002 | -0.002 |
| | **uz [m]** | **uz [m]** | **uz [m]** | **uz [m]** | **uz [m]** | **uz [m]** | **uz [m]** | **uz [m]** | **uz [m]** | **uz [m]** |
| | 0.002 | 0.002 | 0.002 | 0.002 | 0.002 | 0.002 | 0.002 | 0.002 | 0.002 | 0.002 |
| **SILS_Static** | **uy [m]** | **uy [m]** | **uy [m]** | **uy [m]** | **uy [m]** | **uy [m]** | **uy [m]** | **uy [m]** | **uy [m]** | **uy [m]** |
| | -0.089 | -0.092 | -0.095 | -0.091 | -0.093 | -0.241 | -0.244 | -0.246 | -0.262 | -0.227 |
| | **ux [m]** | **ux [m]** | **ux [m]** | **ux [m]** | **ux [m]** | **ux [m]** | **ux [m]** | **ux [m]** | **ux [m]** | **ux [m]** |
| | -0.002 | -0.002 | -0.002 | -0.002 | -0.002 | -0.007 | -0.007 | -0.007 | -0.007 | -0.007 |
| | **uz [m]** | **uz [m]** | **uz [m]** | **uz [m]** | **uz [m]** | **uz [m]** | **uz [m]** | **uz [m]** | **uz [m]** | **uz [m]** |
| | 0.002 | 0.002 | 0.002 | 0.002 | 0.002 | 0.003 | 0.003 | 0.003 | 0.003 | 0.003 |

In Table 19 all the loading combinations selected by the output of the global IBDAS model are summarized. They are both static and seismic and refer to different limit state: ULS, SLS2 and SILS. As stated before in the seismic subgroup the two adopted criteria to select the worst combinations provided two different loading combinations while in the static subgroup the two criteria provided the same loading combinations. That is why in the Table 19 a total of 9 loading combinations are reported. For each loading combination the two separate vectors of the loading on the two legs of the tower are reported.

In the Table 20 the average displacement computed for the two separate legs of the foundation of the Sicilia tower and the rigid rotation of the base are reported for all the loading conditions reported in the Table 19. The most significant results have already been described and discussed in the previous lines of this paragraph. In the following some general comments will be made:

- the maximum computed settlement is about 45 cm and refers to a SILS seismic combination while the maximum rotation towards the seashore is about 0.17 (%) and derives from ULS seismic combination; under static loading combinations this values are significantly lower being the maximum settlement about 24 cm and the maximum rotation towards the seashore about 0.01 (%). In the writers' opinion movements computed with a static approach taking into account seismic forces should be considered as extremely exaggerated and almost neglected if, as in this case, proper dynamic analyses of the soil-structure interaction have been carried out and reported elsewhere.
- the maximum rotation of the two legs towards each other (rotation parallel to the seashore) is about 0.06 (%) and the value occurs under a SILS loading combination; under SLS2 loading conditions the maximum rotation is significantly lower reaching the value of about 0.025 (%);
- the maximum horizontal displacement towards the seashore is about 3.1 cm and refers to SILS seismic combination; the maximum horizontal displacement referred to only static combination is less than 1 cm.

*Table 19* Worst loading combinations selected by the output of the IBDAS model

| SICILIA FOUNDATION - IBDAS RESULTS | | | | | | | | | | |
|---|---|---|---|---|---|---|---|---|---|---|
| | | s[m] | y[m] | z[m] | Ps[MN] | Py[MN] | Pz[MN] | Ms[MNm] | My[MNm] | Mz[MNm] |
| seismic | SILS | -1650 | -39.225 | -15 | -51 | -115 | -6077 | 11530 | -1835 | 71 |
| | SILS | -1650 | 39.225 | -15 | -48 | -215 | -4617 | 7256 | -1679 | -155 |
| | SILS | -1650 | -39.225 | -15 | -1226 | -38 | -2513 | 431 | -31223 | -970 |
| | SILS | -1650 | 39.225 | -15 | -1186 | -98 | -2627 | -1224 | -30253 | -74 |
| | ULS | -1650 | -39.225 | -15 | -44 | -112 | -4680 | 5003 | -1095 | 97 |
| | ULS | -1650 | 39.225 | -15 | -42 | -195 | -4248 | 1717 | -1039 | -135 |
| | ULS | -1650 | -39.225 | -15 | -1111 | -28 | -2674 | 1412 | -29515 | -940 |

| | | | | | | | | | | |
|---|---|---|---|---|---|---|---|---|---|---|
| | ULS | -1650 | 39.225 | -15 | -1077 | -90 | -2621 | -334 | -28145 | -162 |
| | SLS2 | -1650 | -39.225 | -15 | -24 | -33 | -3692 | 2976 | -1405 | 131 |
| | SLS2 | -1650 | 39.225 | -15 | -23 | -108 | -3485 | 220 | -1442 | -122 |
| | SLS2 | -1650 | -39.225 | -15 | -658 | 2 | -2835 | 1209 | -11698 | -404 |
| | SLS2 | -1650 | 39.225 | -15 | -641 | -66 | -2836 | -1027 | -11256 | -62 |
| static | SILS | -1650 | -39.225 | -15 | -15 | -1 | -4564 | 12930 | -1886 | 151 |
| | SILS | -1650 | 39.225 | -15 | -15 | -95 | -2908 | 9086 | -2001 | -100 |
| | ULS | -1650 | -39.225 | -15 | -11 | -4 | -3276 | 5730 | -1138 | 167 |
| | ULS | -1650 | 39.225 | -15 | -12 | -81 | -2733 | 2864 | -1323 | -87 |
| | SLS2 | -1650 | -39.225 | -15 | -9 | 3 | -3141 | 4699 | -1402 | 166 |
| | SLS2 | -1650 | 39.225 | -15 | -9 | -71 | -2713 | 2058 | -1563 | -96 |

*Table 20* Computed displacements and rotations of the two legs of the foundation of Sicilia tower.

| | | Leg location | Horizontal displacement parallel to the seashore | Vertical displacement | Horizontal displacement towards the seashore | Rotation towards the seashore | Rotation parallel to the seashore |
|---|---|---|---|---|---|---|---|
| | | | uy [m] | uz [m] | us [m] | Ry (%) | Rs (%) |
| Seismic | SILS_maxPz | (y+) | 0.006 | -0.257 | 0.002 | -0.0084 | 0.0179 |
| | | (y-) | -0.003 | -0.450 | 0.003 | -0.0023 | 0.0490 |
| | SILS_mingr | (y+) | 0.006 | -0.092 | -0.027 | -0.1161 | 0.0202 |
| | | (y-) | 0.001 | -0.085 | -0.028 | -0.1162 | 0.0111 |
| | ULS_maxPz | (y+) | 0.007 | -0.254 | 0.002 | -0.0070 | 0.0203 |
| | | (y-) | 0.005 | -0.331 | -0.001 | 0.0090 | 0.0141 |
| | ULS_mingr | (y+) | 0.006 | -0.102 | -0.030 | -0.1660 | 0.0156 |
| | | (y-) | 0.000 | -0.108 | -0.031 | -0.1769 | 0.0159 |
| | SLS2_maxPz | (y+) | 0.004 | -0.129 | 0.002 | -0.0076 | 0.0224 |
| | | (y-) | 0.000 | -0.147 | 0.002 | -0.0045 | 0.0235 |
| | SLS2_mingr | (y+) | 0.003 | -0.085 | -0.014 | -0.0263 | 0.0200 |

| | | | | | | | |
|---|---|---|---|---|---|---|---|
| | | (y-) | -0.001 | -0.085 | -0.014 | -0.0260 | 0.0171 |
| Static | SILS | (y+) | -0.002 | -0.092 | 0.002 | -0.0105 | 0.0030 |
| | | (y-) | -0.007 | -0.244 | 0.003 | -0.0076 | 0.0630 |
| | ULS | (y+) | 0.001 | -0.080 | 0.002 | -0.0084 | 0.0067 |
| | | (y-) | -0.003 | -0.127 | 0.002 | -0.0066 | 0.0378 |
| | SLS2 | (y+) | 0.002 | -0.071 | 0.002 | -0.0070 | 0.0139 |
| | | (y-) | -0.002 | -0.101 | 0.002 | -0.0048 | 0.0252 |

In Figure 51 a partial view of the new ULS load combinations provided by the updated IBDAS model is plotted. Vertical load Pv and total shear load Ph (obtained combining Ps and Py) are reported. On the right side where only seismic combinations are plotted the square marks represent the old ULS loading combinations. In Figure 52 another partial view of the new ULS load combinations provided by the updated IBDAS model is plotted. The figure refers to bending moments in the two orthogonal vertical planes. Again the square marks represent the old ULS loading combinations.

To make the comparison the old ULS loading conditions have been transported down to the elevation of -15 asl and divided by the two footings.

From both figures it can be appreciated that in both cases the new loads are sometimes larger than the old ones.

In Figure 53 the values of $\gamma$R obtained by bearing capacity hand made calculations are plotted against the main sets of loading (Pv, Ph, My). In the same figure the square marks represent the results obtained in the section 5 of the report with the old ULS loading combinations. From the figure it can be appreciated that the situation after the updated loads is a bit changed. However as stated before the bearing capacity calculations are still fully satisfactory. The ULS cases analysed with the FEM 3D model are all the circular full marks included in a circular empty mark.

In Figure 54 the settlement ($u_z$), the horizontal total displacement ($u_h$), the separate horizontal displacements ($u_s$ and $u_y$) and the rotation ($r_y$ and $r_s$) obtained by FEM 3D calculations for SILS and SLS2 worst loading conditions are plotted. For comparison in the same plot the bold marks are used to represent the results obtained by old SILS AND SLS2 loading conditions. The figure reports separately the static loading combinations and the seismic ones.

It can be appreciated that with some new seismic loading combinations a bit larger displacement arise. As already stated before the writers opinion is that the main objective of this report and of the included calculations was to verify the foundation of the Sicilia tower under ULS loading. The displacement of the foundation under static SILS and SLS2 loadings are still to be considered as a reliable output of the report while for seismic loading combinations the analyses provided by this report may lead to a significant overestimation of the displacement. More reliable fully dynamic analyses of soil-structure interaction have been carried out in this design stage of the bridge over Messina strait and their results are reported elsewhere.

As a concluding remark it is worth mentioning that values of tower rotation slightly higher than the allowable threshold value of 0.1% were obtained for three seismic loading conditions related to the Structural Integrity Limit States (SILS) (Figure 54). These results were given for completeness, but it is to be recalled that evaluation of displacements and rotations using pseudo-static loading combinations may result unrealistic and excessively conservative. For the Serviceability Limit States (SLS), no loading combination induce rotation in excess to the specified threshold value.

For the evaluation of the maximum rotation induced in the tower by seismic loading conditions, reference can be made to the dynamic interaction analyses that were carried in the time domain, applying real acceleration time histories to an analysis domain in which the tower foundation, the terminal structures and the anchor block were included. These analyses, presented in the report CG1000-P-CL-D-P-SB-A2-00-00-00-00-A_01_Seism_An_ANX, provided, for Sicily tower, maximum values of rotation lower than 0.035 %.

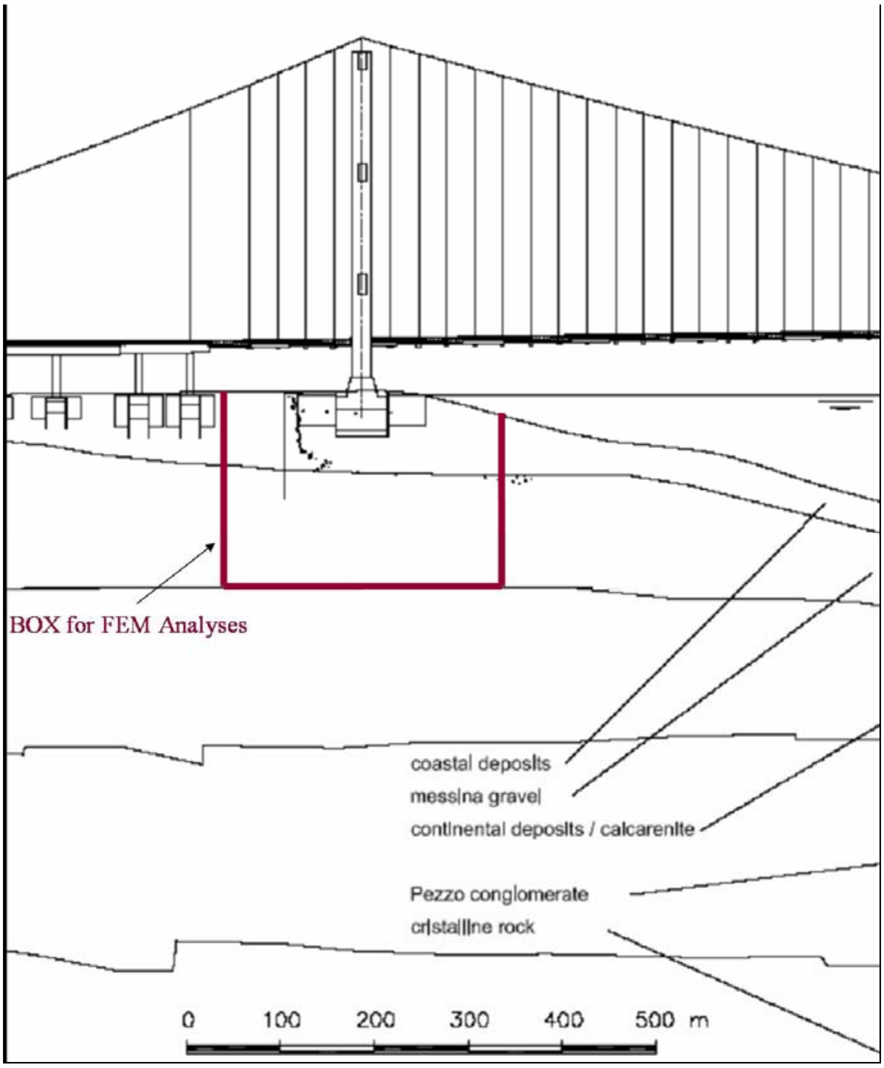


*Figure 1 Soil profile on Sicilian shore of Messina Strait*

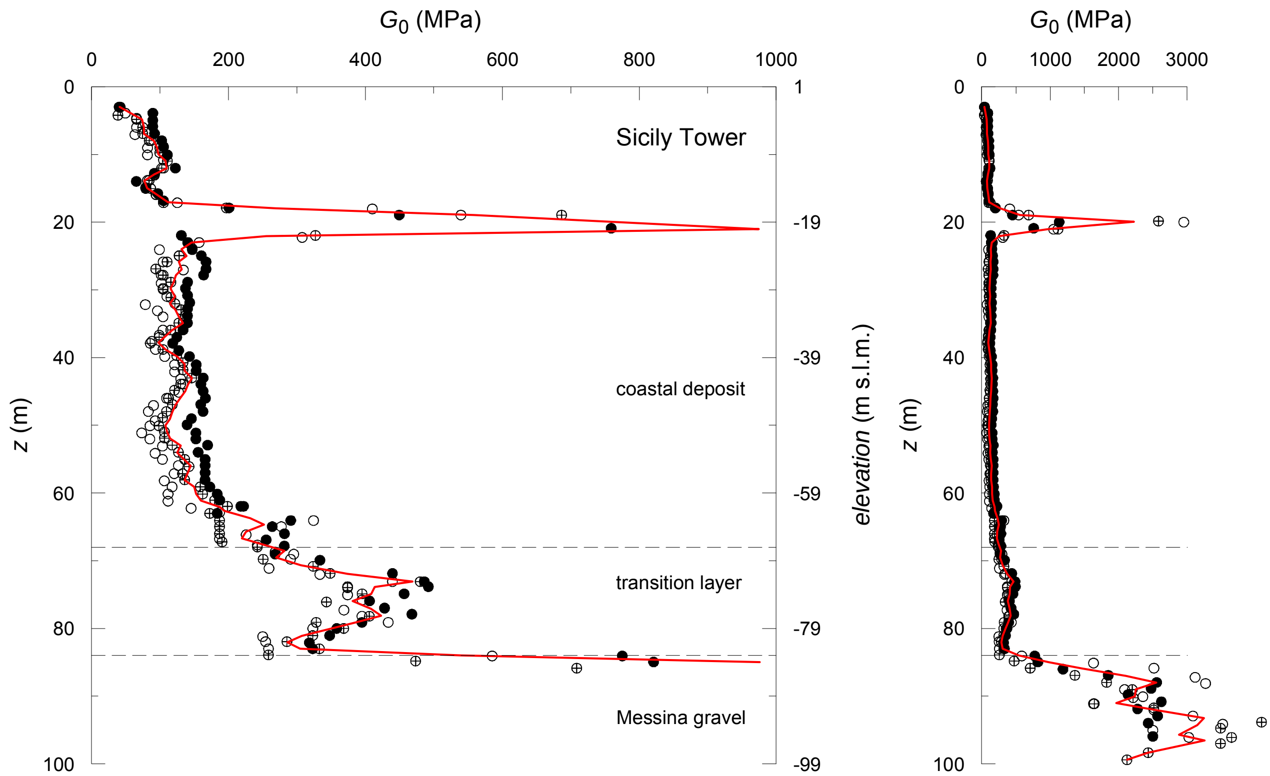


*Figure 2 $G_0$ profile from cross-hole test*

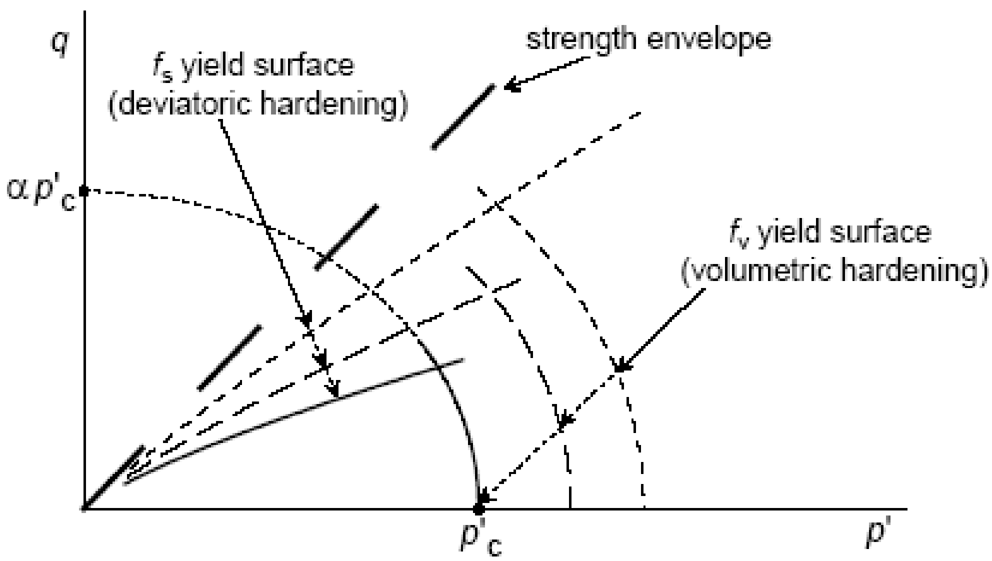


*Figure 3 Yield surfaces of the Hardening Soil model and their evolution*

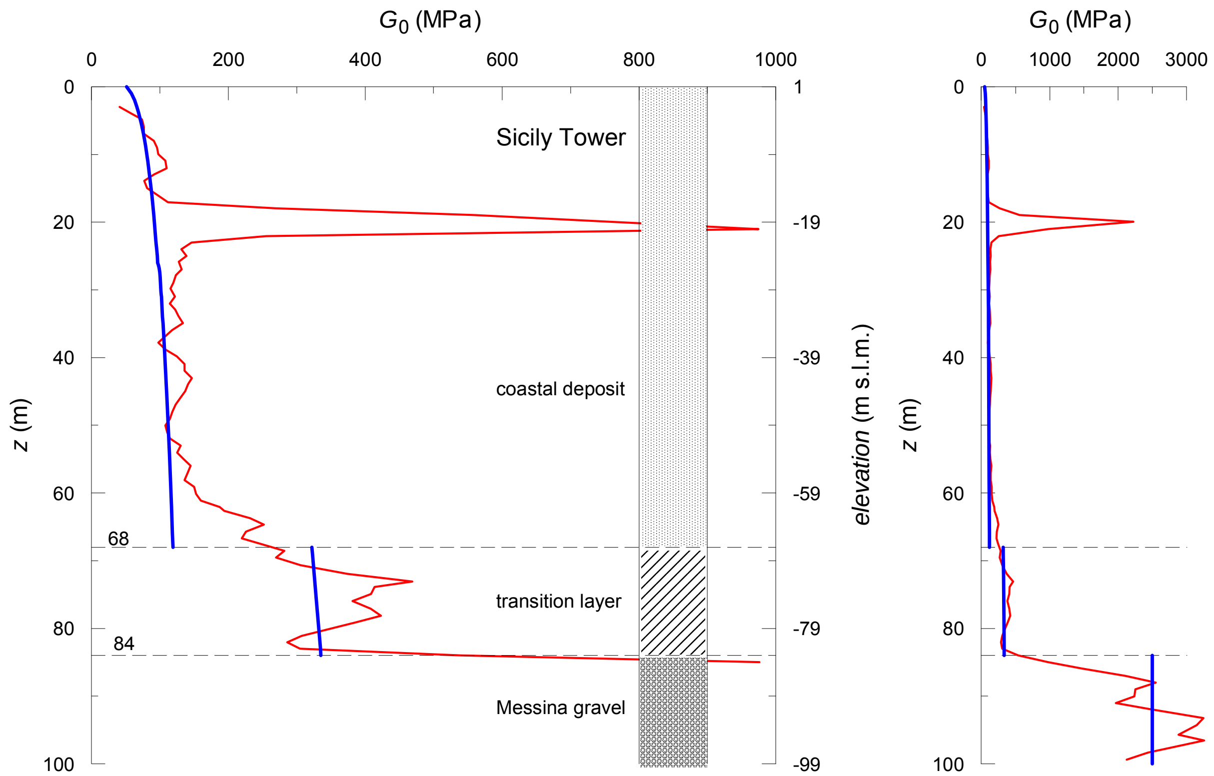


*Figure 4 $G_0$ profile for Plaxis analyses*

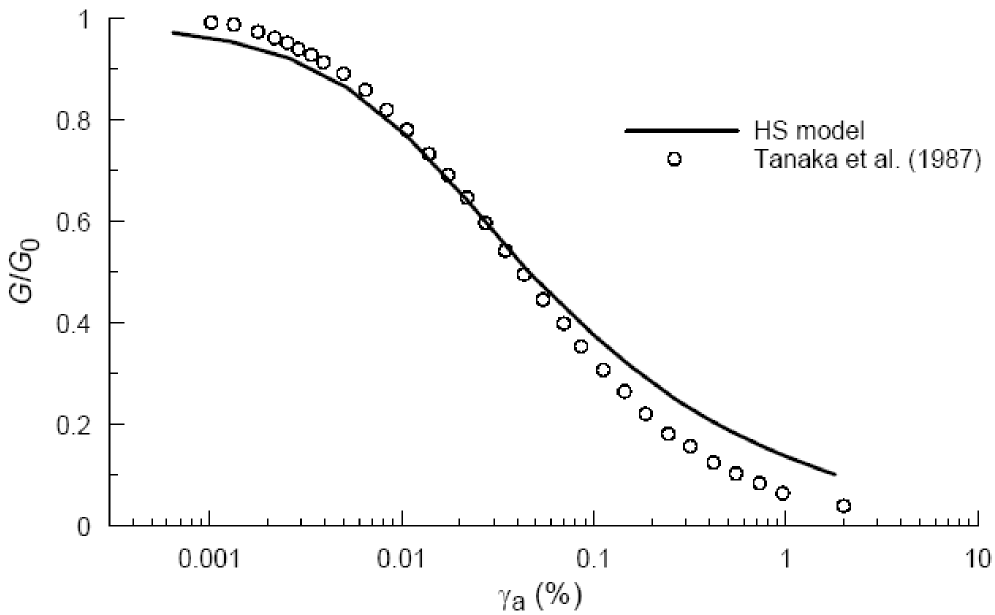


*Figure 5 Comparison between the modulus decay curve predicted by the HS model and that obtained by Tanaka et al (1987)*

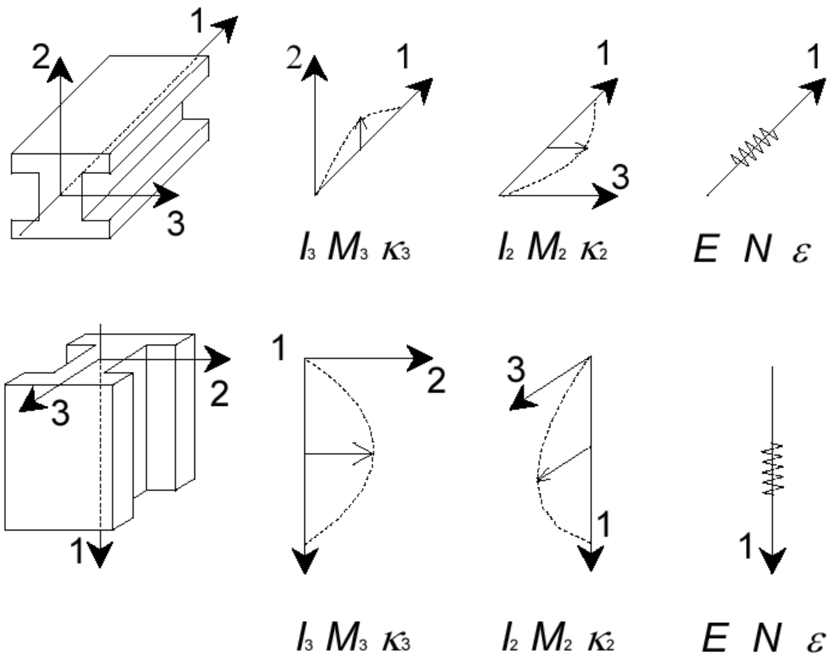


*Figure 6 WALL elements in PLAXIS*

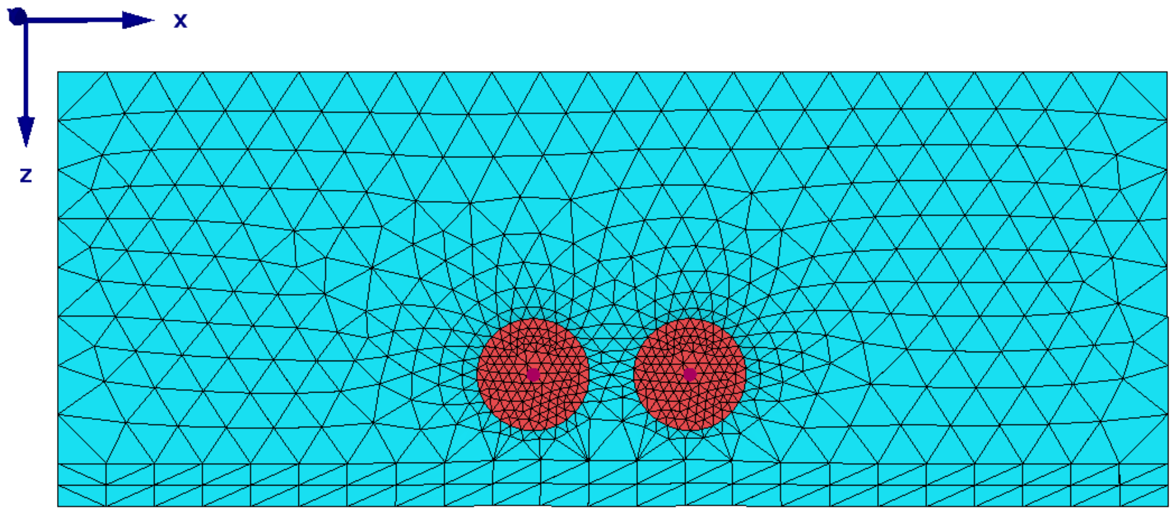


*Figure 7 Plan view of model mesh*

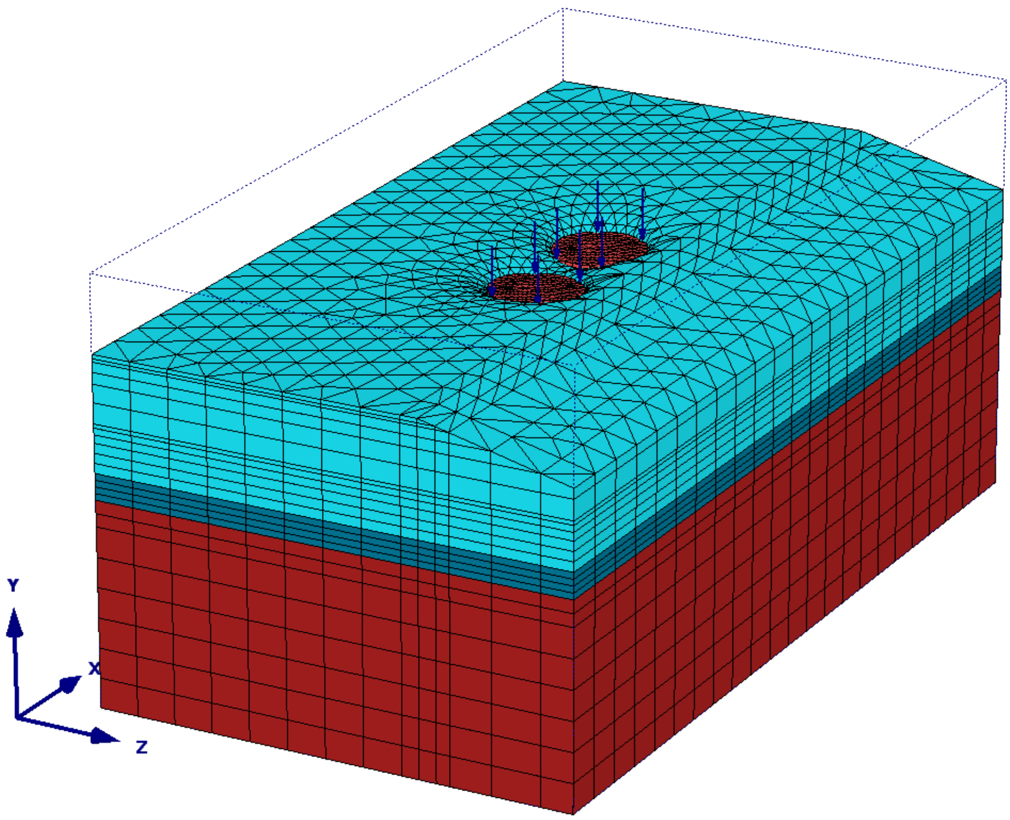


*Figure 8 3D FEM model mesh*

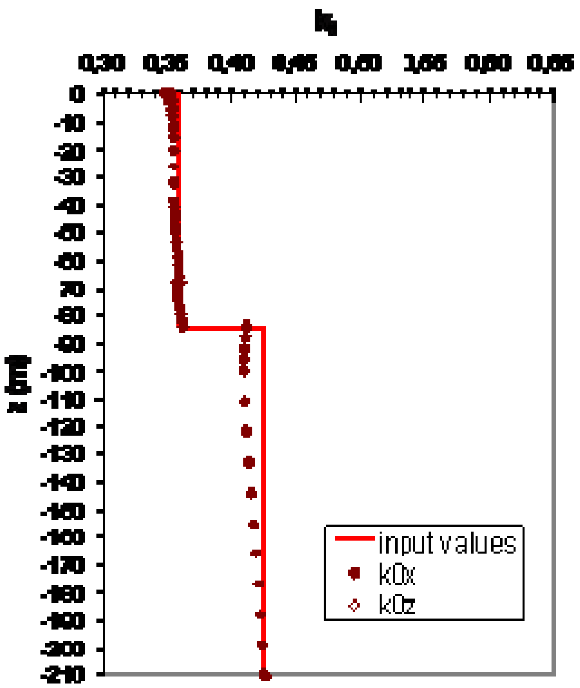


*Figure 9 $k_0$ profile after calculation step 1*

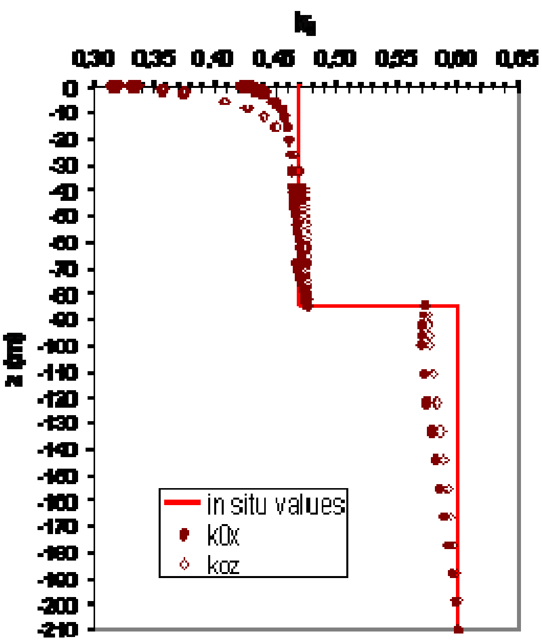


*Figure 10 $k_0$ profile after calculation step 2*

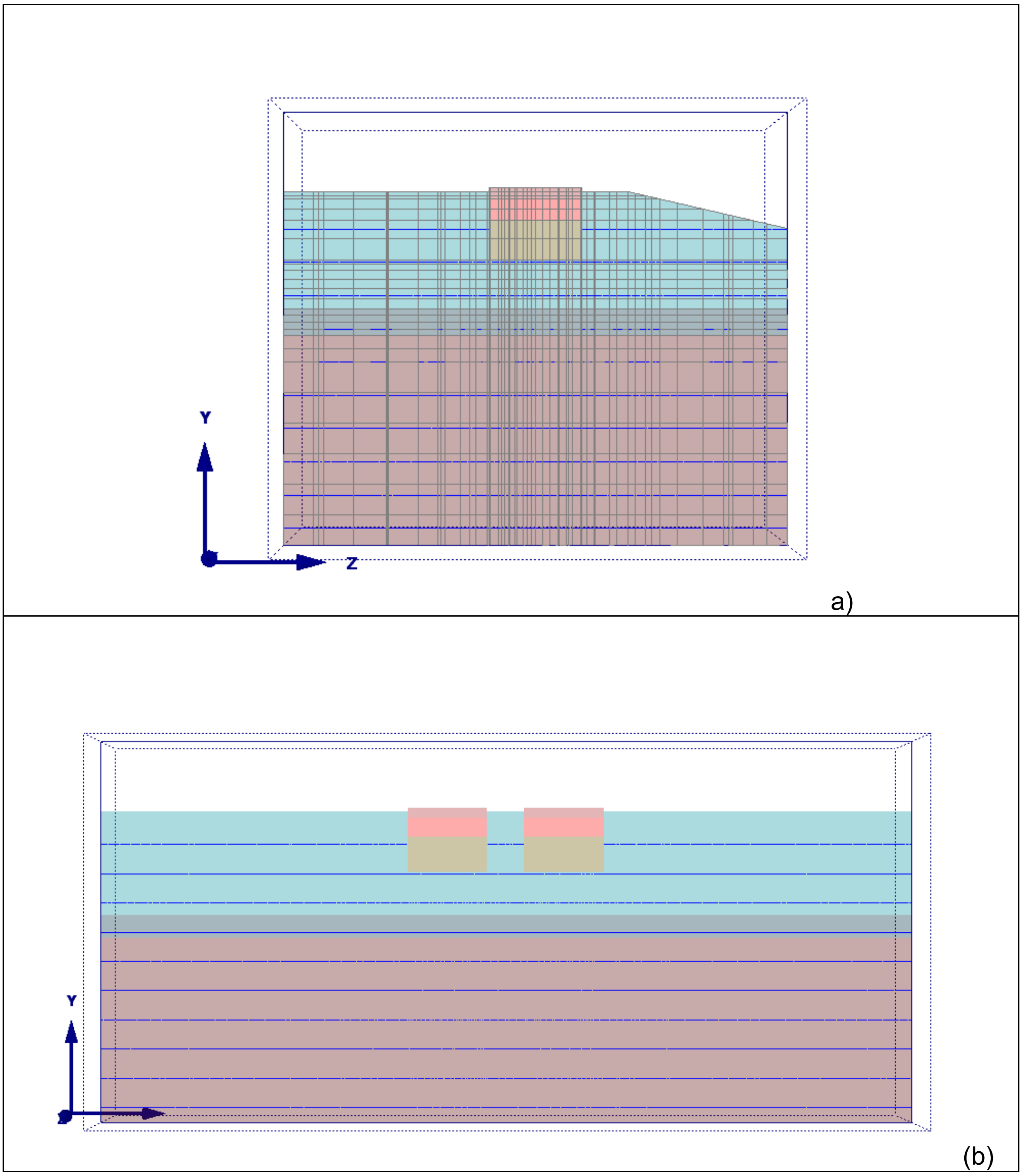


*Figure 11 Sections of the mesh (jet grouting in grey): (a) orthogonal and (b) parallel to the sea*

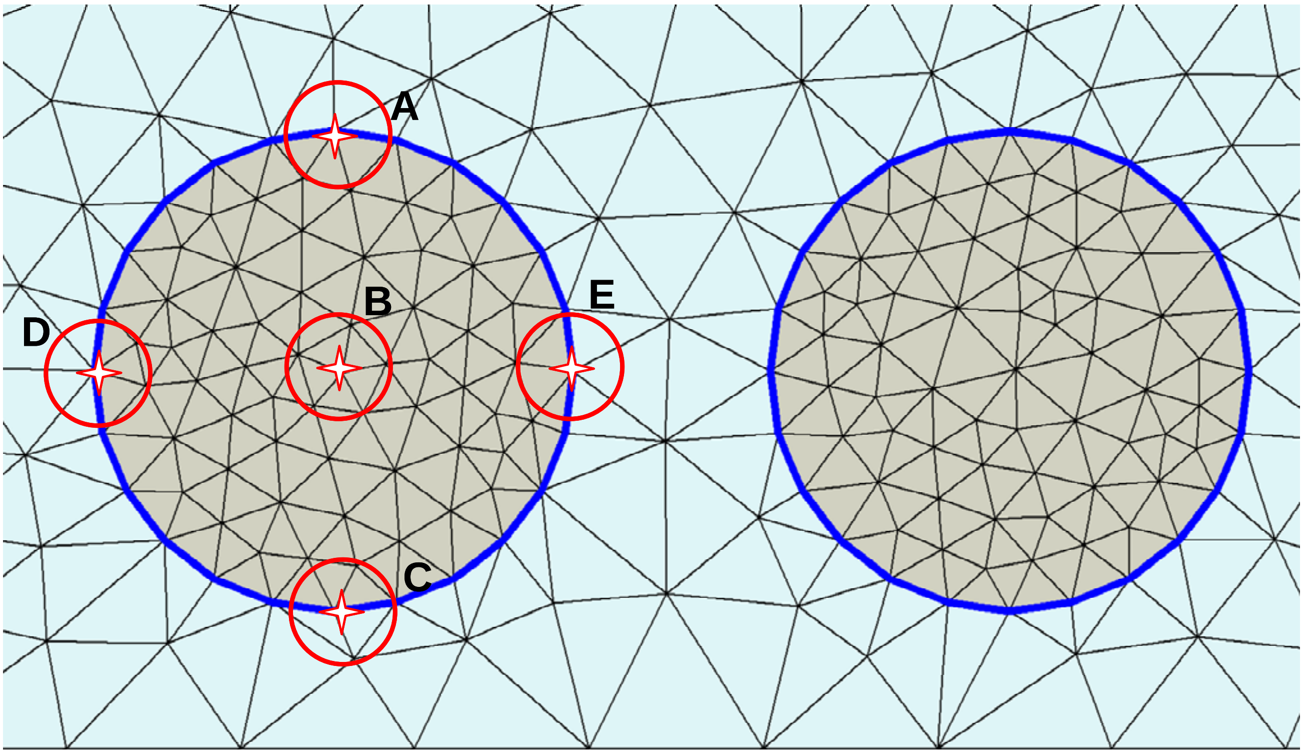


*Figure 12 Location of points at elevation -15,0 m (point C is the nearest to the seashore)*

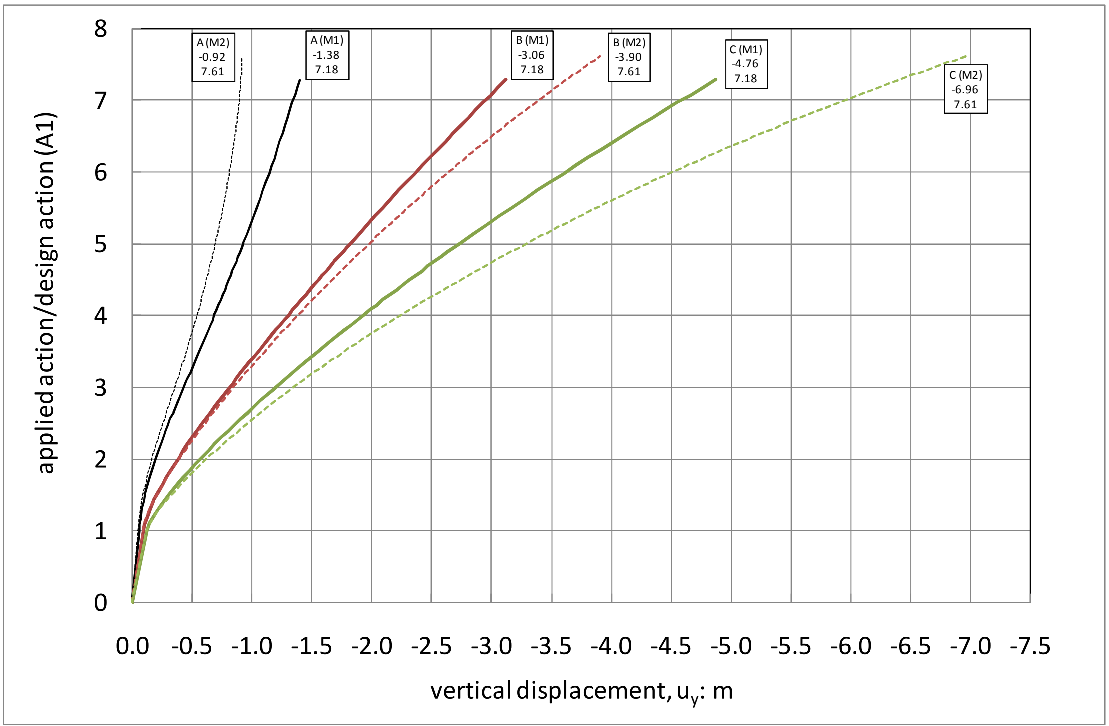


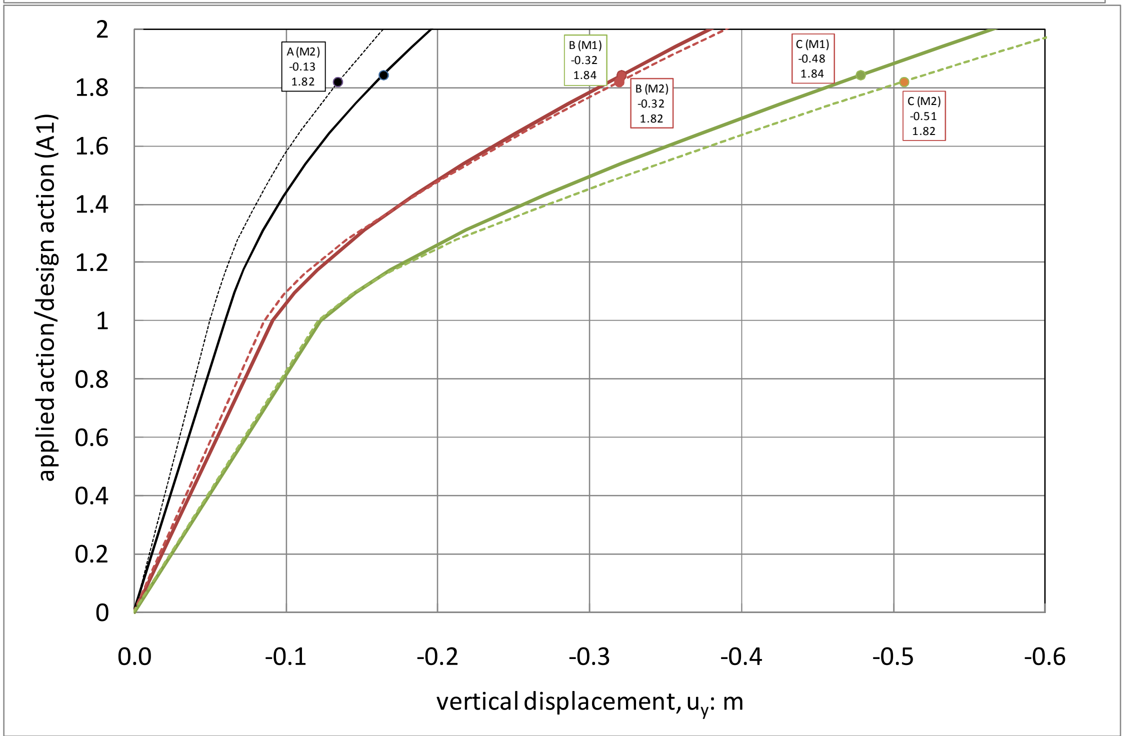


*Figure 13 ULS: Load settlement curves for three points at elevation –15,0 m.*

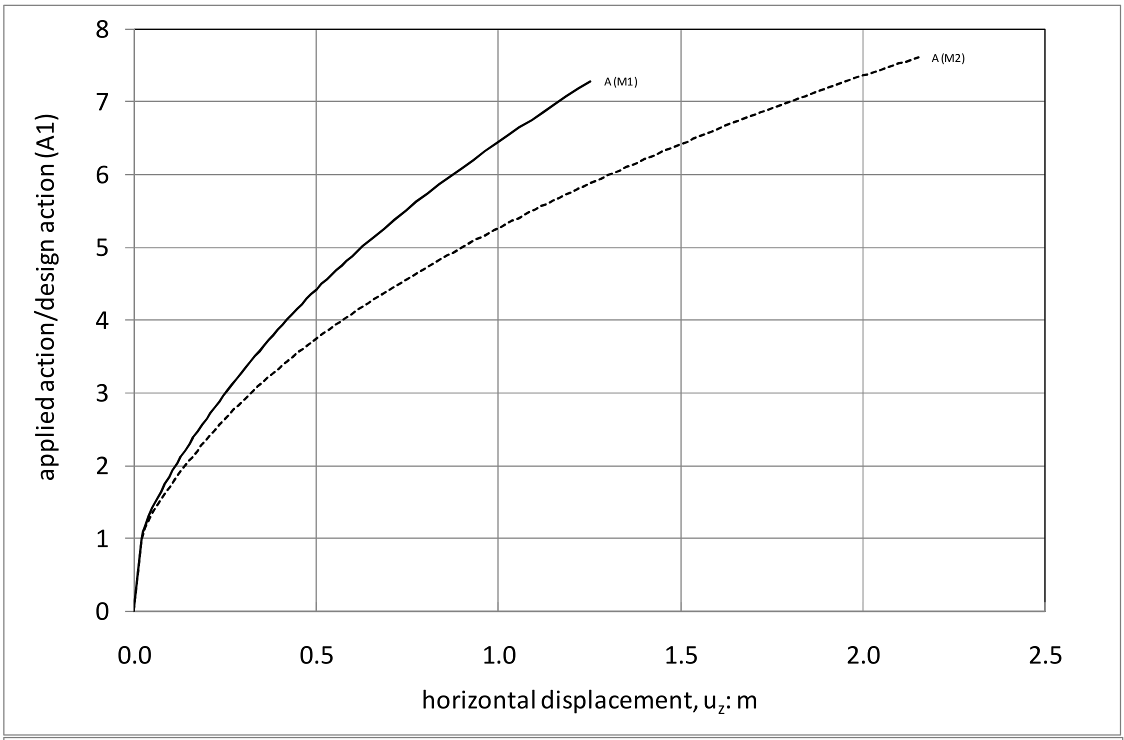


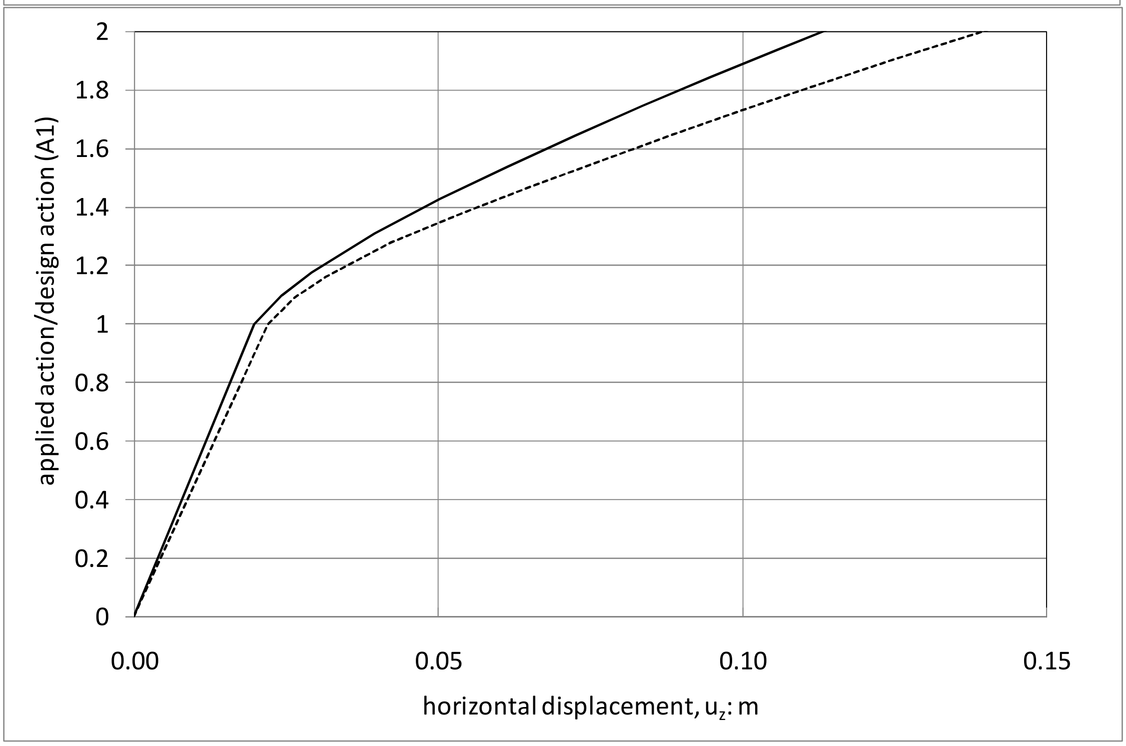


*Figure 14 ULS: Load – horizontal displacement curves for three points at elevation -15,0*

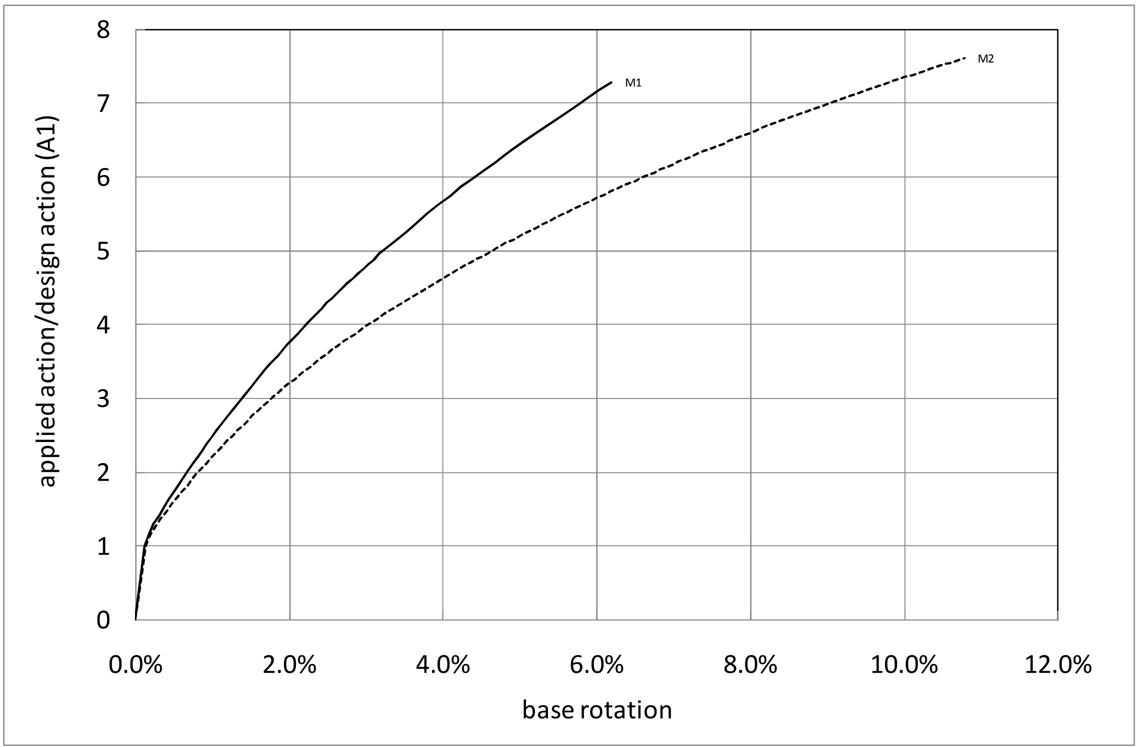


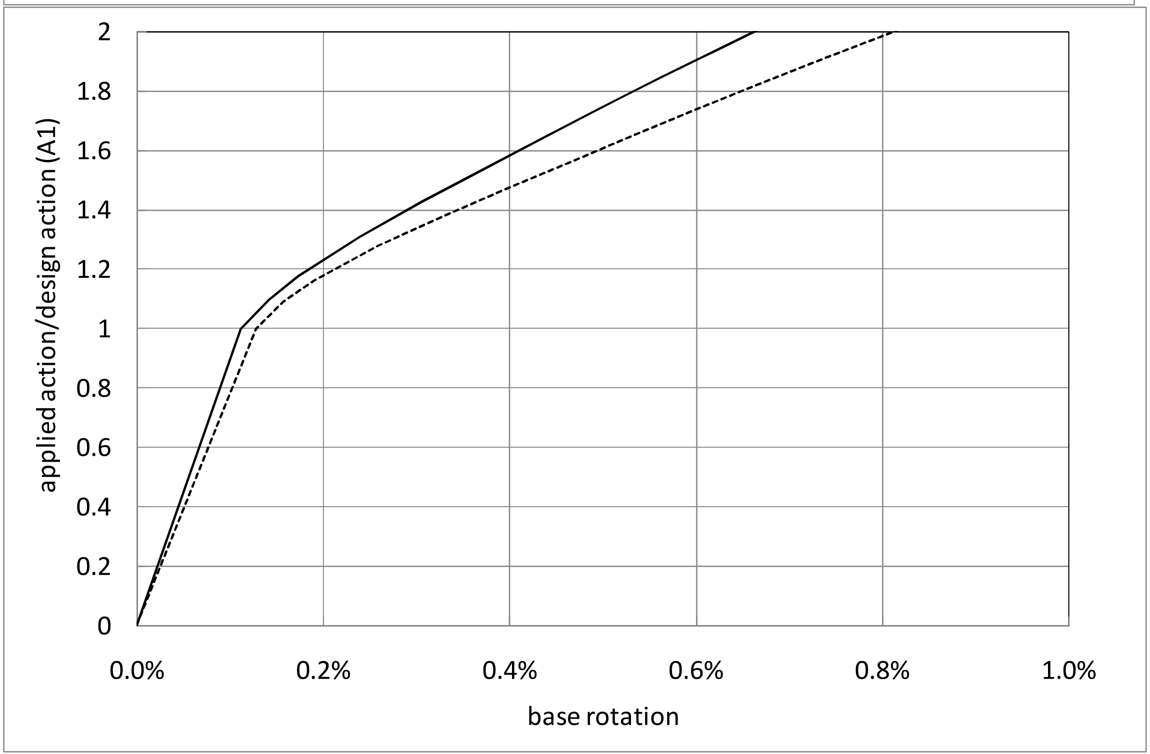


*Figure 15 ULS: Rotations toward the seashore for different analyses*

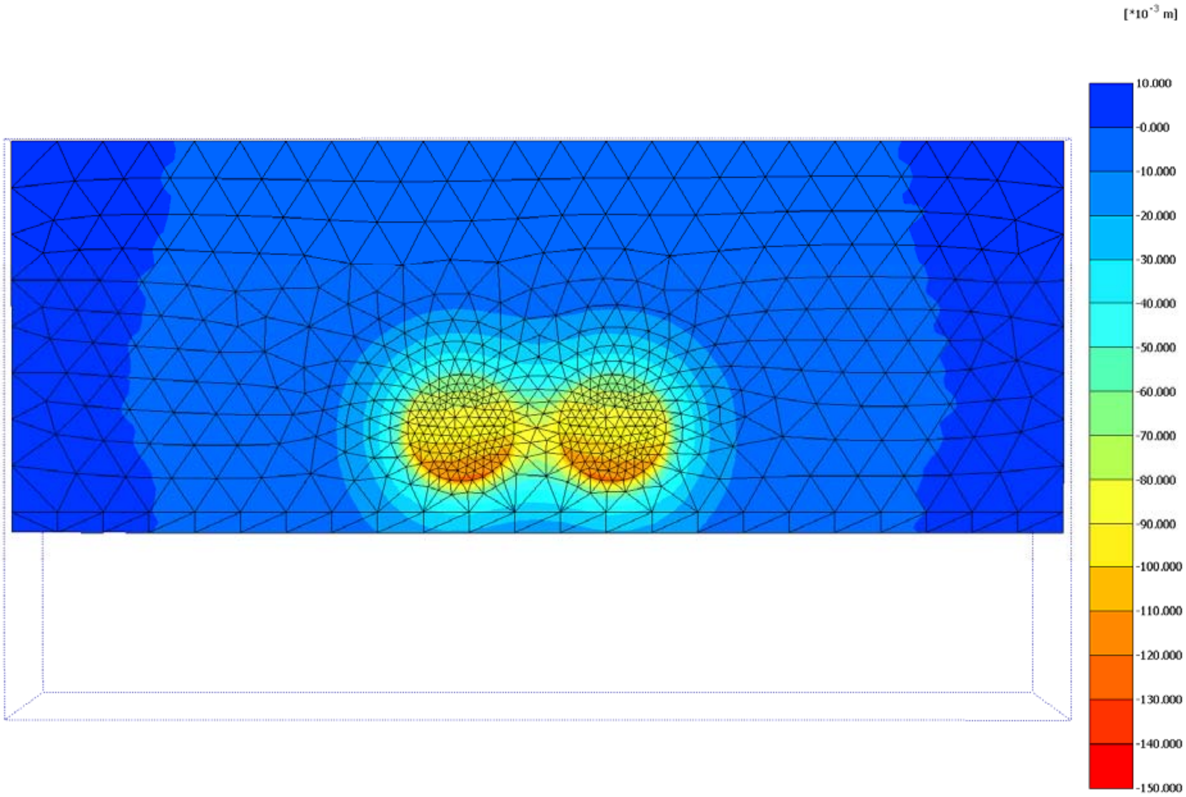


*Figure 16. ULS: Vertical displacements at ground level (+2.5 m asl). Case A1+M1*

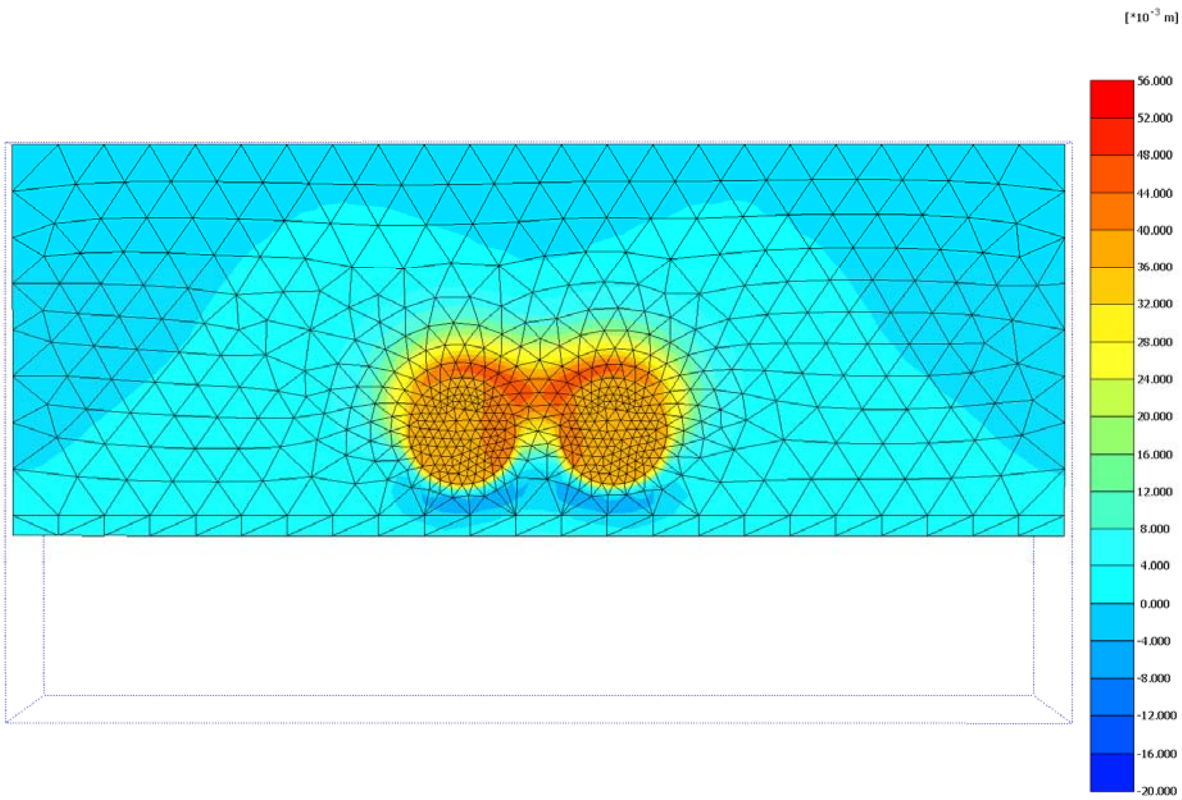


*Figure 17. ULS: Horizontal displacements (positive towards the sea shore) at ground level (+2.5 m asl) Case A1+M1*

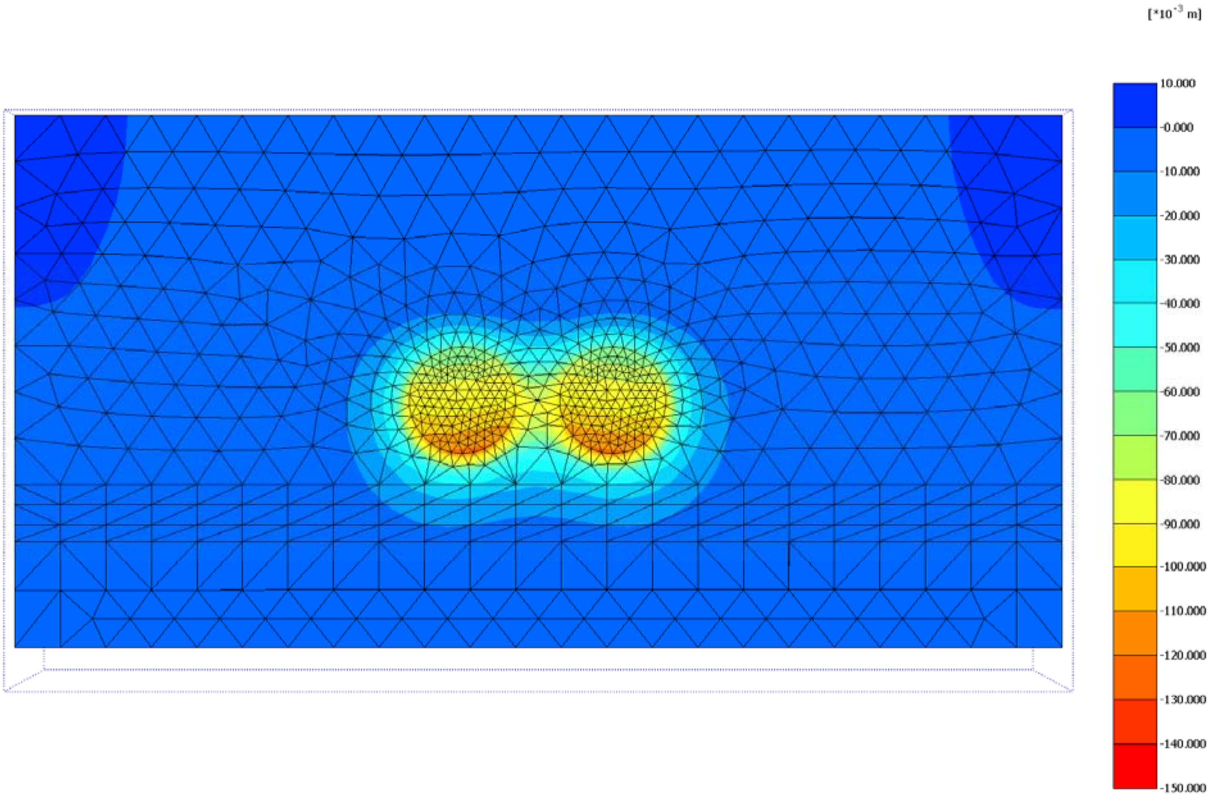


*Figure 18. ULS: Vertical displacements at the footing level (-15 m asl) Case A1+M1*

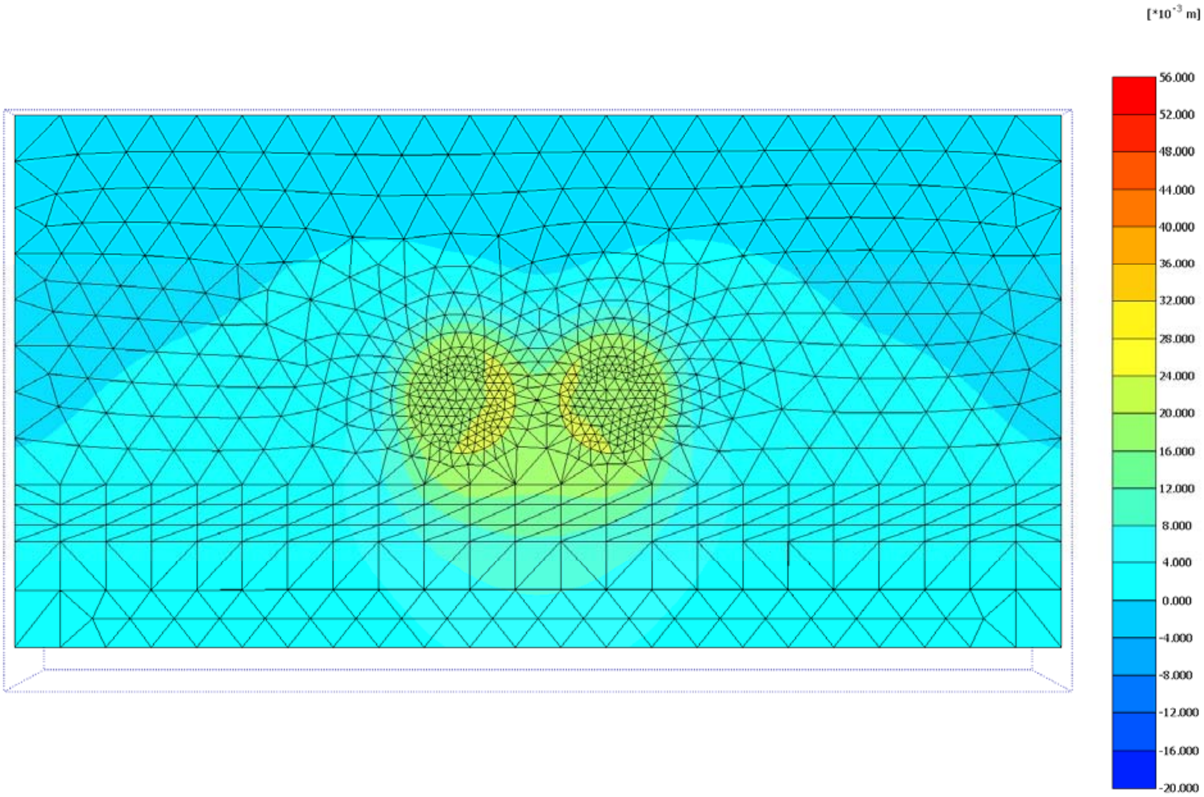


*Figure 19. ULS: Horizontal displacements (positive towards the sea shore) at the footing level (-15 m asl) Case A1+M1*

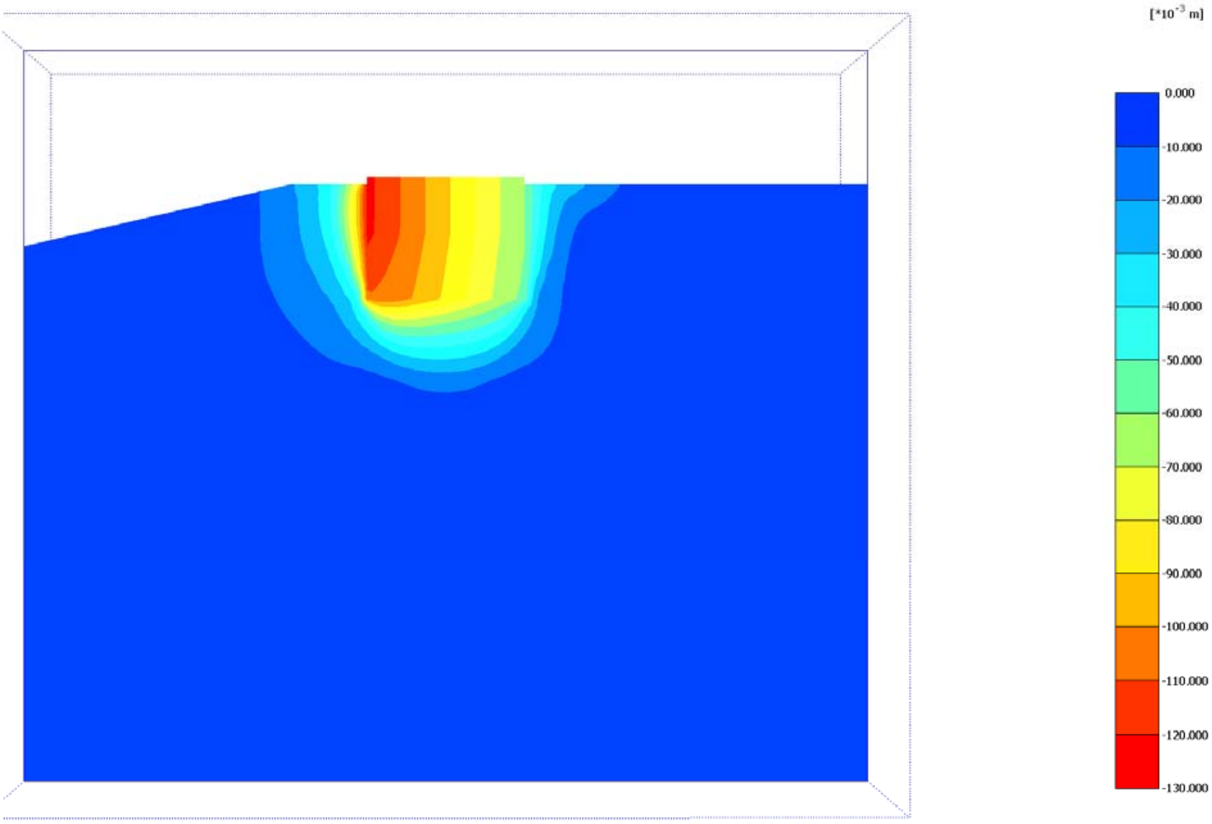


*Figure 20. ULS: Vertical displacements in the section along the tower diameter plane perpendicular to the sea shore Case A1+M1*

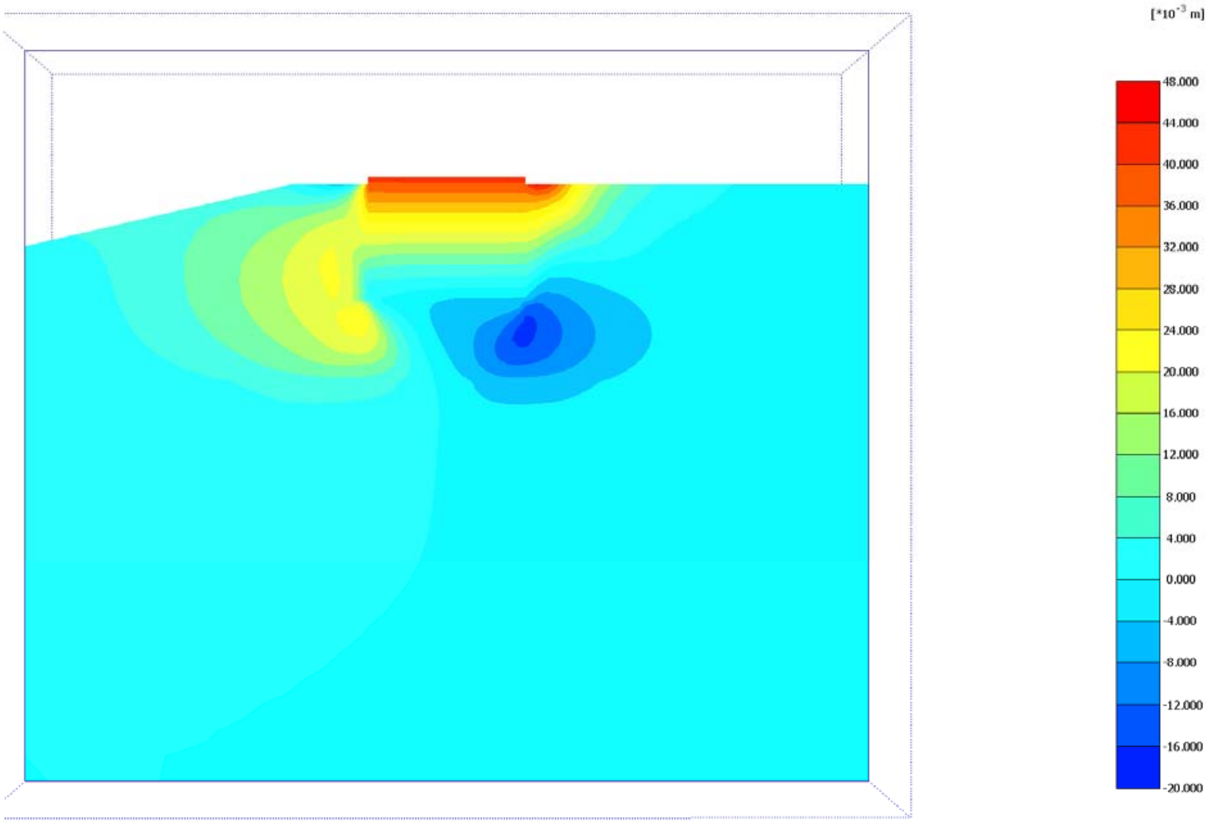


*Figure 21. ULS: Horizontal displacements in the section along the tower diameter plane perpendicular to the sea shore(positive towards the sea shore). Case A1+M1*

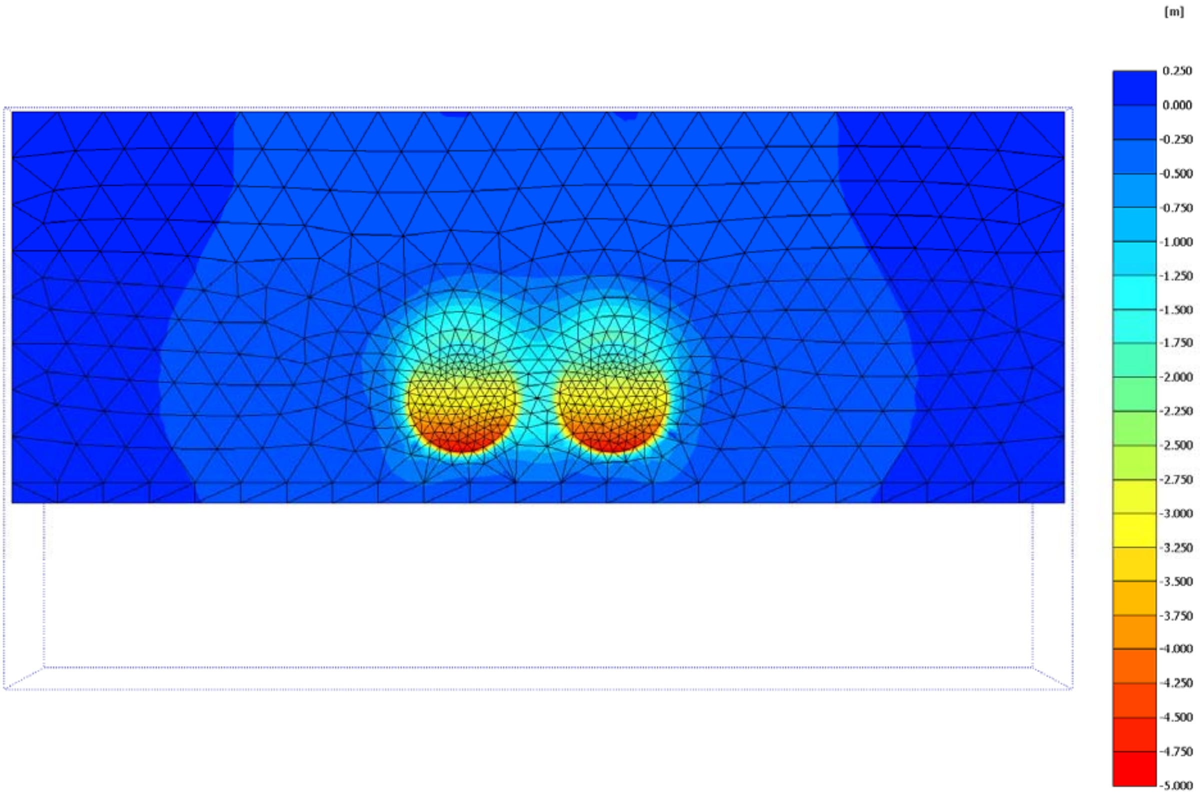


*Figure 22. ULS: Vertical displacements at ground level (+2.5 m asl) at the end of the incremental loading. Case A1+M1*

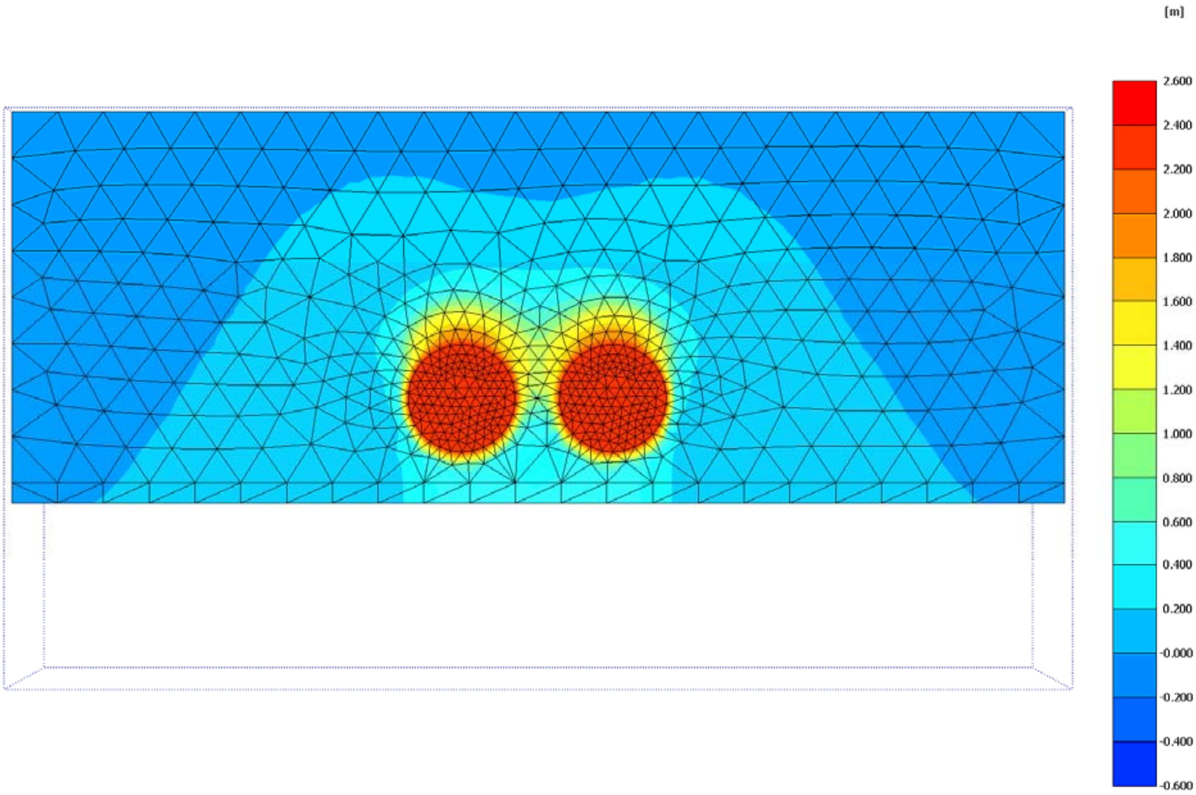


*Figure 23. ULS: Horizontal displacements (positive towards the sea shore) at ground level (+2.5 m asl) at the end of the incremental loading. Case A1+M1*

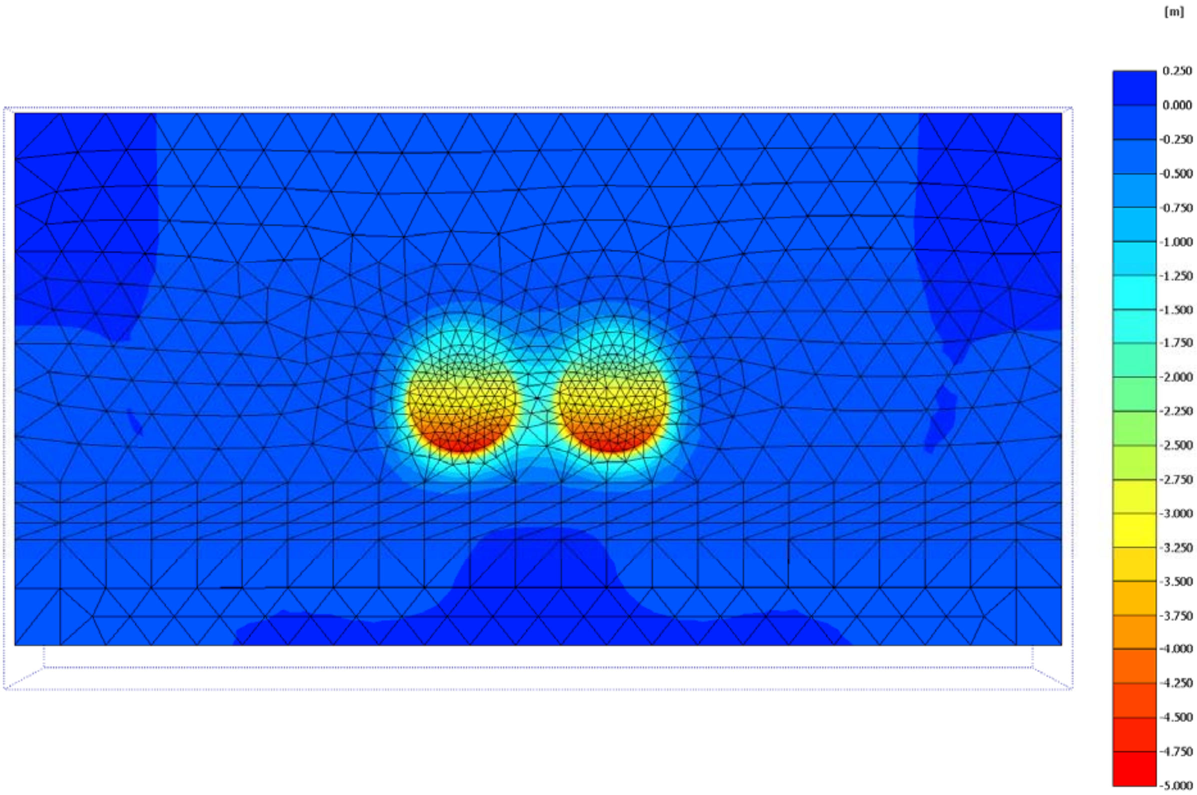


*Figure 24*. ULS: *Vertical displacements at the footing level (-15 m asl) at the end of the incremental loading. Case A1+M1*

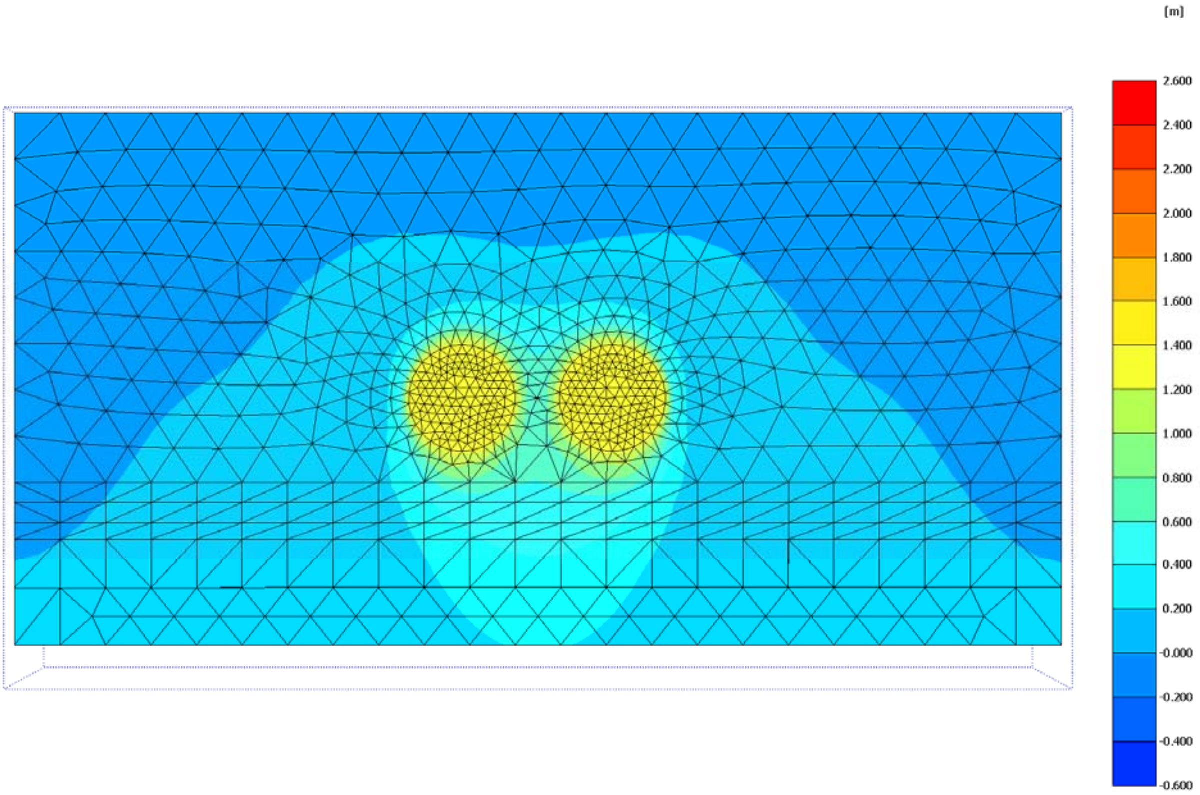


*Figure 25. ULS: Horizontal displacements (positive towards the sea shore) at the footing level (-15 m asl) at the end of the incremental loading Case A1+M1*

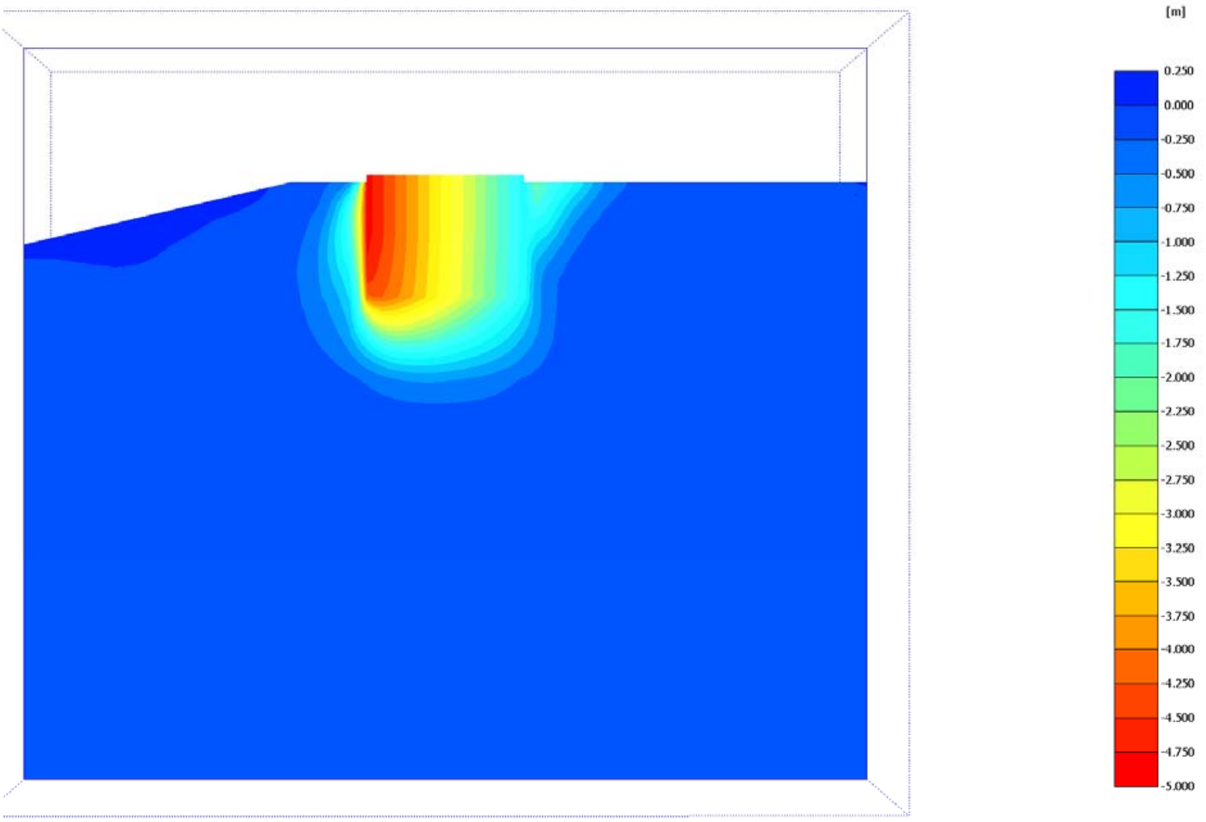


*Figure 26 ULS: Vertical displacements in the section along the tower diameter plane perpendicular to the sea shore at the end of the incremental loading. Case A1+M1*

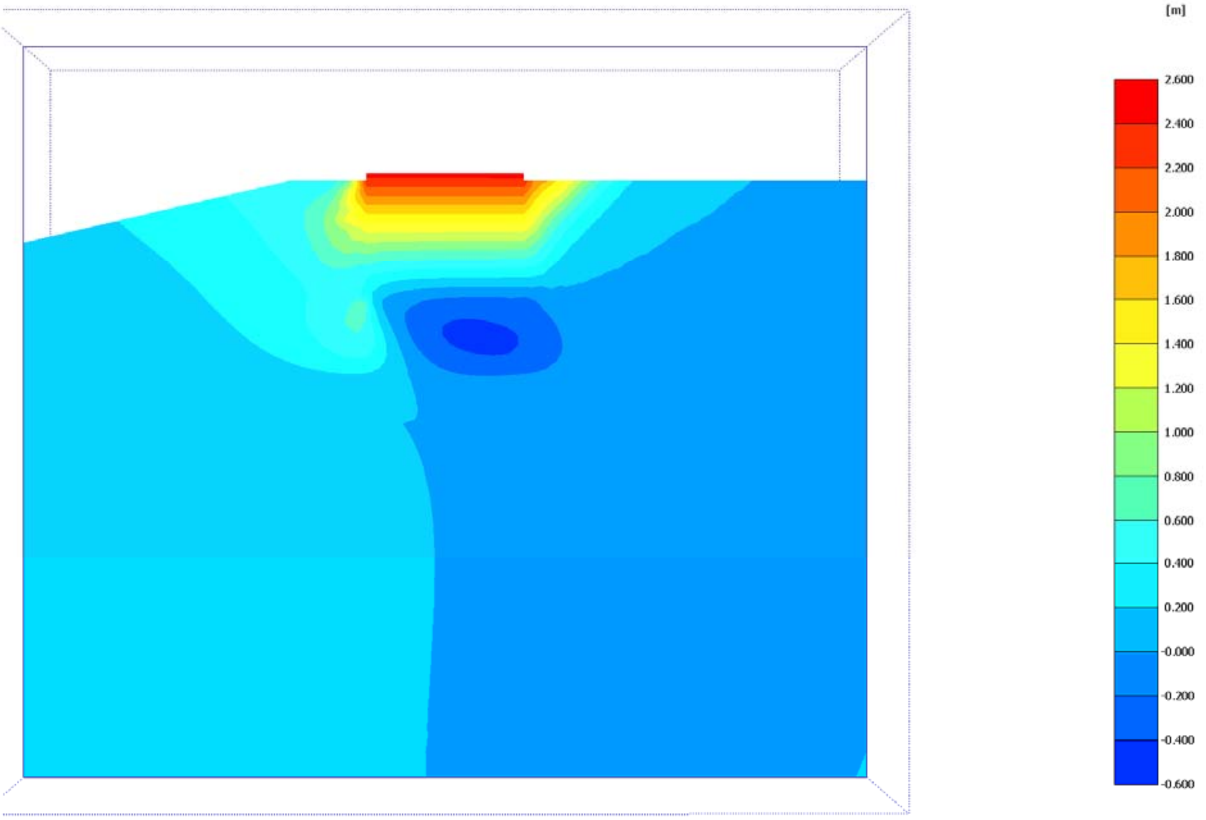


*Figure 27 ULS: Horizontal displacements in the section along the tower diameter plane perpendicular to the sea shore at the end of the incremental loading Case A1+M1*

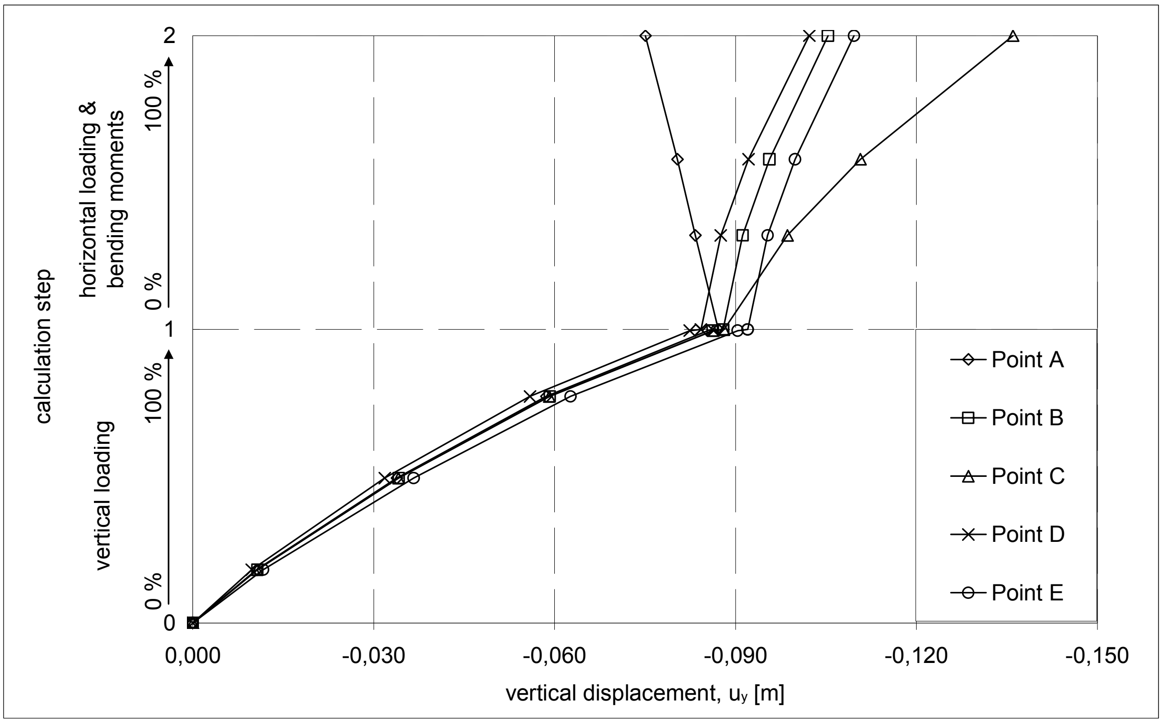


*Figure 28 SILS: Load-settlement curves for five points at elevation –15,0 m.*

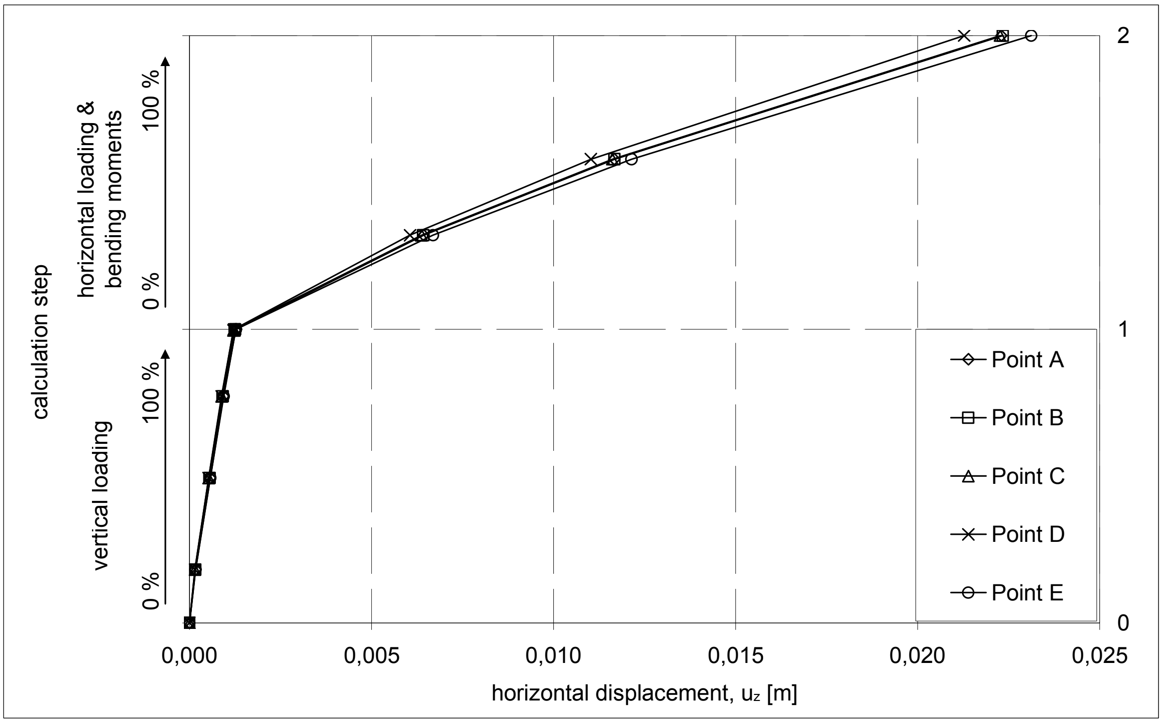


*Figure 29 SILS: Load – horizontal displacement curves for three points at elevation -15,0*

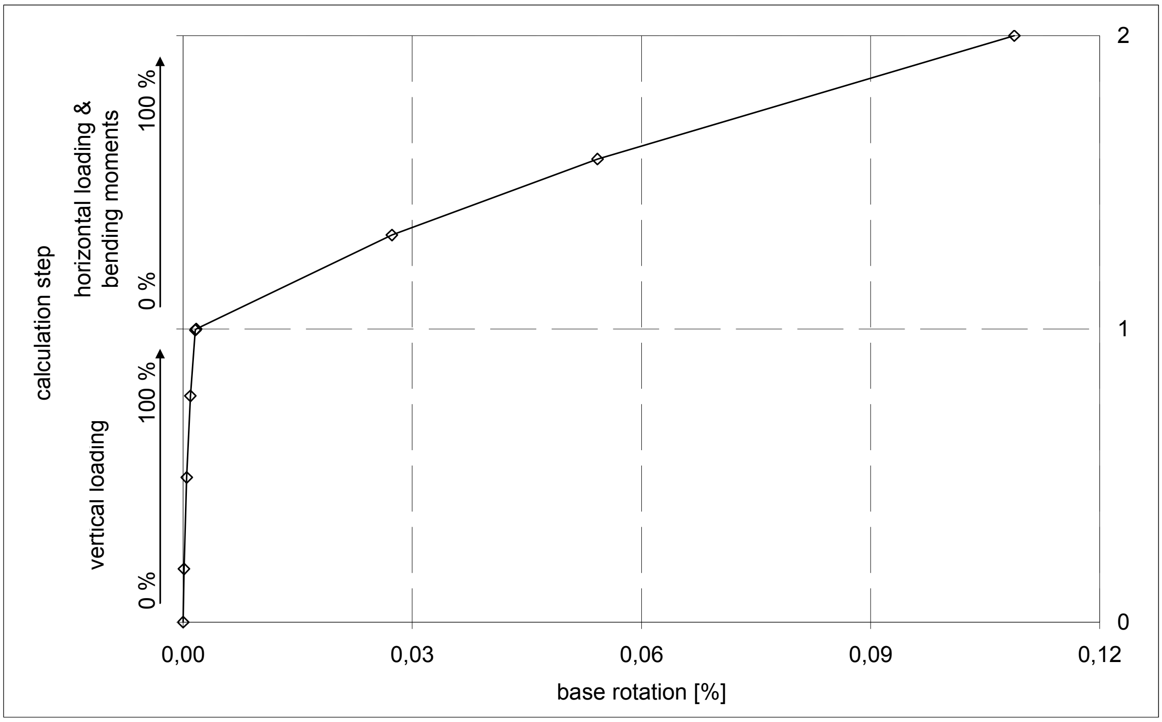


*Figure 30 SILS: Rotations toward the seashore*

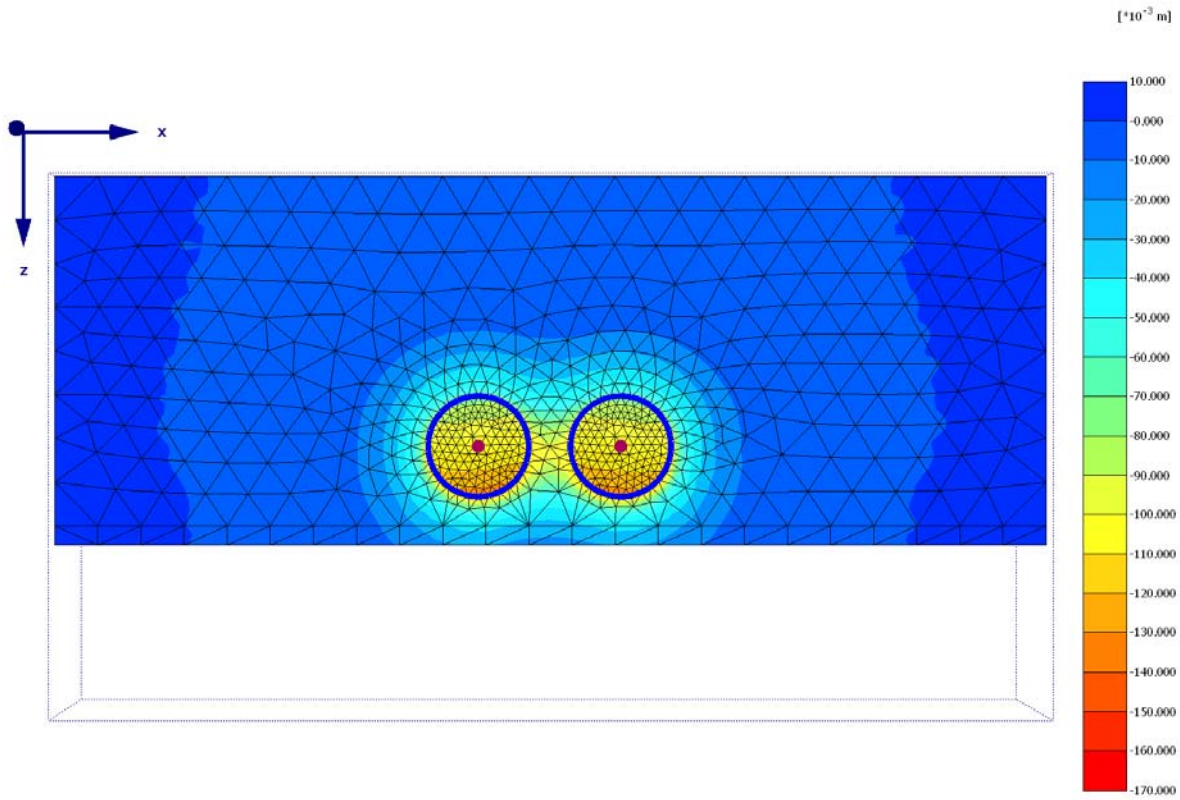


*Figure 31. SILS: Vertical displacements at ground level (+2.5 m asl)*

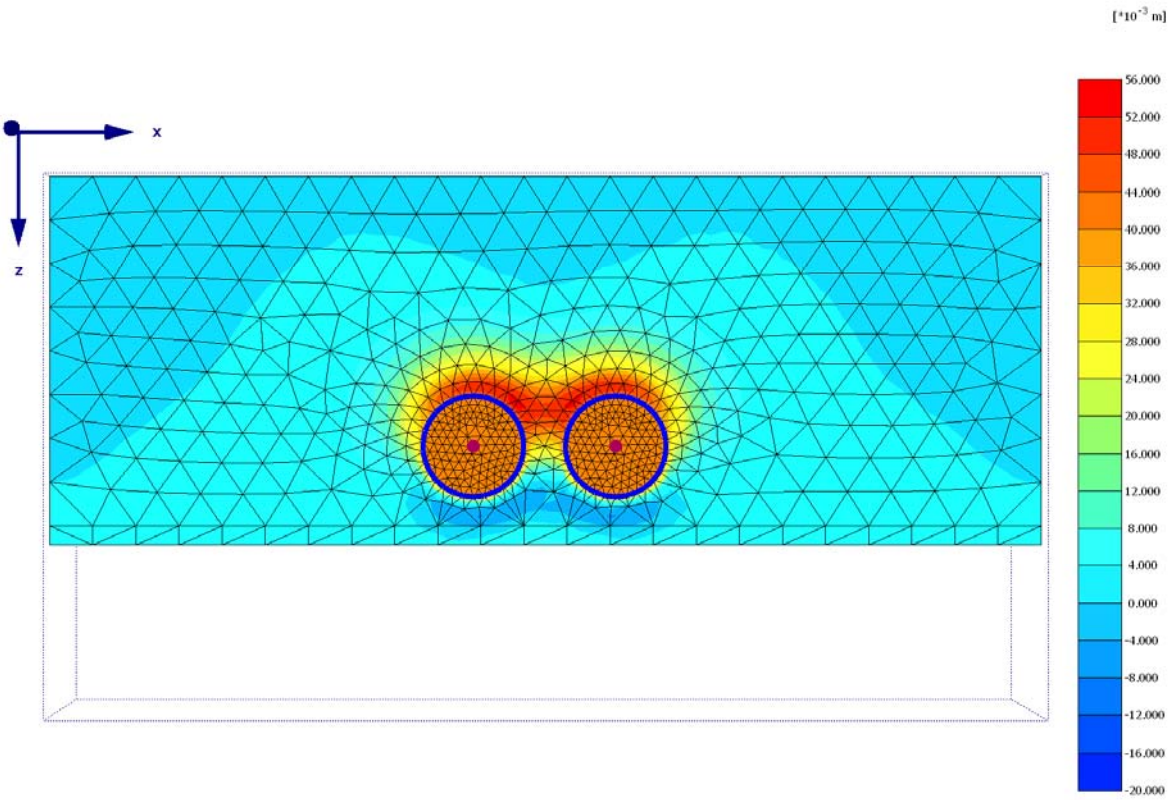


*Figure 32. SILS: Horizontal displacements (positive towards the sea shore) at ground level (+2.5 m asl)*

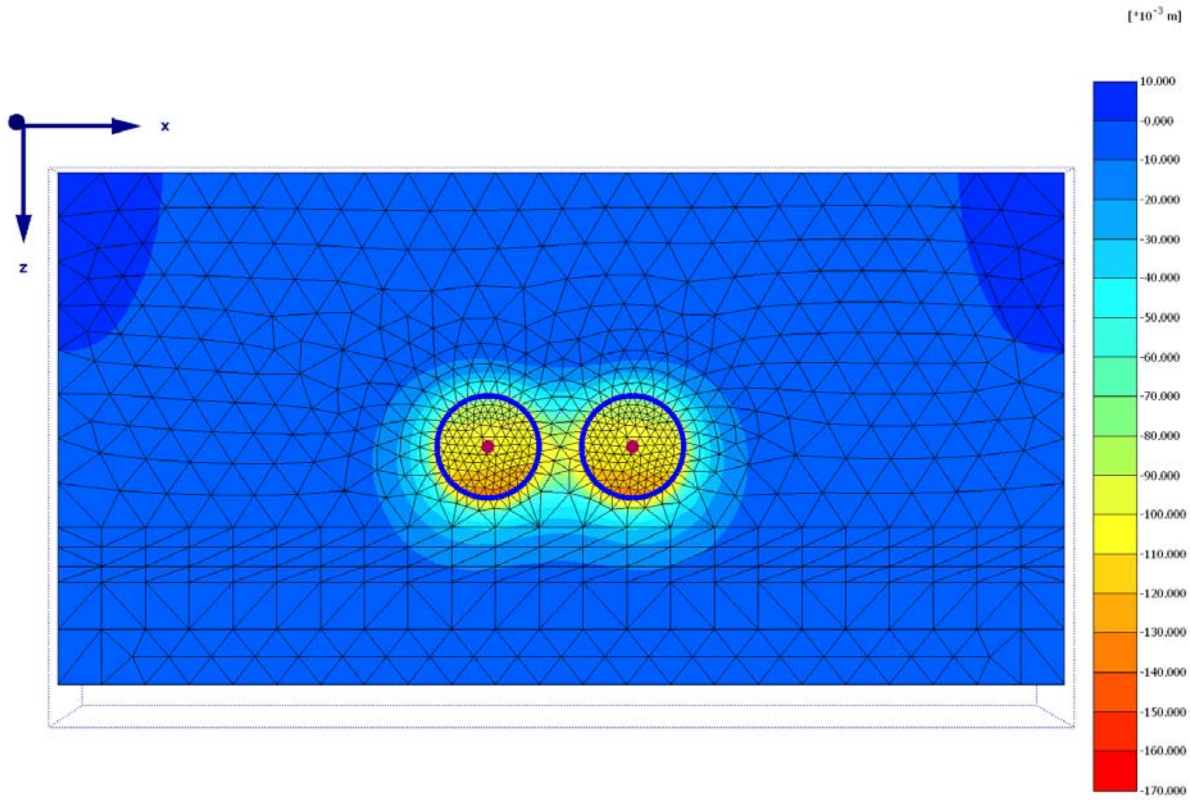


*Figure 33. SILS: Vertical displacements at the footing level (-15 m asl)*

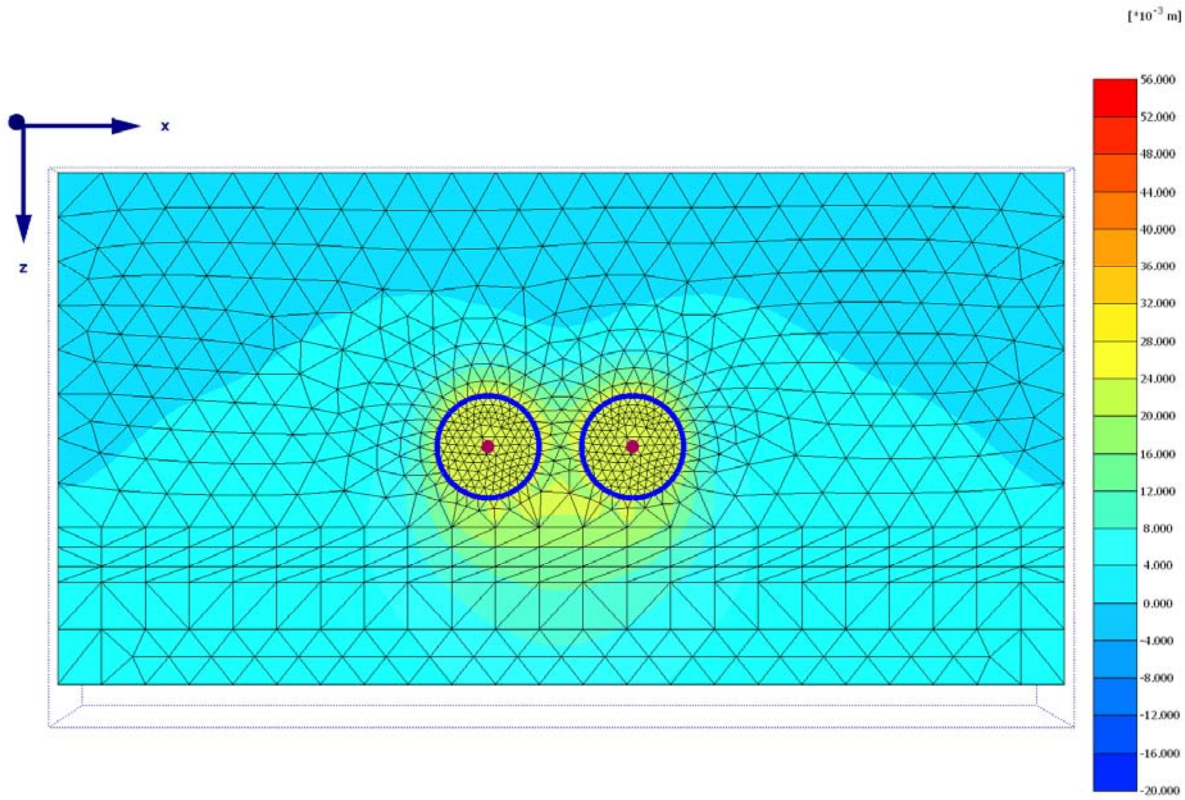


*Figure 34. SILS: Horizontal displacements (positive towards the sea shore) at the footing level (-15 m asl)*

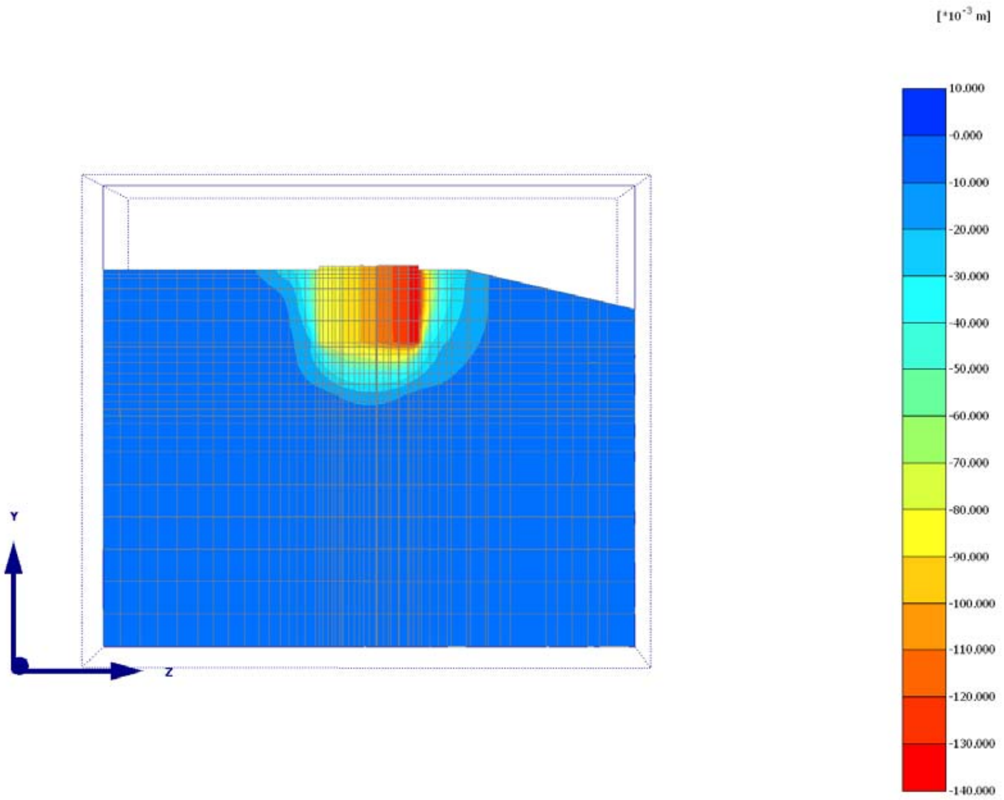


*Figure 35. SILS: Vertical displacements in the section along the tower diameter plane perpendicular to the sea shore.*

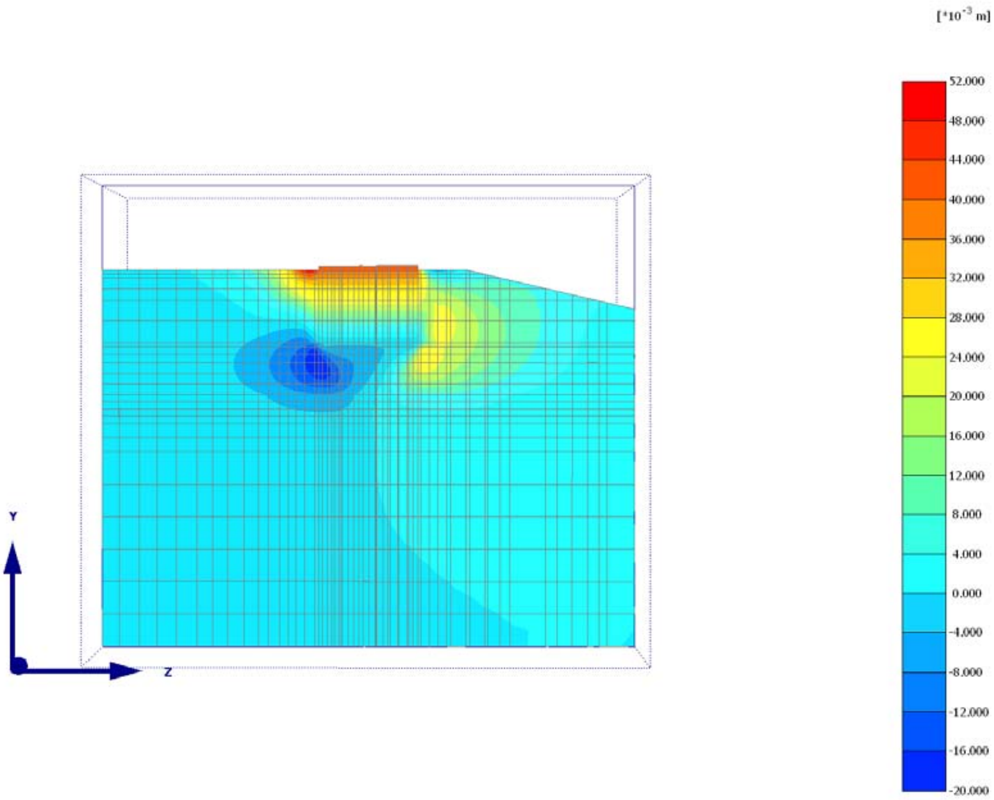


*Figure 36. SILS: Horizontal displacements in the section along the tower diameter plane perpendicular to the sea shore(positive towards the sea shore)*

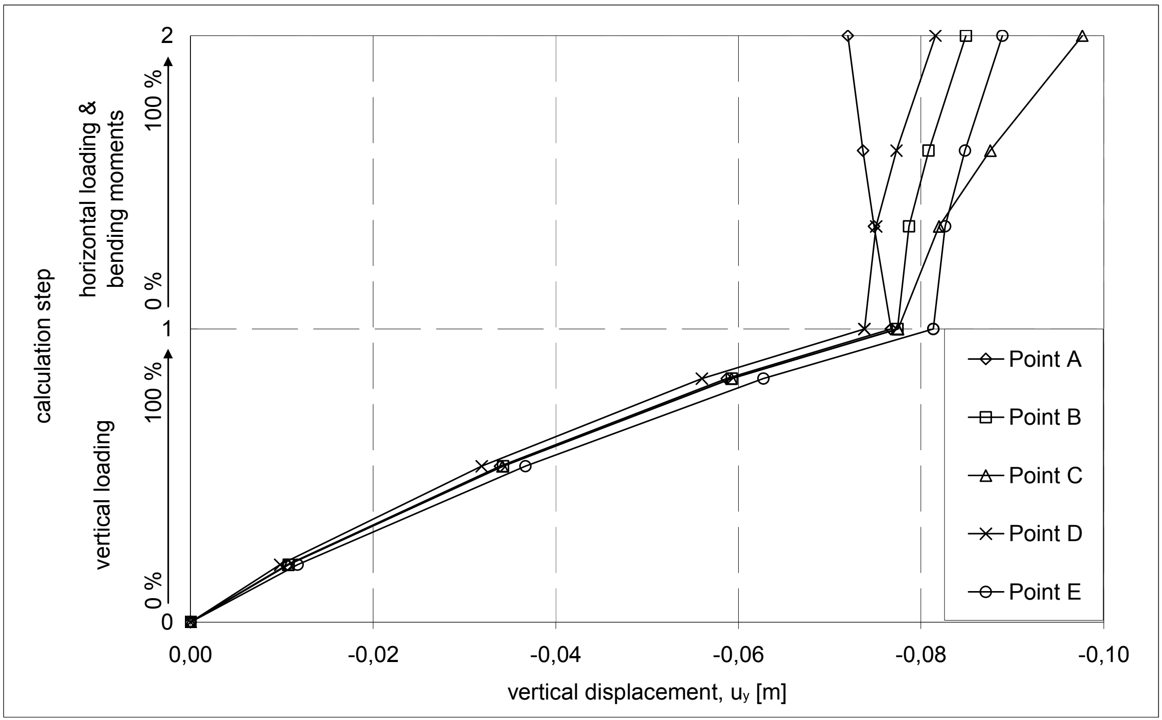


*Figure 37 SLS2: Load-settlement curves for five points at elevation –15,0 m.*

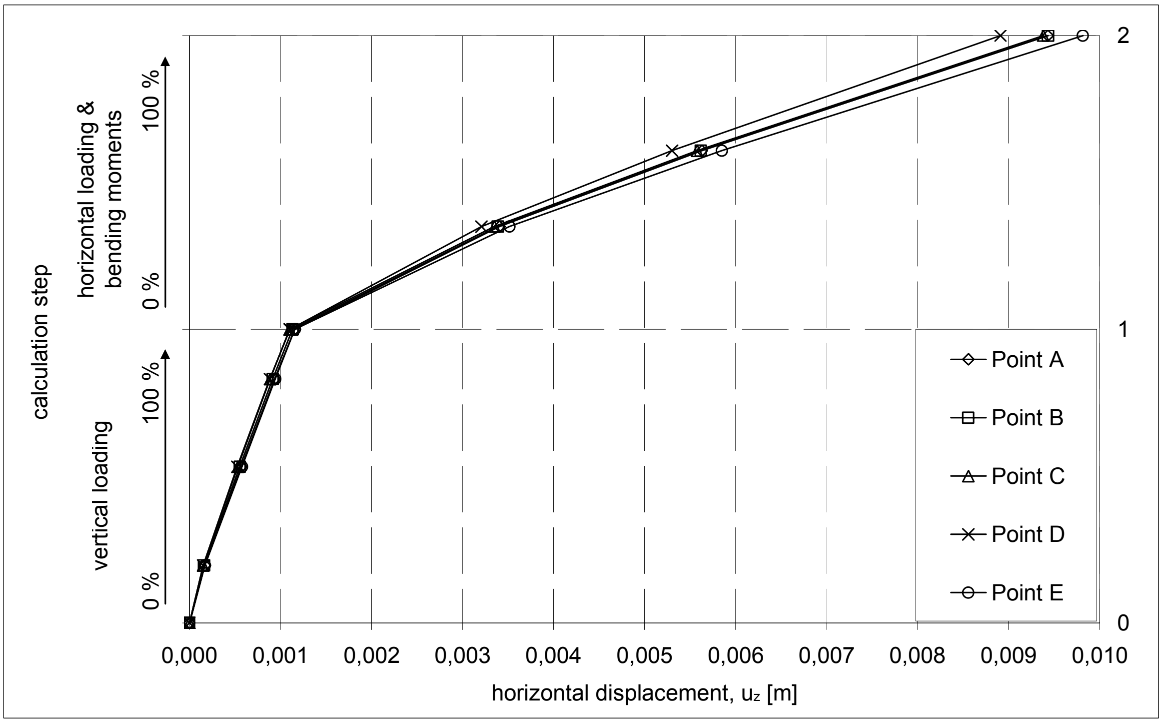


*Figure 38 SLS2: Load – horizontal displacement curves for three points at elevation -15,0*

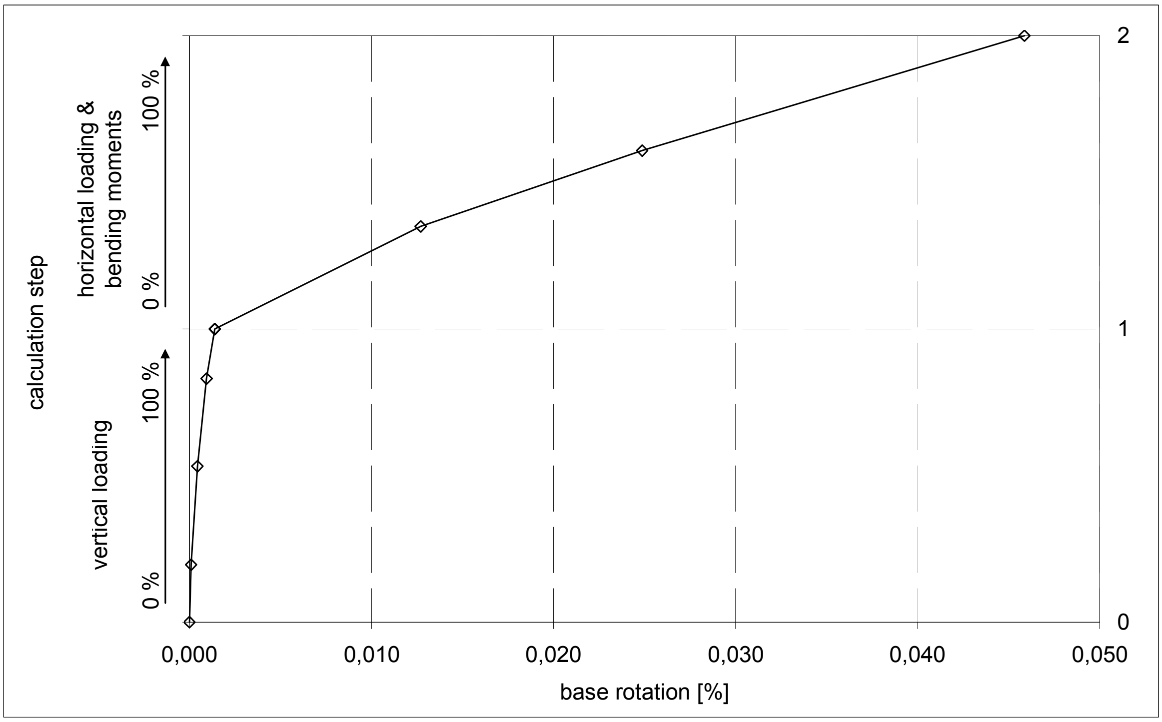


*Figure 39 SLS2: Rotations toward the seashore*

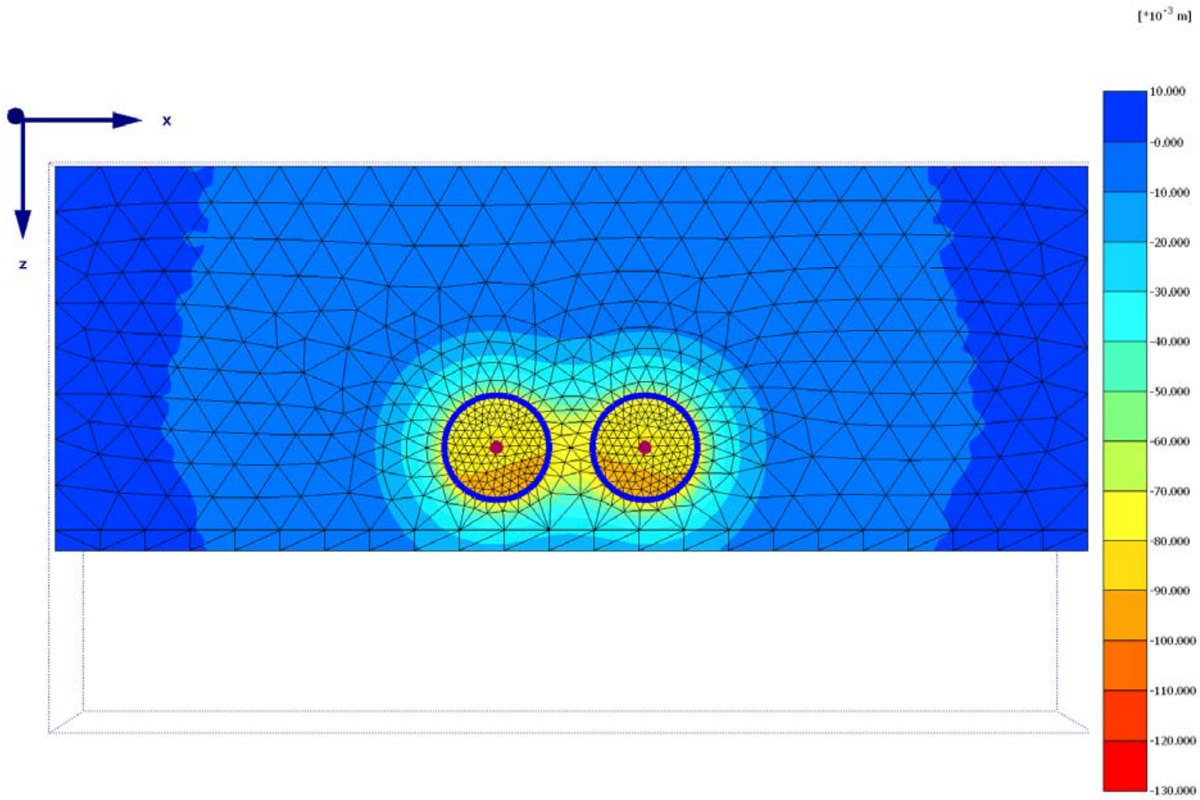


*Figure 40. SLS2: Vertical displacements at ground level (+2.5 m asl)*

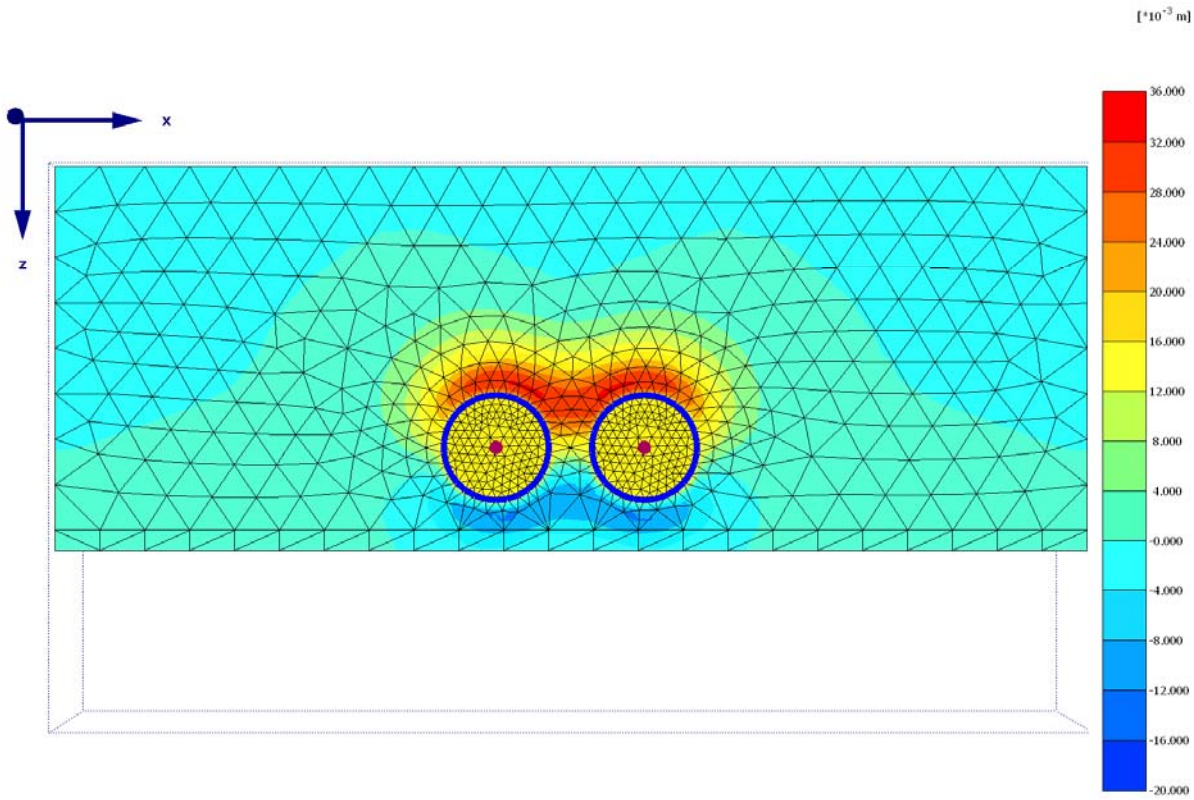


*Figure 41. SLS2: Horizontal displacements (positive towards the sea shore) at ground level (+2.5 m asl)*

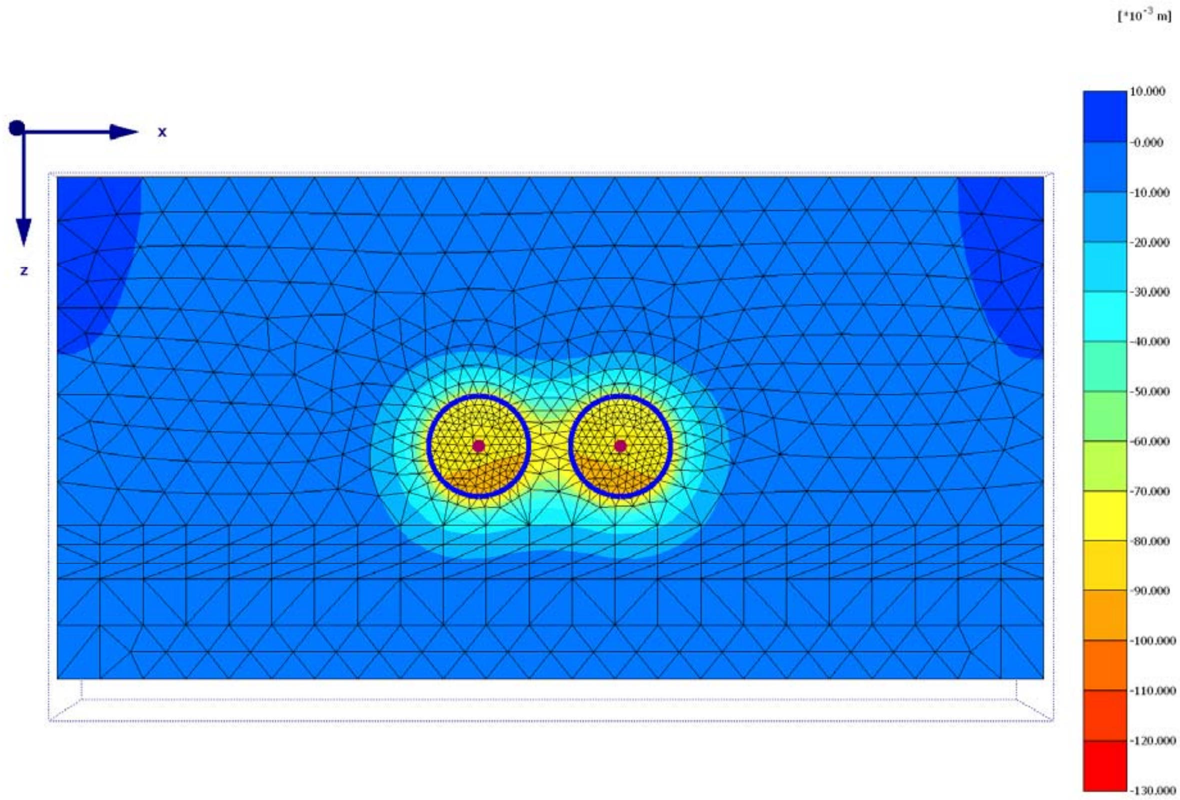


*Figure 42. SLS2: Vertical displacements at the footing level (-15 m a.s.l.)*

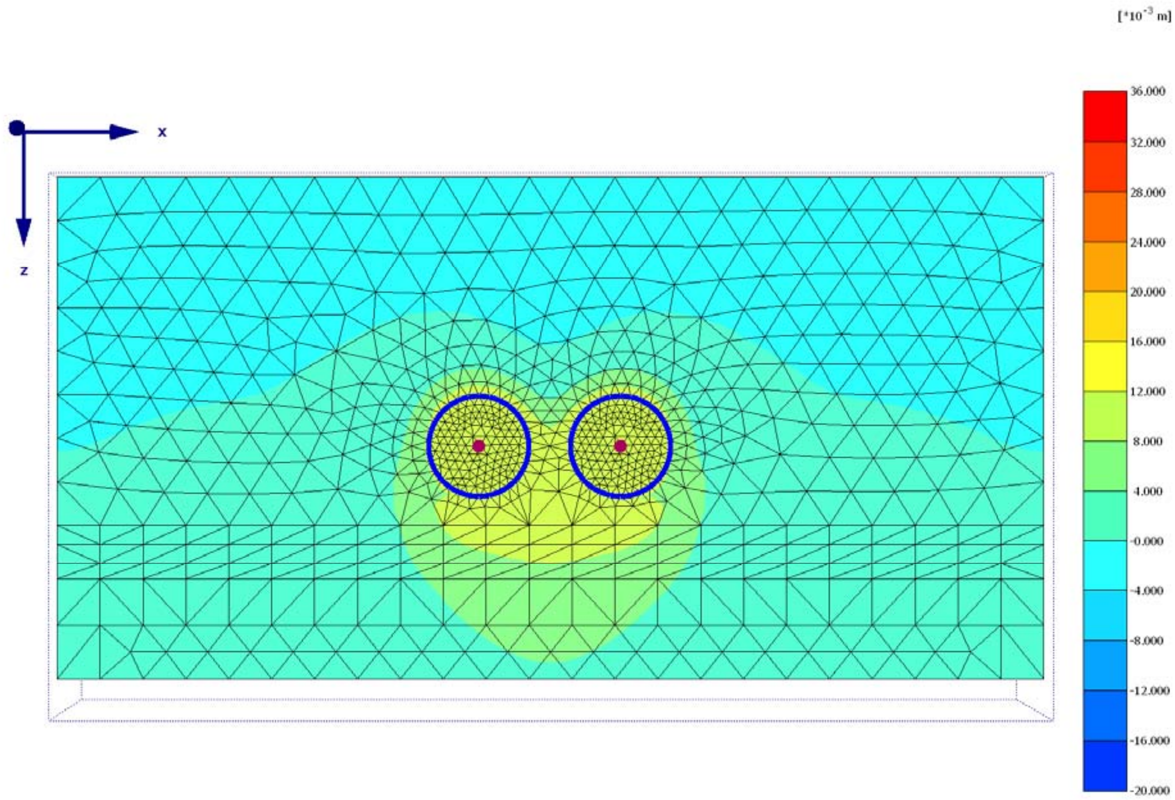


*Figure 43. SLS2: Horizontal displacements (positive towards the sea shore) at the footing level (-15 m asl)*

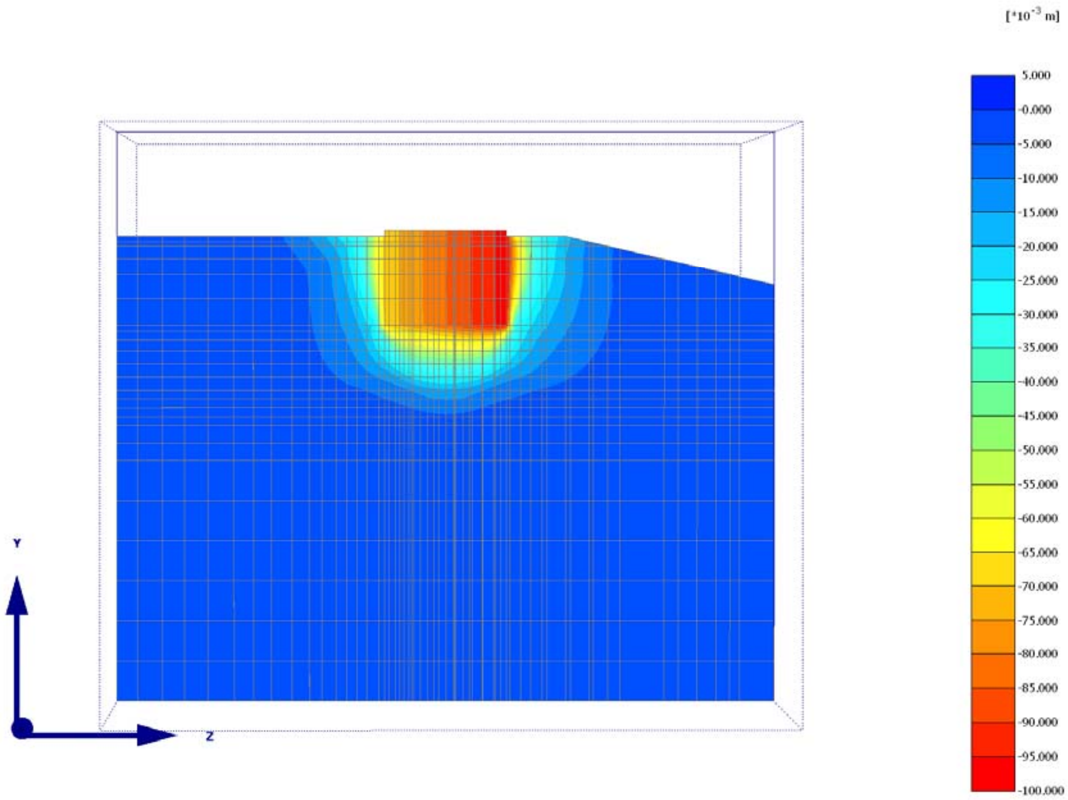


*Figure 44. SLS2: Vertical displacements in the section along the tower diameter plane perpendicular to the sea shore.*

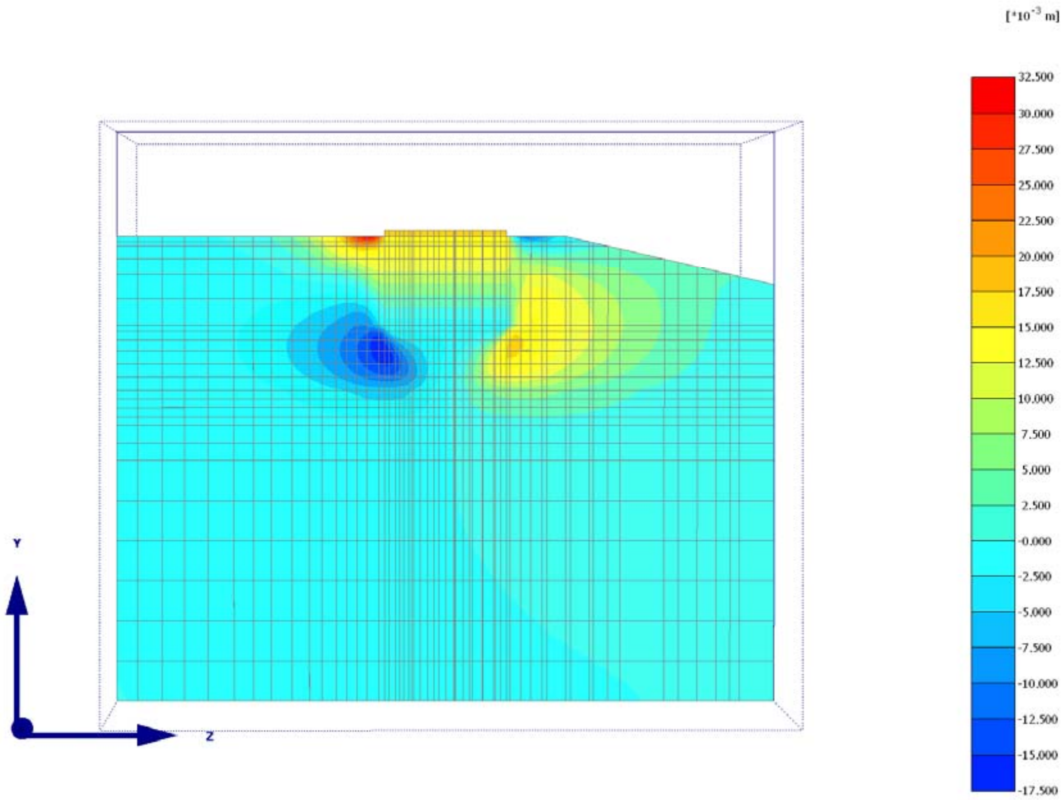


*Figure 45. SILS: Horizontal displacements in the section along the tower diameter plane perpendicular to the sea shore(positive towards the sea shore)*

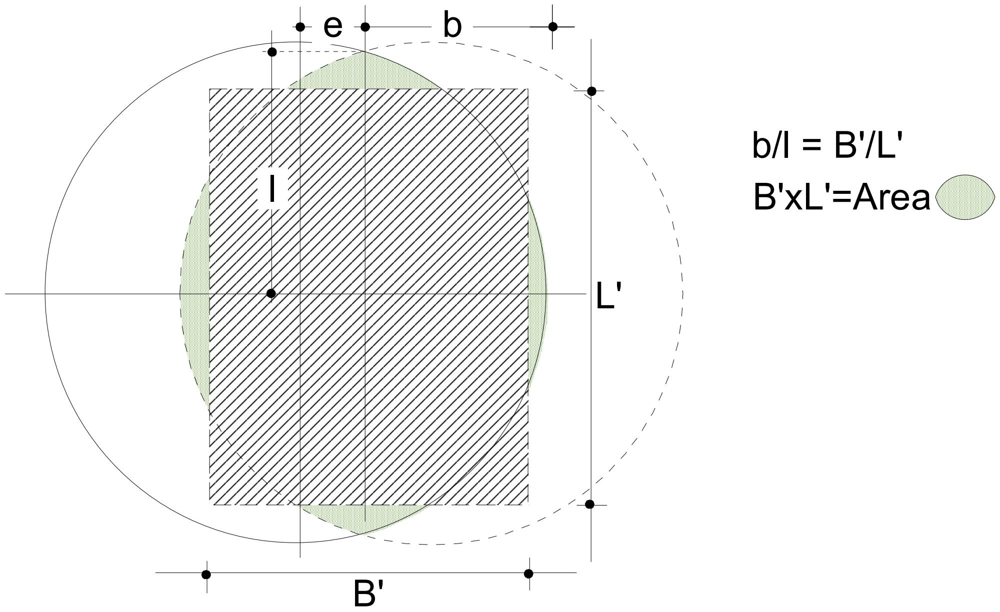


*Figure 46 Equivalent foundation for bearing capacity calculation*

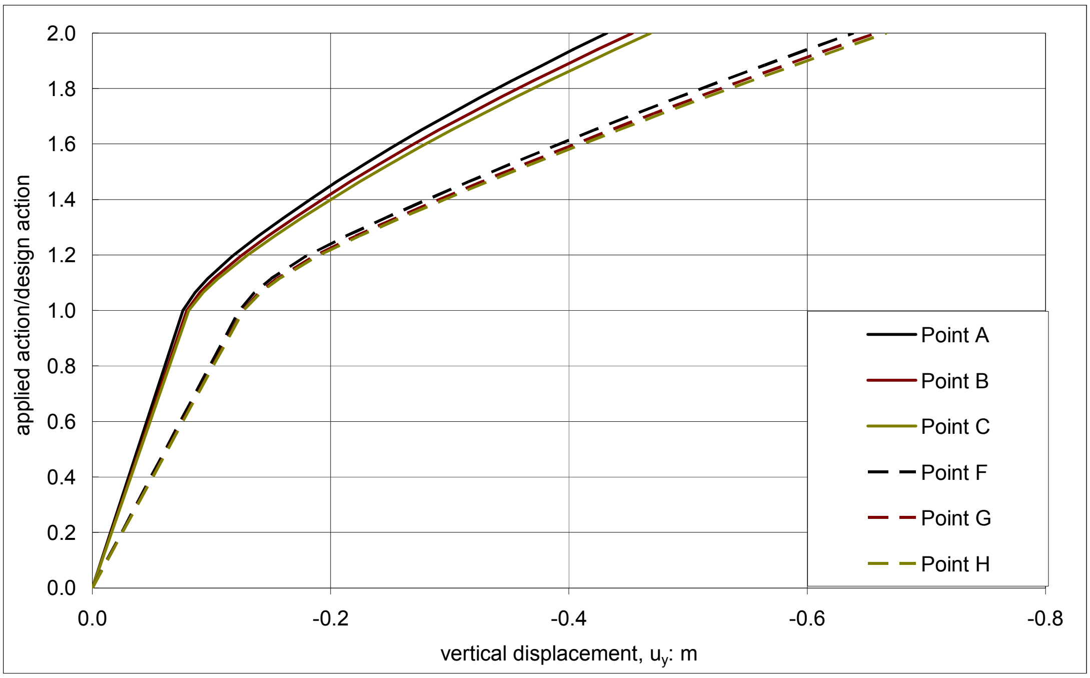


a)

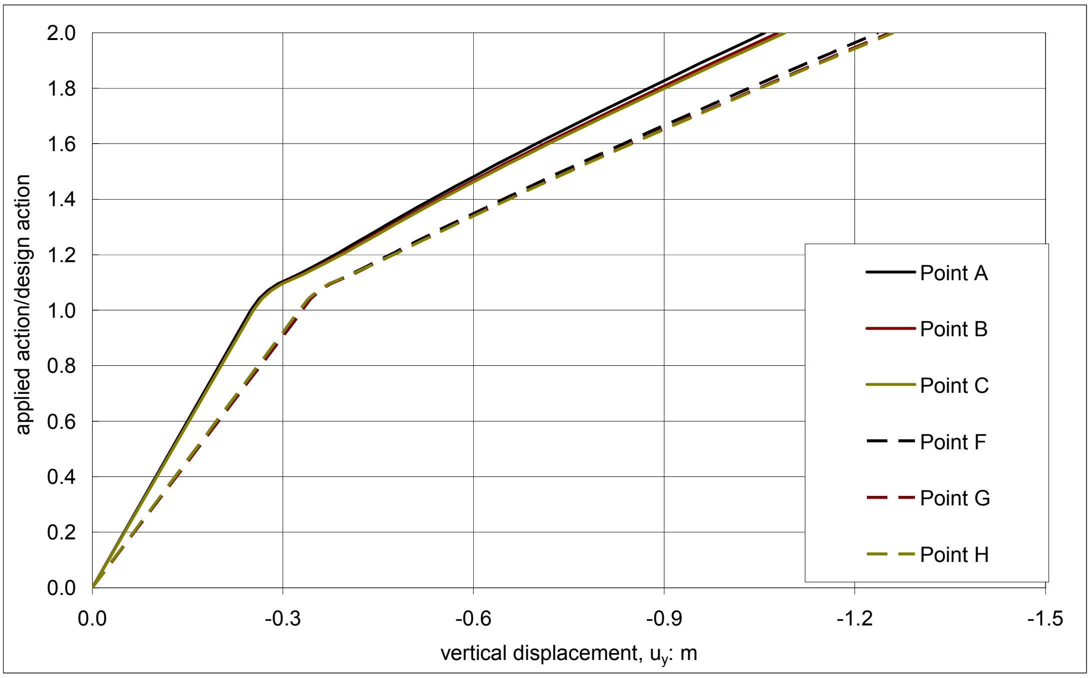


b)

*Figure 47 Load-settlement curves for the two foundations of Sicily towers ULS a) static worst combination; b) seismic worst combination*

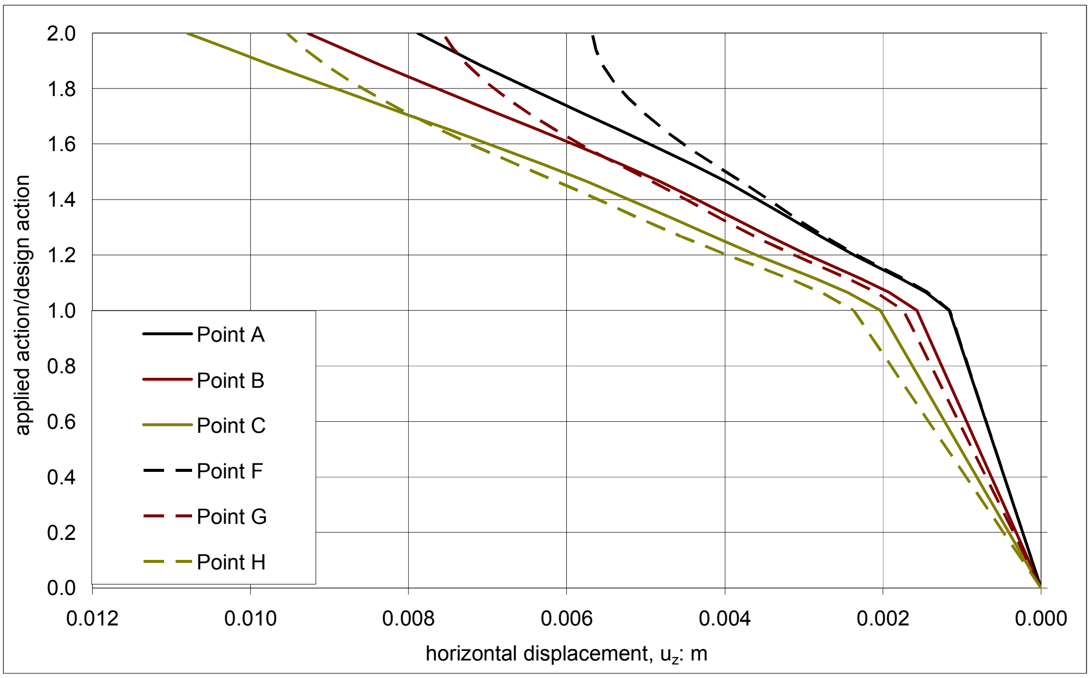


a)

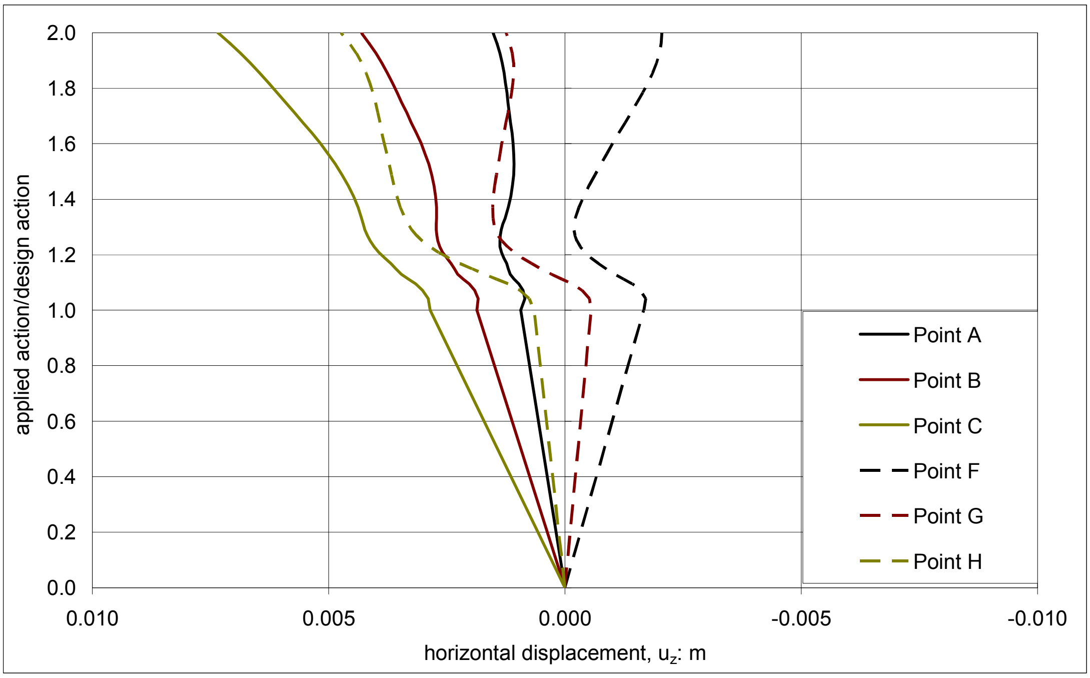


b)

*Figure 48 Load-horizontal displacement ($u_z$ towards the seashore) for the two foundations of Sicily towers ULS a) static worst combination; b) seismic worst combination*

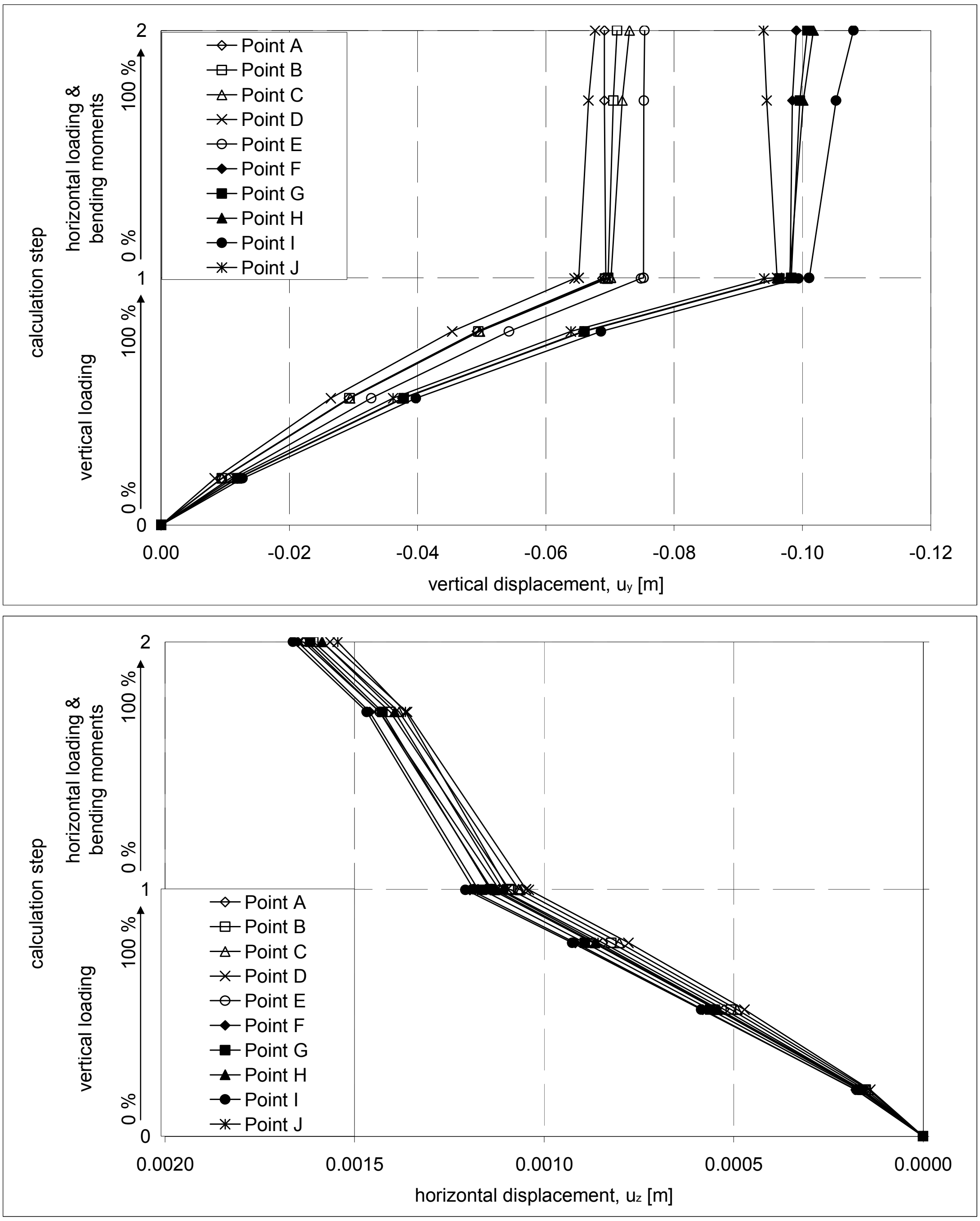


*Figure 49* Vertical settlement and horizontal displacement towards the seashore for both legs of the Sicily towers under SLS2 worst static condition

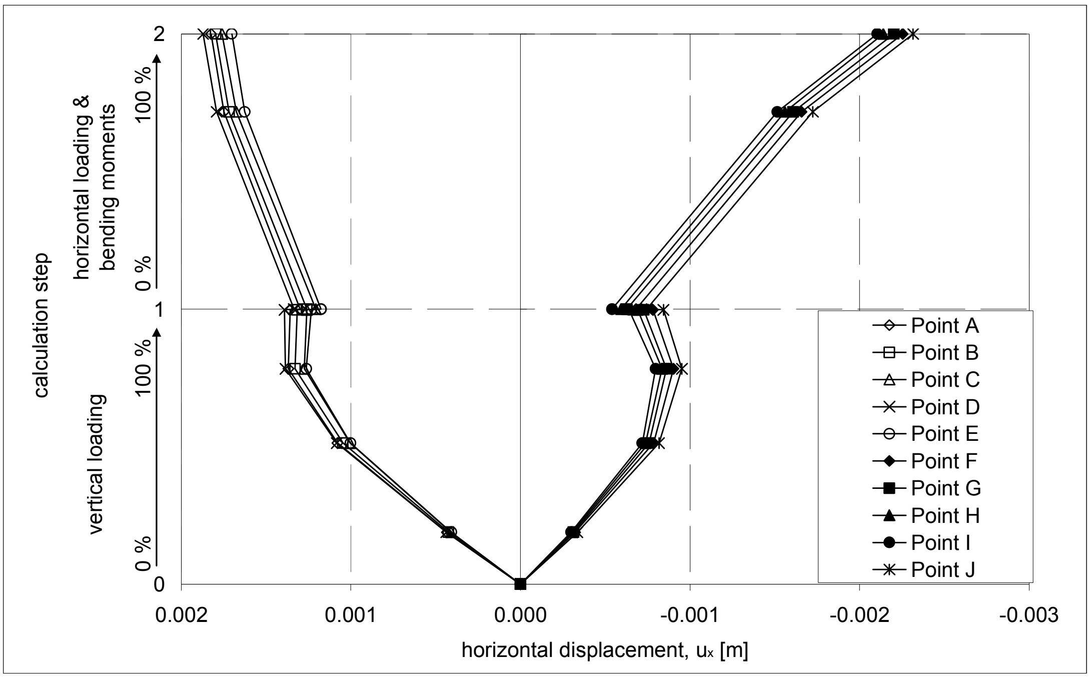


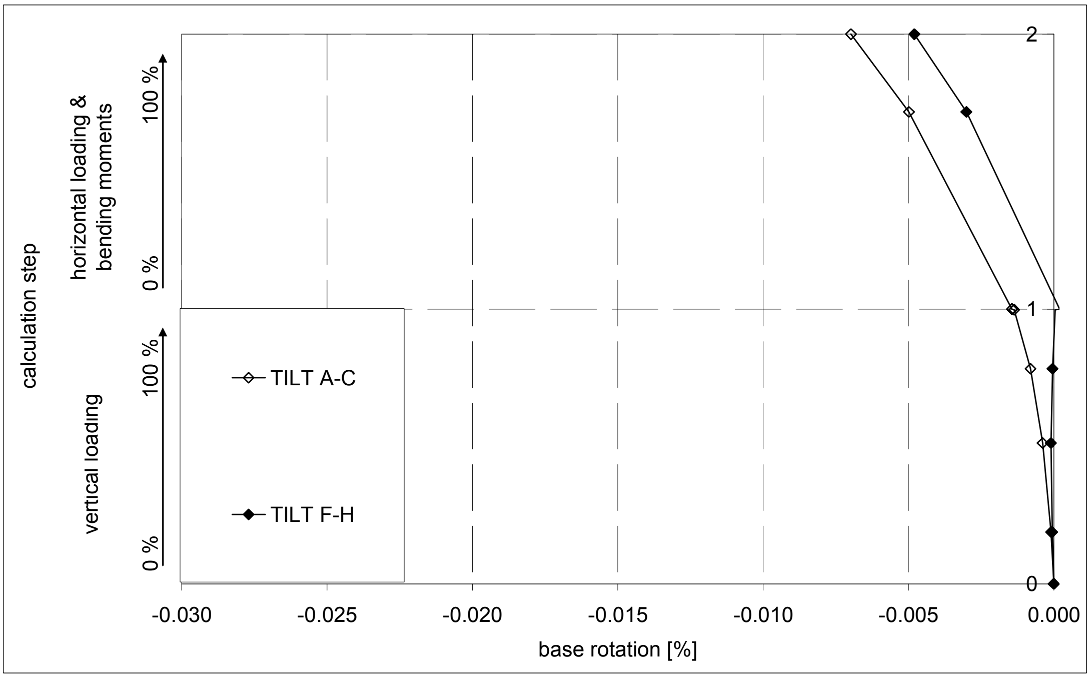


*Figure 50* Horizontal displacement parallel to the seashore and rotations towards the seashore for for both legs of the Sicily tower under SLS2 worst static condition

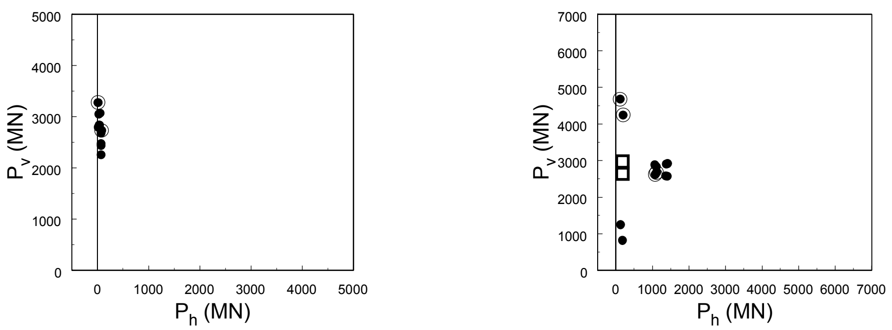

*Figure 51 New ULS static(left) and seismic(right)loading conditions from IBDAS(Pv=vertical load, Ph=horizontal load at level -15 asl)*

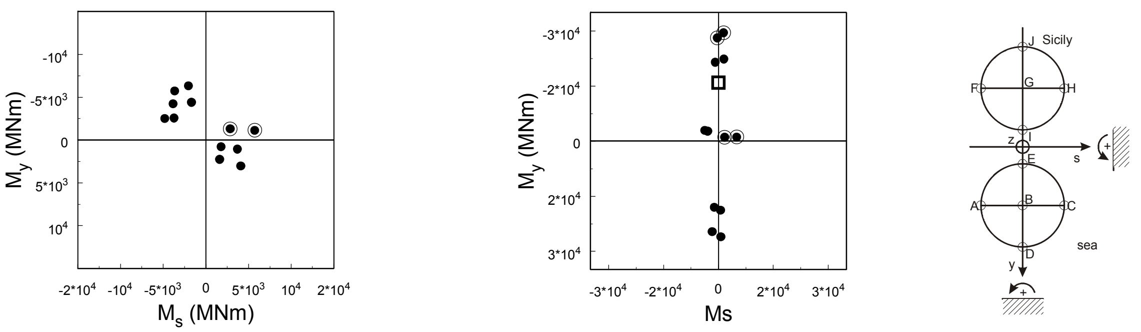

*Figure 52 New ULS static(left) and seismic(right)loading conditions from IBDAS(My=moments in the vertical plane orthogonal to the seashore, Ms=moments in the vertical plane parallel to the seashore at level -15 asl)*

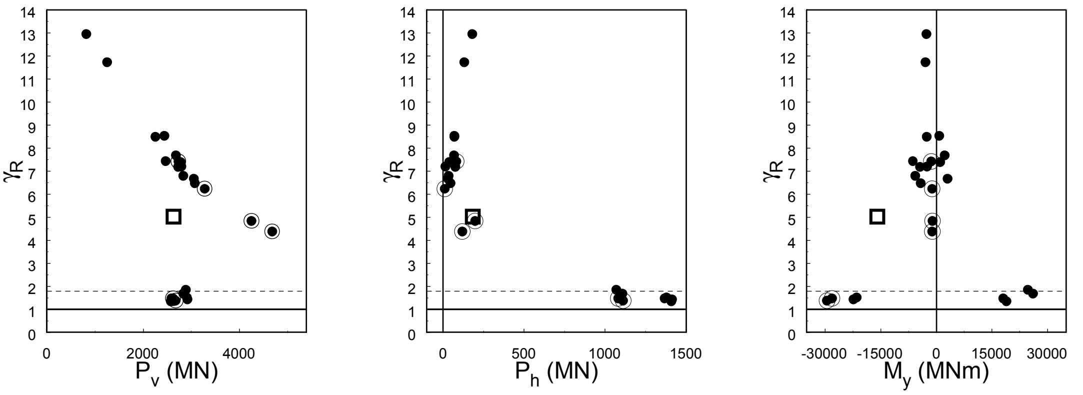


*Figure 53 Values of $\gamma R$ obtained by hand calculations for ULS loading conditions from IBDAS updated model*

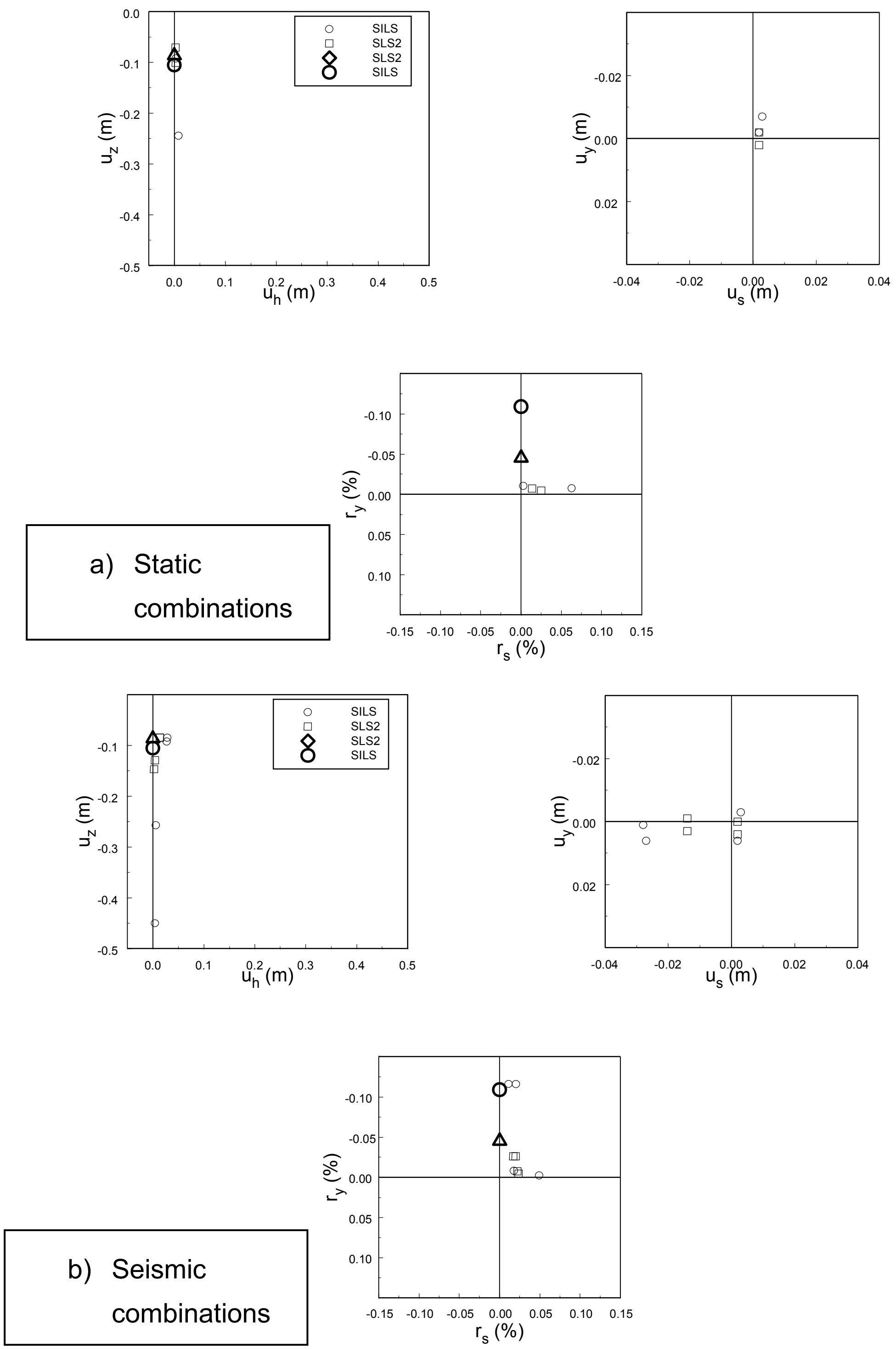


*Figure 54 Displacement and rotation via FEM 3D model for new SILS and SLS2 loading conditions with the worst $\gamma R$ ($u_z$=vertical, $u_h$=horizontal, $r_y$ =rotation in a vertical plane orthogonal to the seashore, $r_s$ rotation in a vertical plane parallel to the seashore): a) static ; b) seismic*

# 7 Appendix A – Comparison between loads from IBDAS global model 3.3 b and 3.3 f

The previous calculations reported in section 6 of the document were based on loads provided by IBDAS global model 3.3 b. New loads have been provided to the writers by the IBDAS global model 3.3 f. A comparison has been carried out based on the ULS checks by hands calculations on the safety factors and also directly comparing the loads on the two legs of the Sicily towers foundations. The main conclusions are summarized in the following points:

a) in general terms partial safety factors increase with the latest loads (IBDAS 3.3f): ULS worst loading combination is characterized now by a value of $\gamma R$= 1.82 which is significantly higher than the values reported in section 6 and furthermore fully satisfies the new Italian code (NTC 2008); this is mainly due to a reduction (15-20%) of shear forces under seismic combinations at the base of the legs;

b) all the other load changes are generally well within ± 5% of the previous ones allowing to state that the load-displacement relationships provided in the section 6 are still valid.